

**Dissertation der Fakultät für Biologie der  
Ludwig-Maximilians-Universität München**

***Foxc1 regulates Pecam-1 Expression in embryonic  
Endothelial Progenitor Cells***

Eingereicht von **Mathias Lamparter**

München, 15. Januar 2008

**Angefertigt am Institut für Klinische Molekularbiologie und Tumorgenetik,  
Helmholtz Zentrum München – Deutsches Forschungszentrum für Gesundheit  
und Umwelt, und Division of Cardiovascular Medicine, Vanderbilt University  
Medical Center, Nashville, TN, USA**

**Erster Gutachter: Prof. Dr. Dirk Eick**

**Zweiter Gutachter: Prof. Dr. Manfred Schliwa**

**Tag der mündlichen Prüfung: 02. Juli 2008**

SUMMARY .....	1
1. INTRODUCTION .....	3
1.1 The Vascular System .....	3
1.2 De novo formation of the vasculature – Vasculogenesis.....	3
1.3 Expansion and maturation of the vasculature – Angiogenesis.....	4
1.4 The vasculature in disease states .....	5
1.5 Characteristics of adult EPCs .....	5
1.6 EPC promote neovascularization .....	6
1.7 Molecular control of blood vessel formation .....	6
1.7.1 VEGF and VEGF-Receptors .....	7
1.7.2 Angiopoietins and Tie-Receptors.....	8
1.7.3 Ephrins and Eph Receptors.....	8
1.7.4 Extracellular Matrix and Cell Adhesion Molecules.....	8
1.7.5 Other signaling pathways involved in vascular development.....	9
1.7.6 Cytokines.....	10
1.7.7 Angiogenic inhibitors .....	10
1.7.8 Haemodynamic forces.....	10
1.8 Transcriptional control of vascular formation.....	10
1.8.1 Ets transcription factors.....	11
1.8.2 Basic Helix-Loop-Helix Transcription Factors .....	11
1.8.3 Homeobox Transcription Factors.....	12
1.8.4 Further Transcription Factors .....	12
1.8.5 Hypoxia and HIF $\alpha$ .....	12
1.9 Embryonic endothelial progenitor cells (eEPCs) as a model system .....	13
1.10 Foxc1 and Foxc2 are induced during eEPC <i>in vitro</i> differentiation.....	14
1.11 Forkhead (Fox) Transcription Factors.....	14
1.11.1 General characteristics of Fox Genes .....	14
1.11.2 Nomenclature of Fox Genes.....	15
1.11.3 Chromosomal organization of Fox genes .....	15
1.11.4 Fox Genes in Development .....	16
1.11.5 Fox Genes in Signaling Pathways .....	17
1.11.6 Fox Genes in Human Diseases.....	18
1.11.7 Fox Genes in the Adult Organism.....	19

1.12 The <i>FoxC</i> subfamily - <i>Foxc1</i> and <i>Foxc2</i> .....	19
1.12.1 Expression Patterns .....	19
1.12.2 Abnormalities in <i>FoxC</i> mutant embryos.....	20
1.12.3 <i>Foxc1</i> and <i>Foxc2</i> - signaling pathways and target gene activation.....	21
1.13 Aims of the Ph.D. Project.....	22
2. MATERIAL and METHODS.....	23
2.1 Tissue Culture.....	23
2.1.1 Cell lines.....	23
2.1.2 Tissue culture media .....	24
2.1.3 Passage of cell cultures.....	24
2.1.4 Freezing and thawing of cell lines.....	25
2.1.5 Transfection of cell lines .....	25
2.2 Molecular biology techniques.....	26
2.2.1 Total RNA isolation.....	26
2.2.2 Reverse Transcriptase-Polymerase Chain Reaction (RT-PCR) .....	27
2.2.3 Polymerase Chain Reaction (PCR) .....	28
2.2.4 PCR Primer Design .....	29
2.2.5 DNA Sequencing.....	29
2.2.6 Plasmid DNA preparation .....	31
2.2.7 Transformation of CaCl <sub>2</sub> -competent DH5 $\alpha$ E.coli .....	32
2.2.8 DNA restriction digests .....	33
2.2.9 DNA ligation .....	34
2.2.10 Plasmid Constructs.....	34
2.2.11 Agarose gel electrophoresis .....	37
2.2.12 Ethanol Precipitation of DNA .....	38
2.3 Quantitative Real-Time Amplification (qPCR) .....	38
2.3.1 LightCycler Real-Time PCR System.....	38
2.3.2 iQ5 Real-Time PCR System.....	40
2.4 Fluorescence Activated Cell Sorting (FACS) Analysis .....	42
2.5 Microscopy and Fluorescence Microscopy .....	43
2.6 Immunofluorescence.....	43
2.7 Promoter-Luciferase Assays .....	44
2.8 Western Blot .....	46

2.9 Chromatin Immunoprecipitation .....	48
2.10 Online Databases and Bioinformatics Programs.....	51
3. RESULTS .....	53
3.1 Expression of Fox genes in eEPCs.....	53
3.2 Foxc1 and Foxc2 regulate expression of <i>Pecam-1</i> in eEPCs .....	56
3.3 <i>Pecam-1</i> as an endothelial target gene of Foxc1 .....	60
3.4 Cis-regulatory areas of the <i>Pecam-1</i> promoter .....	61
3.5 <i>Pecam-1</i> promoter and enhancer analysis in different cell lines .....	62
3.6 Foxc1 activates transcription through the 5'-flanking 3.5kb-fragment .....	65
3.7 The distal 5'-flanking 3.5kb-fragment responds specifically to Foxc1 .....	66
3.8 Foxc1 activates transcription specifically in eEPCs .....	68
3.9 Endogenous <i>Pecam-1</i> RNA analysis matches promoter activation studies....	70
3.10 Dose-dependent activation of the <i>Pecam-1</i> promoter by Foxc1 .....	71
3.11 Activation of the <i>Pecam-1</i> promoter takes place in multiple, independently isolated eEPC clones.....	72
3.12 <i>Pecam-1</i> promoter activity – Summary .....	73
3.13 Localization of Foxc1-responsive sites.....	74
3.14 Analysis of the <i>Pecam-1</i> promoter using Bioinformatic Tools .....	76
3.15 The (TTTGT) <sub>n</sub> motif is found at the human <i>PECAM-1</i> locus .....	78
3.16 Deletion of the repeat motif abolishes promoter activity.....	81
3.17 Foxc1 binds the (TTTGT) <sub>n</sub> motif on native chromatin.....	83
3.18 Results – Summary.....	86
4. DISCUSSION .....	87
4.1 <i>Pecam-1</i> basal promoter activity reflects endogenous transcript levels.....	87
4.2 Foxc1 induced <i>Pecam-1</i> expression reflects an eEPC-specific mechanism ...	88
4.3 <i>Pecam-1</i> expression is controlled by multiple factors.....	89
4.4 Expression of <i>Pecam-1</i> in isolated embryonic angioblasts requires a specific upstream regulatory element .....	90
4.5 Loss of Foxc1 does not affect pan-endothelial <i>Pecam-1</i> expression .....	92
4.6 Foxc1 binds a microsatellite repeat in the 5'-area of the mouse <i>Pecam-1</i> gene .....	93
4.7 The activity of the upstream element depends on the number of microsatellite repeat motifs .....	95
4.8 The repeat number compensates the loss of the consensus motif .....	96

4.9 Fox proteins can bind low-affinity sites.....	97
4.10 Microsatellite repeats represent species-specific transcriptional elements ...	97
4.11 Variation in transcription factor binding sites across species .....	99
4.12 Difference between Foxc1 and Foxc2 functions .....	100
4.13 Foxc1 as regulator of vascular adhesion molecules?.....	101
4.14 Conclusion .....	102
REFERENCES .....	104
SUPPLEMENTAL TABLE.....	123
ABBREVIATIONS.....	125
ACKNOWLEDGMENTS .....	127
LIST OF PUBLICATIONS.....	129

**SUMMARY**

The formation of the vascular network in the embryo is a highly complex event that is controlled on multiple levels in a spatial and temporal manner. Initial formation takes place by vasculogenesis, i.e. the de novo formation of a primitive vessel network by mesodermal endothelial progenitor cells. Subsequent remodeling and expansion into a mature, diverse vasculature is undergone by angiogenesis, which refers to the proliferation of pre-existing endothelial cells. Both processes are controlled by a number of molecular signals such as receptor/ligand complexes, adhesion and matrix molecules as well as signaling intermediates that have been uncovered in the past years. However, the transcriptional mechanisms that regulate the initial differentiation of endothelial progenitor cells to mature tissue are not well-understood. We have used mouse embryonic endothelial progenitor cells (eEPCs) derived from E7.5 embryos – when vascular structures begin to form - as an *in vitro* model to study the process of endothelial cell maturation. We found that *Foxc1* and *Foxc2*, two members of the winged/helix Forkhead transcription factor family, are induced during cAMP-stimulated differentiation of eEPCs *in vitro*. Forkhead transcription factors comprise of a group of DNA binding proteins that act as trans-activators as well as trans-repressors at target gene cis-regulatory areas and are involved in a wide variety of biological processes in animals and fungi. Because *Foxc1* and *Foxc2* have been also implicated in cardiovascular development, we investigated their role during eEPC-differentiation. The work described in this Ph.D. thesis provides evidence that *Foxc1* contributes to the de novo activation of the vascular-specific gene *Pecam-1* (platelet endothelial adhesion molecule-1). In contrast, *Foxc1* appears to down-regulate *Pecam-1* expression in mature endothelial cells. *In vitro* promoter analysis revealed that the de novo activation of *Pecam-1* in response to *Foxc1* is mediated by a distal upstream regulatory element. Further analysis uncovered that *Foxc1* does not bind to a bone fide Fox binding site, but to a microsatellite sequence consisting of repeats of the Fox binding site core 'TTTGT' motif. Stepwise deletion of this repeat motif gradually reduces the ability of *Foxc1* to activate the *Pecam-1* promoter *in vitro*. Chromatin immunoprecipitation assays showed that *Foxc1* protein has the capability to bind to the (TTTGT)<sub>n</sub> pentanucleotide repeat motif in the chromosomal context *in vivo*. Interestingly, the suppression of the *Pecam-1* gene in adult endothelial cell lines

appears to be mediated by a different element immediately upstream from the transcription initiation site. In summary, our study identified a new transcriptional control mechanism for the de novo *Pecam-1* expression in immature embryonic EPCs, thus providing new insight into to the understanding of vascular specific gene expression.



## **1. INTRODUCTION**

### **1.1 The Vascular System**

As the first functional organ to develop in the embryo, the cardiovascular system plays a critical role during vertebrate development and homeostasis. Arising primarily from cells of mesodermal origin, it provides the embryonic tissues with oxygen and nutrients [1]. Blood vessels appear almost simultaneously during embryogenesis at different anatomical sites including the extraembryonic yolk sac membrane, the proximal lateral mesoderm and the allantois. Endothelial cells form the major compartment of the blood vessels where they line the innermost layer (luminal side) and are involved in multiple processes such as cell trafficking, nutrients and oxygen delivery, regulation of the vasomotor tone, maintenance of blood circulation as well as expansion of the vasculature through proliferation [2]. Endothelial cells contain distinctive morphological properties such as the presence of Weibel-Palade bodies and caveolae [3] as well as distinct molecular features, e.g. the expression of specific genes [4].

### **1.2 De novo formation of the vasculature – Vasculogenesis**

The initial event of blood vessel formation during embryonic development is called vasculogenesis, which describes the in situ and de novo assembly of vascular structures from differentiating progenitor cells [5]. Mesodermal cells migrate through the primitive streak and begin to differentiate to endothelial progenitor cells in lateral and posterior areas, such as the head mesenchyme and posterior lateral plate mesoderm. In particular, progenitor cells appear within the cranial region in a bilateral distribution along the midline and begin to form the pre-endocardial tubes [6]; these will later fuse and give rise to the endocardium (the inner layer) of the primitive embryonic heart and the major blood vessels [5, 7]. As development progresses, endothelial progenitor cells gradually appear in most areas of the intraembryonic mesoderm (except the notochord and the prechordal plate) in vascular “hot spots”

where they assemble into the primitive de novo vascular network of the embryo [8]. In parallel to intraembryonic vasculogenesis, the extraembryonic blood vessels form first in the yolk sac where cells within the inner, mesodermal layer assemble in clusters called blood islands [9]. The Flk-1<sup>+</sup>/Tal1<sup>+</sup> cells in the blood islands differentiate at the perimeter into endothelial progenitors, whereas those in the center lose Flk-1 (or VEGFR2) expression and give rise to extraembryonic Flk-1<sup>-</sup>/Tal1<sup>+</sup> hematopoietic precursors [6]. Morphogenetic observations and the close association of early blood and endothelial cells led to the idea of a common precursor for both endothelial and hematopoietic progenitor cells in the yolk sac, called the hemangioblast [9, 10].

### **1.3 Expansion and maturation of the vasculature – Angiogenesis**

Whereas the primitive vascular plexus in the yolk sac and the major intra-embryonic vessels are formed by vasculogenesis, subsequent remodeling and expansion of the vasculature takes place by angiogenesis, i.e. the proliferation, sprouting and migration of pre-existing endothelial cells at the onset of embryonic circulation [11, 12], yielding an extended network of arteries, veins, capillaries, and lymphatics. Several intra-embryonic tissues such as the kidney, thymus, brain, limb and choroid plexus are solely vascularized by angiogenesis, whereas certain endodermal tissues, such as lung or the liver undergo blood vessel formation by vasculogenesis [13, 14]. Angiogenesis also occurs by non-sprouting intussusceptive microvascular growth (IMG), i.e., the splitting of the existing vasculature by transluminal pillars or transendothelial bridges [15, 16].

Vessel maturation is achieved by recruitment of supporting smooth muscle cells (SMCs) and pericytes and production of extracellular matrix (ECM) to stabilize the nascent vessels. Pericytes form a layer and surround the endothelium in capillaries and post-capillary venules, whereas large vessels, such as arteries, are surrounded by mural cells (SMCs), that form a multilayer around the elastic artery wall [17, 18]. Depending on their final localization during development, SMCs differ in their origin, e.g. the first SMCs in the embryo derive from mesoderm cells, pericytes in the

forebrain derive from neural crest cells and SMCs around vessels that lead to the heart originate from the epicardium (the outer layer of the heart) [19].

Under physiological conditions, the adult endothelium is quiescent and the majority of endothelial cells do not undergo cell division in postnatal life. However, vascular remodeling and the pro-angiogenic activity do not entirely cease during adulthood but remain active during the pro-angiogenic activity in the corpus luteum during the female reproductive cycle [20, 21].

#### **1.4 The vasculature in disease states**

The vascular system plays a critical role in many human diseases. Abnormal remodeling of the vasculature can lead to psoriasis (hypervascularity of skin vessels) and pulmonary hypertension [22]. Increased vascularization can cause retinopathy (damage of the retina in the eye) [23] and rheumatoid arthritis. Atherosclerosis (occlusion of arteries) is an abnormal deposition of SMCs and mononuclear cells in the artery wall, mainly triggered through over-expressed inflammatory cytokines [24]. In addition, postnatal angiogenesis is activated during pathological conditions like wound healing or tissue ischemia. Moreover, tumor growth depends on the tumor's ability to induce blood vessel growth through angiogenesis or vasculogenesis [12, 25]. The main goals of clinical research in the field of vessel growth are to block vascularization in diseases like retinopathy or cancer and to enhance neovascularization in patients who suffered myocardial infarction and stroke or have peripheral vascular diseases.

#### **1.5 Characteristics of adult EPCs**

Postnatal blood vessel growth, for example during vascular disease states, mostly depends on the proliferation of mature, pre-existing endothelial cells or angiogenesis [12]. However, within the last years, numerous studies showed that mononuclear bone marrow or peripheral blood precursor cells have the potential to take part in the formation of new blood vessels, a process called adult or neo-vasculogenesis [12,

26, 27]. Those endothelial progenitor cells (EPCs) are characterized as CD34<sup>+</sup>/Flk-1<sup>+</sup> cells. In the bone marrow, human EPCs also express CD133 (formerly AC133), a surface antigen of hematopoietic precursors, in contrast to circulating EPCs that have lower expression of CD133 [28-32]. However, no specific antigen profile has been uncovered to characterize EPCs as a distinct cell type from other mononuclear cells in the bone marrow and peripheral blood. Past studies suggest that EPCs do not consist of a unique cell population but are probably derived from a subpopulation of mononuclear cells, which acquire endothelial characteristics when recruited to ischemic or angiogenic environments. In accordance, EPCs also express myeloid monocytic markers like CD14 [33].

### **1.6 EPC promote neovascularization**

Since the original publications about ten years ago, numerous studies demonstrated the potency of bone marrow mononuclear cells to differentiate to EPCs and then endothelial cells [28-30, 34-36]. By using various animal models of disease, these experiments provided evidence about the involvement of EPCs in blood vessel growth in ischemic myocardium [37-39], ischemic hindlimb [33-35, 40, 41], in cerebral ischemic tissue [42], or during tumor growth [43, 44]. Collectively, these studies showed that EPCs home specifically to areas of active angiogenesis, associate closely with the vascular wall and participate in vessel formation, mostly through the stimulation of angiogenesis and enhanced tissue recovery.

The increasing importance of modulating vascular growth in clinical therapies during disease states has fostered intensive studies to uncover the molecular and cellular mechanisms that guide blood vessel growth during both, embryonic and postnatal vascularization.

### **1.7 Molecular control of blood vessel formation**

Vascular formation is a complex, highly organized mechanism, relying on the correct spatial and temporal expression of specific sets of genes, that eventually result into

the formation of the vascular network [14, 45, 46]. Different molecular factors carry out distinct functions, such as endothelial growth stimulation or regulation of vessel maturation. Among them are e.g. extracellular ligands and their receptors, cell adhesion molecules, extracellular matrix components and intracellular signaling intermediates. The initiation of embryonic endothelial specification is driven by Fibroblast Growth Factor-2 (Fgf2) [47]. During subsequent vascular formation, three families of receptor tyrosine kinases and their ligands play major roles: the VEGF (Vascular Endothelial Growth Factor) family and their receptors [48, 49], the angiopoietins and their Tie receptors [50], and the ephrins and their Eph receptors [51].

### 1.7.1 VEGF and VEGF-Receptors

VEGF signaling is crucial to achieve a continued vascularization of the developing embryo, including organs such as heart and brain, as well as growth of the major blood vessels. The VEGF family consists of six members, VEGF-A – VEGF-E and PlGF (Placental Growth Factor). Three VEGF-receptor tyrosine kinases (VEGFR1-VEGFR3) have been identified. VEGFR1 (Flt-1) and VEGFR2 (Flk-1) are expressed on the vascular endothelium, whereas VEGFR3 (Flt-4) is restricted to lymphatic endothelium [52].

VEGF-A (usually termed VEGF) has the ability to induce proliferation, differentiation and migration of endothelial progenitor cells *in vivo* and *in vitro* and it is essential in both processes of vasculogenesis and angiogenesis [51]. Mutations of VEGF or VEGFR2 lead to early embryonic lethality. In the adult, lack of VEGF affects mainly wound healing or the ovarian corpus lutei [53]. The second VEGF receptor, Flt-1 (VEGFR1) modulates VEGF signaling through Flk-1 (VEGFR2) and is involved in hemangioblast commitment. VEGF signaling is also modulated by the members of the neuropilin (NRP) family, which form a family of transmembrane proteins and bind members of the VEGF family, thus functioning as regulators of vasculogenesis [54]. Further, members of the neuropilin family differentially mark the arterial-venous system, with NRP-1 being expressed in arterial ECs, whereas NRP-2 is found on venous endothelium and later on lymphatic vessels [55].

### 1.7.2 Angiopoietins and Tie-Receptors

Angiopoietins, which comprise four secreted proteins (Ang1, Ang2, Ang3, and Ang4), and their receptors, the Ties (Tie-1 and Tie-2) function subsequent to the action of VEGF and have an important role in vessel maturation or destabilization by regulating processes such as endothelial sprouting, vessel wall remodeling and mural cell recruitment [50]. Ang1 counters the function of VEGF by promoting and maximizing the tight contact between ECs and underlying support cells, thus maintaining the quiescence and stabilization of the vessel [56]. In turn, a second Tie-2 ligand - Ang2 - acts as a natural antagonist of Ang1 and leads to opposite effects like de-stabilization of the vessel wall [57].

### 1.7.3 Ephrins and Eph Receptors

Artery-vein cell fate is genetically programmed by numerous factors, including members of the Eph/ephrin family, which are expressed differentially in arterial and venous ECs. The Eph Family consists of at least 14 members and their counterparts, the ephrins, of at least 8 members. This receptor/ligand system stands out inasmuch that both, the receptor and its ligand must be membrane-bound to induce signaling into the cell [53]. Knockout studies showed that ephrinB2 and EphB4 are involved in the important specification of arterial and venous vessel identity, with EphB4 being expressed in veins whereas ephrinB2 marking arteries [58-60]. Mutations in both *ephrin-B2* and *Eph-B4* lead to embryonic lethality at E9.5, showing failure to remodel the primitive vascular plexus into arteries and veins.

### 1.7.4 Extracellular Matrix and Cell Adhesion Molecules

Matrix Metalloproteinases (MMPs) are zinc-dependent enzymes that partake in degrading the extracellular matrix during angiogenesis, thus permitting ECs to migrate into the surrounding tissue [45]. Their function is countered during vessel formation by circulating tissue-localized inhibitors of matrix metalloproteinases (TIMPs) [61].

The assembly of migrating ECs into solid cords is established by cell-cell contacts through adhesion molecules, e.g. Pecam-1 (Platelet-Endothelial Cell Adhesion Molecule-1) [62] and members of the cadherin surface molecule family such as N-cadherin (Neuronal-Cadherin) and VE-cadherin (Vascular endothelial-cadherin), which are expressed in ECs [63-65]. Integrins, a family of transmembrane proteins, mediate cell adhesion to proteins of the extracellular matrix and partake in the regulation of angiogenesis [66, 67], e.g. the integrin family member  $\alpha_v\beta_3$  is expressed on angioblasts where it functions during EC maturation and vessel formation [68].

Extracellular matrix molecules such as fibronectin support the formation of the basic vascular network [69]. During vessel maturation, fibronectin decreases and ECs synthesize collagen type IV and laminin that support the stability of the vascular tubes [70].

#### 1.7.5 Other signaling pathways involved in vascular development

The Notch-Delta pathway is involved in driving the differentiation of the primitive vessel network toward a hierarchy of mature vascular beds and controls arterial cell fate as well as homeostatic functions of mature arteries [71, 72]. This pathway is a highly conserved mechanism comprising of four receptors (Notch 1-4) and five ligands (Jagged-1 and -2 and Delta-1,-3,-4), and all these factors have been shown to have expression patterns in different components such as arteries, veins, capillaries, and mural cells. Mutations in Notch receptors, ligands and downstream components lead to strong vascular defects [73].

During maturation of newly formed vessels, members of the transforming growth factor-beta (TGF $\beta$ ) and platelet derived growth factor (PDGF) family inhibit proliferation and migration of ECs [18, 74]. PDGF-B is secreted by ECs in response to VEGF, and lack of PDGF-B leads to impaired pericyte recruitment [75]. Pleiotropic TGF $\beta$ -signaling consists of an essential role during vascular development, controlling EC migration as well as maturation [76].

### 1.7.6 Cytokines

Several cytokines such as GM-CSF (Granulocyte-Monocyte Colony Stimulating Factor) or SDF-1 (Stromal Cell-Derived Factor-1) stimulate the migration of EPCs from the bone marrow to sites of neovascularization in adults [41, 77-79].

### 1.7.7 Angiogenic inhibitors

Besides numerous pro-angiogenic factors, several naturally occurring inhibitors of angiogenesis exist [45], among them thrombospondin, angiostatin or endostatin [80, 81].

### 1.7.8 Haemodynamic forces

Next to oxygen and genetic factors, the vascular system is shaped by the influence of haemodynamic forces, such as shear stress, i.e. the tangential, mechanical force acting upon the surface of the endothelium [14, 82]. Blood flow dynamics was shown to induce changes in vessel branching angles to allow optimization of flow, and shear stress has been suggested to be a driving force for the release of angiogenic signals [83].

## **1.8 Transcriptional control of vascular formation**

Besides extracellular signaling factors, surface receptors, and matrix molecules that have been described during blood vessel growth, factors also regulate vascular development on the transcriptional level and control the genetic regulation of endothelial differentiation. During development, transcription factors serve as master switches in activating the expression of tissue and cell-line specific genes. Unlike during developmental processes such as hematopoiesis or myogenesis, where a wide set of important transcriptional regulators have been uncovered in the past, only a few transcriptional regulators of vascular development are known to date [84].



### 1.8.1 Ets transcription factors

The majority of the identified transcription factors during vascular development are activators of the expression of e.g. certain tyrosine kinase receptors like *Tie1* and *Tie2* or *Flk-1* (VEGF receptor 2) and *Flt-1* (VEGF receptor 1). Regulatory elements in the genomic regions of these genes were shown to contain binding sites for members of the Ets-family of transcription factors, e.g. Ets-1, Ets-2, and Fli-1 [85-89]. For example, *Tie1* and *Tie2* were strongly activated by the Ets-family members NERF and ELF-1 [85, 86], with the latter one being strongly enriched in developing chicken embryos. In addition, the Ets-factor Fli-1 is enriched in the developing vasculature of zebrafish [88] and was shown to be a critical factor of vascular development in both, the zebrafish and E11.5 Fli-1 knockout mice, which display loss of vascular integrity [88, 89]. Ectopic expression of the transcription factor *SCL/Tal1* in zebrafish mesoderm allowed identification of an important role of this gene in vasculogenesis, hematopoiesis and endothelial differentiation [90]. In addition, *SCL/Tal1* is expressed in both, mouse and zebrafish embryos, where it can be detected in the developing vasculature [90, 91]. The Gata transcription factor family member Gata-2 was shown to be strongly expressed in endothelial cells and serves as an important regulator of the expression of vascular-specific genes, such as *Flk-1*, *Icam-2* (Intercellular Adhesion Molecule-2), *eNOS* (endothelial nitric oxide synthase) and *Pecam-1* [87, 92-94].

### 1.8.2 Basic Helix-Loop-Helix Transcription Factors

Basic Helix-Loop-Helix (bHLH) transcription factors are involved in the formation of the vasculature. The bHLH protein Tfeb was shown to be required for the vascularization of the placenta [95] and the transcription factor HESR1 is upregulated during vascular tube formation, where in turn it downregulates the expression of *Flk-1*, thus lowering the responsiveness of ECs to VEGF, eventually resulting into increased vessel maturation [96].

### 1.8.3 Homeobox Transcription Factors

Capillary morphogenesis is under the partial control of the homeobox gene *HoxB3*, with ectopic overexpression of this gene resulting into increased capillary density in the chorioallantoic membrane of embryos [97, 98]. The related homeobox transcription factor HoxD3 was shown to regulate the expression levels of integrin  $\alpha_v\beta_3$  on endothelial cells [99] and endothelial differentiation is enhanced after overexpression of the homeobox transcription factor gene *hex* in zebrafish embryos [100].

### 1.8.4 Further Transcription Factors

Further transcription factors required for endothelial differentiation include the immediate-early gene *Fra1* - an AP-1 transcription factor family member - whose deletion leads to a reduced number of endothelial cells in the placenta [101]. The zinc-finger transcription factor gene *VeZF1* is expressed specifically in endothelial cells and their progenitors as well as ECs of the dorsal aorta, the branchial arch artery and the endocardium [102] and its expression co-localizes with *Flk-1*. The zinc-finger transcription factor gene *LKLF* is expressed in non-vascular and vascular cells, and its loss leads to abnormalities during the late stages of vascular formation [103].

### 1.8.5 Hypoxia and HIF $\alpha$

Hypoxia serves as a master stimulus in promoting the growth of new blood vessels, thereby inducing the expression of transcription factors that mediate this response. Among them is the bHLH-PAS domain transcription factor *HIF1 $\alpha$*  (hypoxia inducible factor 1 $\alpha$ ) that mediates the expression of angiogenic genes, such as *VEGF* during low-oxygen conditions [104, 105].

Signaling pathways that partake in the transcriptional induction of vascular and angiogenic genes involve the PI3-kinase (Phosphoinositide 3-kinases) pathway, that modulates *VEGF* induction by hypoxia. The catalytic subunit p110 induces HIF1 $\alpha$  activity in response to hypoxia [106], and the mitogen-activated protein kinases p42 and p44 have been shown to modulate HIF1 $\alpha$  activity through phosphorylation [107].

## **1.9 Embryonic endothelial progenitor cells (eEPCs) as a model system**

As mentioned above, bone marrow derived progenitor cells with endothelial potential partake in postnatal neovascularization processes. A number of endothelial lineages have been established in the past for *in vitro* studies to disclose the cellular processes of vessel development, including mature lines from diverse vascular beds of different species as well as CD34<sup>+</sup> progenitor cells [4]. In order to gain further insight into the molecular mechanisms of endothelial cell growth and differentiation, our group took advantage of an embryonic endothelial progenitor (eEPC) line that was isolated by Hatzopoulos and coworkers [108].

These cells were cultured from intra-embryonic egg cylinders of trypsin-dissociated mouse embryos at day 7.5 during midgestation, prior to the formation of the cardiovascular system. They represent a subpopulation of the first angioblasts in the embryo proper during development and show unlimited stem cell-like growth and properties of endothelial progenitor cells. Expression profile analysis indicates that these cells are derived from the embryonic proximal lateral mesoderm and represent an early pro-endocardial population. They express the stem-cell marker *c-Kit* as well as early endothelial markers like *thrombomodulin* and *Tie2*. In culture, they show a round to spindle-like shape and bind to GSL I B4 isolectin that interacts specifically with ECs and EPCs [109]. RNase protection assays - a method for gene expression studies - revealed that retinoic acid and cyclic adenosine monophosphate (cAMP) are capable to induce differentiation of these embryonic endothelial progenitor cells (eEPCs) toward more mature endothelial cells that express endothelium specific *Flk-1* and *vWF* [109]. Furthermore, eEPCs can differentiate and form tube-like structures when plated in Matrigel (an extra-cellular matrix basement material) [109]. Taking together, the data showed that these embryonic mesodermal cells have the properties of EPCs and can differentiate into mature ECs. Interestingly, eEPCs do not express endothelial progenitor marker genes such as CD34 [40, 110] or *Flk-1* [111] before retinoic acid/cAMP treatment, but they show high levels of the endothelial surface protein *Tie2*. They display unlimited growth potential *ex vivo* with population doublings every 24 hours. Further, eEPCs were shown to retain their properties of endothelial progenitor cells after *ex vivo* culturing and they form vascular structures after injection into host chick embryos. Animal models showed

incorporation of eEPCs into the tumor microvasculature in lung carcinomas in mice [112] and eEPCs displayed intensive therapeutic potential inside damaged tissue in models of ischemic hind limb and myocardial infarction [113, 114]. Moreover, using eEPCs, it was shown that homing of progenitor cells from the circulation to the tumor vasculature is mediated by adhesive mechanisms that resemble the interaction of activated leukocytes with the vessel wall and involve ESL-1 (E-selectin ligand) and PSGL-1 (P-selectin ligand) expressed on eEPCs, and their respective receptors – E-selectin and P-selectin – expressed on resident endothelial cells [112].

In summary, embryonic EPCs have provided a new tool and allowed us to gain further insight into the molecular and cellular biology of endothelial progenitor cells and their behavior in postnatal vasculogenesis and organ vascularization.

### **1.10 Foxc1 and Foxc2 are induced during eEPC *in vitro* differentiation**

In order to elucidate new vascular specific regulatory factors, the eEPC transcriptome was analyzed by means of Affymetrix GeneChip, which uncovered a number of genes induced or suppressed during *in vitro* differentiation. Among the induced genes were *Foxc1* and *Foxc2*, two closely related members of the Forkhead/winged helix (Fox) transcription factor gene family [115, 116].

### **1.11 Forkhead (Fox) Transcription Factors**

#### **1.11.1 General characteristics of Fox Genes**

Fox genes encode a subclass of the helix-turn-helix class of transcription factors and comprise a monophyletic group of DNA binding proteins with an approximately 110-amino acid conserved monomeric DNA binding domain [117], called the Fox (Forkhead) domain. The structure of the Fox domain is based on a helix-turn-helix core of three  $\alpha$ -helices, flanked by two looped wings [118], giving Fox proteins the alternative name winged helix proteins, due to this butterfly-like three-dimensional structure [116, 119]. The *Drosophila melanogaster* *forkhead* gene and the rat *Foxa1*

gene were the first identified members of this gene family [120, 121] and since then, Fox genes have been identified in numerous species, ranging from yeast to mammals [115, 116]. Because of their wide functional variety in biological processes, there is no simplified scheme of a general function of all members of the Fox gene family. Fox transcription factors have been shown to act as trans-activators as well as trans-repressors and unlike most helix-turn-helix proteins, Fox proteins bind as monomers to an asymmetric target sequence and are most likely to activate gene expression directly by opening up the chromatin structure close to the target gene locus [122]. In addition, little is known about the interactions of Fox proteins with the basic transcriptional machinery, although *Foxf2* has been shown to interact with the general transcriptional regulators TBP and TFIIB in vitro [123].

### 1.11.2 Nomenclature of Fox Genes

Chordate Fox genes are divided into 17 subclasses, or clades, namely A-Q, based on the amino acid sequence of the conserved Fox (Forkhead) domain. Kaestner and coworkers revised the nomenclature system for Fox transcription factors, leading to a standardized name system that uses Fox (from Forkhead Box) as a root and divides the members into subfamilies [115]. Each member of a respective subfamily is further defined by a number, e.g. *Foxa2* or *Foxf1*. This ensures a unified nomenclature between species and identifies orthologues family members between species. Comprehensive and updated information about Fox genes is available online under <http://www.biology.pomona.edu/fox.html>.

### 1.11.3 Chromosomal organization of Fox genes

Generally, Fox genes are distributed throughout the whole genome of a species and do not show any physical clustering. However, certain members of the human FOX gene family within the human genome show proximity, e.g. *FOXQ1-FOXF2-FOXC1* (on chromosome locus 6p25.3) or *FOXC2-FOXF1-FOXL1* (locus 16q24.1), giving evidence for ancestrual intra-and inter-chromosomal gene duplications [124]. Ancient loci duplications, followed by sequence divergence, are thought to be responsible for the expansion of the Fox gene family. In some cases, the duplications

date back in evolution before the separation of zebrafish and coelacanths (jawed fish), as for *Foxc1* and *Foxc2*, since these genes are present in both eukaryotic organisms [119]. Most of the vertebrate Fox genes have only a few small introns and some are even intronless, such as *Foxc1*, *Foxc2*, *Foxd1*, *Foxd2* and *Foxg1*, whereas others such as *Foxo1* and *Foxo3* genes have large introns up to 130kb separating the Forkhead domain [116].

#### 1.11.4 Fox Genes in Development

Since the discovery of the first Fox gene, the biological importance of this gene family has become of significance because they partake in a wide variety of biological functions, e.g. cell cycle control, cell differentiation, metabolic control, and developmental processes such as the establishment of the body axis and the development of various tissues from all three germ layers [116, 119].

For example, *Foxh1* was shown to regulate the establishment of the left-right body axis in zebrafish and mouse embryos [125, 126] and mutations in *Foxj1* lead to sinus inversus, i.e. abnormal laterality of the heart [127]. Hair development in mammals involves *Foxq1* and *Foxn1* and mutations in *Foxq1* causes aberrant differentiation of the hair shaft [128] whereas *Foxn1*, that is specifically expressed in the skin and the thymic epithelium, leads to the nude phenotype in newborn mice, that is characterized by the absence of hair and severe immunodeficiencies [129, 130]. Impaired organogenesis also occurs in *Foxi1* *-/-* mice, which display intense inner ear structural dysgenesis and severe hearing impairment [131], due to a lack of *Foxi1* expression in the ectodermal epithelium of the otic vesicle. *Foxe3* is another Fox gene required for specification of ectodermal epithelia, where it controls the proliferation of ectodermal lens cells [132]. *FoxA* genes (*Foxa1*, *Foxa2*, *Foxa3*) are expressed in the vertebrate endoderm and formation of the epithelial gut tubes is impaired in *Foxa2* *-/-* embryos [133, 134]. Other organs relying on Fox gene function involve the lung, where gene expression in the epithelium is controlled by *Foxa1* and *Foxa2* [135] and *Foxj1* [127, 136, 137] as well as *Foxp2* [138], which guide the specification of ciliated cells in the airway epithelium. In contrast, *Foxf1* is expressed in the lateral plate mesoderm and the posterior primitive streak where it drives the separation of the lateral plate into splanchnic and somatic mesoderm [139, 140] and

*Foxb1* deletions were shown to cause embryonic lethality with an open neural tube and dysgenesis of the caudal midbrain [141]. The development and differentiation of neuronal cells is controlled by several members of the Fox gene family such as *Foxg1* that regulates the development of the cerebral hemispheres in the neuroectoderm, where it controls the proliferation of telencephalic neuroepithelial cells [142, 143]. *Foxd3* was shown to regulate and maintain the neural crest stem cell pool in zebrafish [144]. Adult myogenic stem cells require *Foxk1* expression for proper cell cycle regulation and myogenic cell commitment [145].

#### 1.11.5 Fox Genes in Signaling Pathways

Fox genes have been related to a number of important signaling pathways, where they function as downstream activators or repressors of transcription. Mammalian Foxh1 is involved in mediating TGF $\beta$  induced downstream responses during target gene activation. In addition, Foxh1 was shown to form a complex with smad2 and smad4, both intermediate signal transducers downstream of activin signaling, a member of the TGF $\beta$  superfamily [146-149]. Conversely, Foxg1 was shown to inhibit gene activation in response to TGF $\beta$ -type signaling [150, 151]. Sonic hedgehog signaling activates several mammalian Fox genes, such as *Foxa2* in the floorplate of the neural tube or *Foxc2* and *Foxd2* in the presomitic mesoderm and *Foxf1* expression in the sclerotomes was shown to depend on Shh signaling from the notochord [152]. Foxl1 function was linked to Wnt/b-catenin/TCF signaling pathway in the intestinal mesenchyme [153].

Furthermore, FoxO genes have been linked to Akt/PKB (Protein Kinase B) signaling, where they are involved in cell cycle regulation. Phosphorylation by PI3K/PKB leads to arrest of the cell cycle entry in G1 [154] and Foxo4 was shown to be phosphorylated by Ras signaling, placing certain Fox proteins downstream from major signaling pathways [116, 154, 155]. Mammalian *FoxM1* is activated upon the cell's entry into the S-phase and has been implied in the regulation of DNA replication [156].

Despite this wealth of information, the precise genetic program of Fox genes, including their regulators and downstream targets, yet has to be identified for most of the family members.

### 1.11.6 Fox Genes in Human Diseases

Since Fox family members play pivotal functions during organogenesis and in the maintenance of physiological homeostasis, mutations or deletions in human FOX genes, e.g. in the case of *FOXC1*, *FOXC2*, *FOXE1*, *FOXP2*, lead to various human congenital disorders and malformations, such as skeletal, craniofacial, immune and circulatory defects. A majority of the known eight human disorders, that are caused by mutations in Fox genes, are autosomal dominantly inherited. The mutations frequently lie within the highly conserved Forkhead Domain, i.e. the DNA binding domain [116].

In the human genome, *FOXC1* lies in the 6p25 forkhead cluster and mutations of this gene cause Axenfeld-Rieger Syndrom, characterized by defects in eye development, eventually resulting into glaucoma [157-159]. Malformations of the anterior chamber of the eye have also been linked to mutations in *FOXE3* [160] and mutations in *FOXL2* and *FOXC2* cause eyelid defects and lymphedema [161-165]. A fraction of primary endometrial and ovarian cancers exhibit *FOXC1* inactivation, suggesting a tumor suppressor gene role for *FOXC1* [166]. *FOXL2* also has been implicated in premature ovarian failure [167], and *FOXM1* deficiency causes T-cell immunodeficiency and skin disorders [168]. Speech and language disorders in humans have been linked to *FOXP2* [169]. *FOXA1* is overexpressed in esophageal and lung cancer [170], whereas *FOXM1* expression levels were shown to be elevated in pancreatic cancer [171] and in basal cell carcinomas [172]. In acute lymphoid leukemia, fusion proteins consisting of the DNA binding domain of a certain transcription factor and the transactivation domain of FOXO3 or FOXO4 can cause oncogenic transformations [173-175].

There is increasing interest in disclosing the precise biological and molecular function of Fox gene family members, since a profound understanding of their role may lead to novel therapeutics as well as diagnosis and prevention of certain human genetic diseases.



### 1.11.7 Fox Genes in the Adult Organism

Interestingly, many Fox genes show an expanded repertoire of functions in the adult organism, compared to embryonic life. Metabolic control in liver, lung, intestine and pancreatic tissues is one of the major functions of Fox genes in adult tissues, as it was shown for members of the *FoxA* subfamily, by the use of conditional knock out mice [135]. Likewise, a functional switch from embryonic control of morphogenesis to adult control of metabolism in adults is seen for *Foxc2*, which regulates metabolic efficiency in response to the energy content of the diet [176] and *FoxO* subfamily genes were shown to be involved in insulin/IGF signaling in the adult organism [116, 155, 177].

### 1.12 The *FoxC* subfamily - *Foxc1* and *Foxc2*

*Foxc1* and *Foxc2* proteins have nearly identical DNA binding domains, suggesting that they were generated by a duplication event [115]. The role of the mouse *Foxc1* and *Foxc2* genes during embryogenesis and the resulting phenotypes after gene knock out in mice was the subject of extensive research during the last years, implicating these two genes in cardiovascular development [178-181].

#### 1.12.1 Expression Patterns

Initially, *FoxC* genes are expressed in a dorsoventral gradient and they display overlapping expression patterns in several embryonic tissues, e.g. the paraxial, cephalic, and nephrogenic mesoderm [180, 182]. In addition, *FoxC* transcripts are localized in the endothelium and the surrounding mesenchyme of the developing blood vessels and the heart [178, 179, 181, 183, 184] and both genes were shown to be expressed in the nuclei of endothelial and smooth muscle cells in the aorta of the developing embryo [180].

### 1.12.2 Abnormalities in FoxC mutant embryos

For the most part, *Foxc1* and *Foxc2* are partially functionally redundant and display interactive roles during cardiac and renal morphogenesis, since compound heterozygous embryos (*Foxc1* +/- ; *Foxc2* +/-) have similar defects as single null mutant embryos, whereas compound null mutant embryos (*Foxc1* -/- ; *Foxc2* -/-) display much more severe abnormalities. Most compound heterozygotes (*Foxc1* +/- ; *Foxc2* +/-) as well as single homozygotes (*Foxc1* -/- or *Foxc2* -/-) die pre-or perinatally with similar phenotypes, such as cardiovascular, multiple skeletal, urogenic, and ocular defects, as well as ventricular septal defects and pulmonary valve diplasia [178-180, 185-189]. However, blood vessels and somites form to a certain extent in those embryos, suggesting that *Foxc1* and *Foxc2* can compensate for each other to a certain degree in a dose-dependent function. Besides this, compound homozygote *Foxc1*, *Foxc2* mice (*Foxc1* -/- ; *Foxc2* -/-) and compound heterozygous/homozygous embryos (*Foxc1* +/- ; *Foxc2* -/- or *Foxc1* -/- ; *Foxc2* +/-) die in utero with intensified malformations that are more severe than those of each single homozygous null embryo, undermining a dose-dependent function of the two transcription factors [180].

Blood vessels in embryos carrying *Foxc1* and *Foxc2* null mutations are disorganized vascular plexi without proper remodeling into a well-defined system of larger and smaller blood vessels, and compound *Foxc1* +/- ; *Foxc2* -/- embryos display extensive defects in the morphology and remodeling in the head vasculature, and the number, size and organization of the branchial arch arteries is abnormal [180]. Further, the heart shows dysgenesis and is smaller than in wild type animals. In addition, FoxC transcription factors were shown to be involved in the regulation of arterial endothelial cell specification [181]. They directly activate transcription of the Notch ligand *Dll4*, a marker for arterial endothelium, through a Fox-binding site in the *Dll4* promoter. *Foxc1* -/- ; *Foxc2* -/- compound mutants have arteriovenous malformations and lack expression of arterial markers [181], making FoxC proteins important transcriptional regulators in arterial fate determination. Overlapping domains of expression have also been shown in the pro-epicardium, in cardiac neural crest cells and the endocardium, where a lack of *Foxc1* and *Foxc2* may affect the formation of the outflow tract cushions [190]. Because of its expression in cephalic neural crest derived mesenchyme, *Foxc1* mutations lead to hydrocephalus and defects in eye

development in the mutant embryo [187, 191] and craniofacial development is strongly impaired in these null mice, with maxilla and mandible, skull and facial gland developmental defects [188]. *Foxc1* and *Foxc2* were also shown to play a role in the specification of mesoderm to paraxial fate versus intermediate fate [178, 180, 185, 187, 192], and double null mutants show a lack of paraxial mesoderm patterning and somite formation [180].

### 1.12.3 Foxc1 and Foxc2 - signaling pathways and target gene activation

As for other members of the Fox gene family, little is known about the signaling pathways that interact with FoxC transcription factors downstream in the nucleus and so far, transcriptional target genes of FoxC proteins have lacked profound identification. Recent studies showed that the gene *paraxis* - a presumptive and definite paraxial mesoderm marker - contains several Fox binding sites in its promoter region [192], suggesting a direct regulation of that gene by Fox proteins. *Foxc1* was shown to act as a TGF $\beta$ 1 responsive gene in several human cancer cell lines and mesenchymal cells in *Foxc1* null embryo lack proper differentiation into cartilage and do not respond to added Bmp2 and TGF $\beta$ 1 [187], showing that TGF $\beta$  family members can mediate their function involving members of the FoxC gene family.

Further, *Foxc1* was shown to regulate the proliferation of osteoprogenitor cells by controlling Bmp-driven expression of the homeobox transcription factors *Msx2* during calvarial development [193], and the expression of *Foxc1* in turn was shown to be regulated by FGF2 signaling [194]. Together, the proliferation of osteoprogenitor cells is under strict genetic control of Bmp and Fgf signaling, and *Foxc1* was identified as one of the downstream transcriptional regulators. Lack of activity of the T-box transcription factor *Tbx1*, a downstream target of FoxC proteins in the head mesenchyme, has been accounted for craniofacial defects and FoxC proteins were shown to function as intermediate factors in sonic hedgehog signaling during the transcriptional activation of *Tbx1*, that was identified as the first direct target gene of *Foxc1* and *Foxc2* during development [195]. Haploinsufficiency of *Tbx1* is a major

factor of congenital cardiac and craniofacial defects, which are associated with DiGeorge syndrome, linking *FoxC* genes to that congenital disorder [195].

### **1.13 Aims of the Ph.D. Project**

Because of the involvement of *Foxc1* and *Foxc2* in the development of the cardiovascular system and their induction during *in vitro* eEPC-differentiation, these two transcription factors were considered as interesting candidates to study transcriptional mechanisms during the transition from eEPCs to the mature endothelial cell phenotype. Since little is known about FoxC proteins regarding their direct transcriptional targets as well as the transcriptional regulation of endothelial-specific gene expression, this Ph.D. thesis aimed in identifying new transcriptional targets of *Foxc1* and *Foxc2* in the vascular system, using embryonic EPCs as a cellular model system. The identification of mouse *Pecam-1* as a *Foxc1* target gene and the characterization of a distal 5'-flanking *Foxc1* binding site are described herein. Further, core promoter areas and an enhancer from the 2<sup>nd</sup> intron of mouse *Pecam-1* are characterized for their cis-regulatory activity in eEPCs, mature endothelial cells and non-endothelial lines.

## **2. MATERIAL and METHODS**

### **2.1 Tissue Culture**

#### **2.1.1 Cell lines**

For the Ph.D. Thesis, the mouse embryonic endothelial progenitor cell (eEPC) lines FT4b, T17b, and T19b were used for all procedures. The isolation of eEPCs has been described previously by Hatzopoulos and coworkers [108]. In addition, bovine aortic endothelial cells (BAECs - American Type Culture Collection, Manassas, VA, USA), pancreatic endothelial cells (MS1-ECs - American Type Culture Collection), cardiac endothelial cells (H5V-ECs - kind gift from Bin Zhou, Vanderbilt University, Nashville, TN, USA – described in [196]), CGR8 mouse embryonic stem cells (FunGenES Consortium), NIH mouse 3T3 fibroblasts and green monkey (fibroblast-like) kidney Cos7 cells (American Type Culture Collection) were used for the project. Embryonic EPCs were cultured on coated plates (0.1% porcine skin gelatin - Sigma-Aldrich, St. Louis, MS, USA) to enhance attachment of the cells to the surface, and passaged every 3-4 days onto new plates. BAECs, MS1-ECs, H5V-ECs, Cos7 cells, and 3T3 fibroblasts were cultured on 0.1% gelatin-coated plates and passaged every 5-6 days (or when the cell layer reached a density of around 100%). During growth, the cells were washed with 1X PBS (137 mM NaCl, 2,7 mM KCl, 4.3 mM Na<sub>2</sub>HPO<sub>4</sub>, 1,4 mM KH<sub>2</sub>PO<sub>4</sub>, - Sigma-Aldrich) and supplied with fresh medium if the medium color turned into orange, indicating a pH below 7.5.

ES cells were supplied with fresh medium daily to continuously provide active leukemia inhibitory factor (LIF) and prevent premature differentiation. They were cultured on 0.2% gelatin-coated plates (pre-coated for at least 3 hours) and passaged every 2-3 days (or before growing to a density of more than 70%, since a higher density can induce differentiation and thus cause the loss of pluripotency of the ES cells) onto fresh plates. Tissue culture work was carried out in a sterile tissue culture bank (Clean Air Technik BV, Woerden, The Netherlands and NUAIRE Biological Safety Cabinets, Plymouth, MN, USA) and all cell lineages were incubated at 37°C, 5% CO<sub>2</sub>, 21% O<sub>2</sub> in a CO<sub>2</sub> Water Jacketed Incubator (Thermo Forma, Marietta, OH, USA) and cultured on standard tissue culture plastic plates (NUNC

Brand Products, Nalgen Nunc International, Denmark or Sarstedt Inc., Newton, NC, USA).

### 2.1.2 Tissue culture media

Embryonic EPCs were maintained in DULBECCO'S Minimal Essential Medium (DMEM) (4.5 g/Liter Glucose, Mediatech Inc., Herndon, VA, USA or GIBCO Invitrogen Corporation, Carlsbad, CA, USA) supplemented with 20% heat-inactivated Fetal Bovine Serum (55°C - 30 min, GIBCO Invitrogen), 1x Penicillin/Streptomycin (100x Stock - 10,000 units/ml Penicillin, 10 mg/ml Streptomycin, Mediatech or GIBCO Invitrogen), 2 mM L-Glutamine (Mediatech or GIBCO Invitrogen), 25 mM HEPES pH 7.5 (Mediatech), 1x MEM non-essential amino acids (Mediatech or GIBCO Invitrogen), and 0.1 mM  $\beta$ -Mercaptoethanol (Sigma-Aldrich).

BAECs, MS1-ECs, H5V-ECs, Cos7, and NIH 3T3 fibroblasts were maintained in DMEM (4.5 g/Liter Glucose) supplemented with 10% Fetal Bovine Serum, 1X Penicillin/Streptomycin and 2 mM L-Glutamine.

CGR8 ES cells were maintained in Glasgow Minimal Essential Medium (GMEM, Sigma-Aldrich) supplemented with 10% Fetal Bovine Serum, 2 mM L-Glutamine, 0.05 mM  $\beta$ -Mercaptoethanol, and  $5 \times 10^4$  units Leukemia Inhibitory Factor (LIF, Chemicon Millipore Corporation, Billerica, MA, USA).

Prepared tissue culture media were filter-sterilized using a 0.2  $\mu$ m pore size SFCA Serum Filter Unit (Nalgene Filtration Products, Nalgene Nunc International, Rochester, NY, USA).

### 2.1.3 Passage of cell cultures

The split ratios for cell lines were as follows: FT4b, T17b, and T19b eEPCs - 1:20 for 3-4 days; MS1-ECs - 1:10 for 5-6 days; H5V-ECs - 1:5 for 5-6 days; BAECs - 1:10 for 5-6 days; CGR8 ES cells - 1:5 for 3-4 days; Cos7 cells - 1:10 for 5-6 days; 3T3 fibroblasts - 1:10 for 5-6 days. Before splitting, the cell layer was washed with 5 ml (60 mm plates) or 10 ml (100 mm plates) 1X PBS. To detach cells from plates, the

cell layer was incubated for 10 minutes with 1-2 ml of 0.05% Trypsin-EDTA (GIBCO Invitrogen). Trypsinization was stopped with serum through the addition of the respective growth medium. The cell suspension was then spun at 250 g for 5 min to pellet the cells. The supernatant was removed and cells were resuspended in the corresponding fresh growth medium and plated onto freshly gelatin-coated plates.

#### 2.1.4 Freezing and thawing of cell lines

All cell lines were frozen in 90% FBS and 10% Dimethylsulfoxide (DMSO - Sigma-Aldrich). First,  $1-2 \times 10^6$  cells were washed with 1X PBS, trypsinised, resuspended and then spun down (as described above). The supernatant was removed and the cells were resuspended in 4°C cold FBS. Subsequently, DMSO was added to a final concentration of 10%. One ml of the cell suspension was then pipetted into a cryovial (Nalgene Nunc), stored at -20°C for 2 hours and subsequently transferred to -80°C for 2 days. Finally, the frozen cells were long-term stored in liquid nitrogen (around -196°C). To thaw frozen cell stocks, a cryovial was warmed quickly in a 37°C water bath until the cells were thawed. Immediately after, the cells were gently pipetted onto a 100 mm plate containing 25 ml of pre-warmed (37°C) tissue culture growth medium. Cells were then incubated overnight and washed with 1X PBS the following day and supplied with fresh growth medium for further culturing.

#### 2.1.5 Transfection of cell lines

Transfection is a technique that allows the transfer of nucleic acids into eukaryotic cells. To this end, cell lines were transfected with the reagent Lipofectamine 2000 (Invitrogen Corporation, Carlsbad, CA, USA), according to the manufacturer's instructions. Lipofectamine is a cationic liposome reagent that facilitates the contact and fusion of the negatively charged nucleic acid molecules with the phospholipid cell membrane, which also carries a negative net charge [197]. Upon mixture, the DNA molecule binds to a positively charged head group of the liposome containing nitrogen atoms, that interact with the negative phosphate backbone of the nucleic

acid as well as with the negatively charged cell membrane, thus providing a linker to overcome the electrostatic repulsion between the DNA and the cell membrane. The fusion with the cell membrane is carried out by neutral hydrocarbon chains, that are linked to the positively charged head group in the liposomes. After fusion, the nucleic acid-liposome complex penetrates the cell and is also carried into the core by merging with the nuclear membrane, thus exposing the DNA to nuclear proteins, allowing efficient transcription of e.g. genes cloned into expression plasmids. Nucleic acids can eventually integrate into the host genome, resulting into genetically engineered stable cell lines.

In this project, transfection was carried out using a 2-fold excess of  $\mu\text{g}$  Lipofecatiome 2000 compared to  $\mu\text{g}$  of plasmid DNA. E.g., for transfection of a 60 mm cell culture plate (about  $3\text{-}5 \times 10^6$  cells), 8  $\mu\text{g}$  of plasmid DNA was dissolved in 1 ml of OPTIMEM medium (Invitrogen), i.e. a modified minimal essential medium (MEM) that only contains minimal protein levels (insulin and transferrin at 15  $\mu\text{g}/\text{ml}$ ), but has a formulation that allows cells to survive under serum-deprived conditions for several hours. Transfections have to be carried out in a low-serum environment, since serum lipoproteins can interfere with the liposomes. Next to the DNA/OPTIMEM mix, a second mixture containing 1 ml OPTIMEM and 16  $\mu\text{g}$  of Lipofectamine 2000 (liposomes) was set up and incubated for 5 min at room temperature before both mixtures were combined by gentle mixing and incubated for 30 min at room temperature. Finally, the combined mixture was given onto the cells and incubated for 6 hours at  $37^\circ\text{C}$ , followed by addition of 5 ml of regular growth medium to the plate. The cells were then grown further for 24 hours before they were used for downstream applications.

## **2.2 Molecular biology techniques**

### **2.2.1 Total RNA isolation**

The RNA isolation procedure was carried out using the QIAGEN RNeasy<sup>®</sup> Kit (QIAGEN Corporation, Valencia, CA, USA), which is based on a silica-gel membrane system that binds RNA molecules with a length of more than 200bp (RNeasy<sup>®</sup> Mini Handbook, QIAGEN). Cell lysis occurs in the presence of the denaturing agent



isothiocyanate, which also inactivates RNases, thus preventing an enzymatic degradation of RNA. The purification step is based on the highly specific binding of larger RNA molecules, such as mRNA to the membrane, whereas smaller RNAs, e.g. tRNA, are efficiently washed away, together with other contaminants. The binding of RNA is also enhanced by the presence of ethanol. After binding and washing with ethanol-containing washing buffers, the bound RNA is eluted with H<sub>2</sub>O and can be used for further processing.

Generally, for RNA isolation, cell monolayers on plates (around  $5 \times 10^6$  cells) were lysed in 700  $\mu$ l RLT Lysis buffer (RNeasy Kit). DNA digestion (with RNase-Free DNase Set, QIAGEN) was performed to avoid contamination of isolated RNA with genomic DNA. The RNA was eluted in 40-50  $\mu$ l RNase-free water (QIAGEN) and stored at -80°C for future use. RNA concentrations were measured at an OD<sub>260</sub> using an Eppendorf BioPhotometer (Eppendorf Corporation, Hamburg, Germany).

### 2.2.2 Reverse Transcriptase-Polymerase Chain Reaction (RT-PCR)

RT-PCR is a technique to measure expression levels of gene transcripts. In a first step, cDNA is synthesized by Reverse Transcription (RT) using RNA as a template. The molecular reaction is carried out by enzymes called reverse transcriptases, which are RNA-dependant DNA polymerases derived from retroviruses such as the moloney murine leukemia virus [198]. Single-stranded RNA is thereby transcribed into complementary DNA (cDNA), using specific deoxyoligonucleotides, such as oligo(dT), as primers for the enzymatic reaction. The derived single-strand cDNA subsequently serves as template for amplification by Polymerase Chain Reaction (PCR).

The steps for RT-PCR were carried out in an Eppendorf Thermomixer (Eppendorf Corporation) in 1.5 ml tubes. First, 3  $\mu$ g of RNA were added to autoclaved ddH<sub>2</sub>O to a total volume of 15  $\mu$ l. Then, 3,75  $\mu$ l of 80 ng/ $\mu$ l oligo(dT)<sub>15</sub> primer (Promega Corporation, Madison, WI, USA) were added to the mixture. The tubes were incubated at 65°C for 5 min to open up secondary RNA structures and allow the primers to bind to the polyA tails of mRNA molecules. Afterwards, the tubes were put

on ice immediately to avoid refolding of the RNA. Then 11,25 µl of RT-Mix was added to the tubes. RT-Mix contained:

4,5 µl NX buffer (0.4 M KCl, 0.1 M Tris-HCl pH 8,4, 20 mM MgCl<sub>2</sub>, 2% Tween20, all from Sigma-Aldrich), 1.5 µl dNTPs (20mM stock - Amersham Biosciences Piscataway, NJ, USA), 3 µl of 0.1 M β-mercaptoethanol (Sigma-Aldrich), 10 U RNasin (40 U/µl - Promega), 100 units M-MLV Reverse Transcriptase (200 U/µl - Invitrogen). The entire mixture was incubated at 37°C for 55 min, followed by a second incubation step at 95°C for 5 min to inactivate the enzyme and stop further reaction. Finally, 270 µl autoclaved ddH<sub>2</sub>O was added to the reaction to obtain a final cDNA volume of 300 µl at a concentration of about 10 ng/µl. The cDNA was then stored at -20°C for future use.

### 2.2.3 Polymerase Chain Reaction (PCR)

Polymerase Chain Reaction (PCR) is a powerful technique that allows the exponential *in vitro* amplification of a specific region of a template DNA strand [199]. In typical applications, DNA fragments up to the size of 10 kb are amplified. A PCR reaction is divided into cycles that consist of three steps, i.e. (1) denaturation of the DNA double helix at around 95°C; (2) primer annealing between 55-65°C; (3) elongation of the polymerase reaction at 72°C. The cycles are preceded by a denaturation step at around 95°C for several minutes to assure proper opening of the DNA double helix. At the end of the cyclic program, a 5-7 min elongation step is performed before the enzymatic reaction is stopped. The thermostable Taq DNA polymerase from the hot springs thermophilic bacterium *Thermus aquaticus* resists the high denaturation temperatures, thus allowing the reaction to be performed without the requirement to add fresh enzyme during each thermocyclic amplification. PCR amplification was carried out using 20 ng cDNA as template derived from RT-PCR reactions. Oligodeoxynucleotide primer pairs (2 µl) were added to a final concentration of 0.5 µM, together with 0.2 µl deoxynucleotide 5'-triphosphate (dNTP) mix (20 mM of each dNTP – Amersham Biosciences), 2 µl of 10X PCR reaction buffer (0.1 M Tris-HCl pH 8.4, 0.5 M KCl, 15 mM MgCl<sub>2</sub>, all from Sigma-Aldrich), 1 µl DMSO (Sigma-Aldrich) and 1 U Taq DNA polymerase (Promega). The reaction mixture was filled up with ddH<sub>2</sub>O to 20 µl and amplified with a MJ Research PTC-100

Thermo Cycler (Bio-Rad Laboratories, Hercules, CA, USA). The primer sequences and their corresponding thermocyclic program were as follows: *Aldolase* forward 5'-AGCTGTCTGACATCGCTCACCG-3', reverse 5'-CACATACTGGCAGCGCTTCAAG-3' (24 cycles – 65°C annealing); *Pecam-1* forward 5'-G TTCAGCGAGATCCTGAGGGT-3' (35 cycles – 60°C annealing), reverse 5'-GAGGACACTTCCACTTCTGTGTATTC-3'; *Foxc1* forward 5'-GCAGTGAAGGACAAGGAGGAGAAG-3', reverse 5'-TGGAGGCAGCGAGTAGTCGG-3' (35 cycles – 65°C annealing); *Foxc2* forward 5'-CTCTTACGACTGCACCAAATACTG-3', reverse 5'-GAATCTCCACAGAAGTCATTAGGG-3' (35 cycles – 65°C annealing); *Foxa2* forward 5'-AGGAGTGTACTCCAGGCCTATTATG-3', reverse 5'-GTCCGGTACACCAGACTCTTACAT-3' (35 cycles – 60°C annealing). Shown are the sequences for the primarily used RT-PCR primers. A complete list of all primers used in RT-PCR is given in the supplemental file 'primer\_sequences.pdf'.

#### 2.2.4 PCR Primer Design

Primers were designed using the online primer3 tool ([http://fokker.wi.mit.edu/cgi-bin/primer3/primer3\\_www.cgi](http://fokker.wi.mit.edu/cgi-bin/primer3/primer3_www.cgi)). This program allows optimal design of oligonucleotides for PCR by selecting a large number of criteria that specify the working conditions of the primer. Primers were designed to contain the following criteria: an annealing temperature between 60-65°C, a length between 20-25 bp; a PCR amplification product of variable length between 150-800 bp. For cDNA amplification and gene expression studies, if possible, primers were designed to bind in areas representing different exons of the transcript, such enabling the distinction between amplified cDNA and possible impurities of genomic DNA that would also serve as template. Primers were ordered from MWG Biotech (Ebersberg, Germany) or Integrated DNA Technologies (Coralville, IA, USA).

#### 2.2.5 DNA Sequencing

To date, the chain-termination method developed by Frederick Sanger is the standard choice for the sequencing of DNA. The principle of this enzymatic reaction

is based on the use of dideoxynucleotide triphosphates (ddNTPs) that function as nucleic acid chain terminators [200]. The original described method uses single-stranded DNA to be sequenced as template. Modern protocols also use double-stranded DNA that has been denaturated using e.g. alkali, as template. A special DNA polymerase, e.g. E.coli DNA polymerase I, initiates the synthesis of a complementary strand, starting from an oligodeoxynucleotide primer that binds at the 3'-end of the template DNA strand. The key of the reaction lies in the separation into four separate sequencing reactions, that all contain the standard deoxynucleotides, i.e. dATP, dCTP, dGTP, dTTP. In addition, each reaction contains one of four dideoxynucleotides (ddATP, ddCTP, ddGTP, ddTTP), that lack the 3'-OH group required for the enzymatic formation of the phosphodiester bond between two nucleotides during the polymerization of the DNA strand. Thus, the incorporation of a dideoxynucleotide into the elongating DNA strand causes the termination of the polymerization reaction and yields multiple DNA fragments of various, random lengths. The elongated DNA fragments are then separated according to their length by gel electrophoresis using denaturing polyacrylamid gels, and each of the four separate sequencing reactions (containing one of the four ddNTPs) is run in an individual lane. The DNA molecules are visualized through the use of e.g. fluorescence-labeled oligodeoxynucleotide primers during the polymerization reaction. The terminal nucleotide base on the template strand is similar to the dideoxynucleotide used in the individual sequencing reaction and the relative positions of the DNA bands in the gel are used to assemble the nucleotide sequence of the template DNA strand. Modern automated DNA sequencers use a single reaction with all four dideoxy terminator nucleotides at the same time, and with different fluorescent colors on each of them, usually red, green, blue and yellow. The resulting fragments are subsequently separated by electrophoresis, and an ultraviolet laser determines the color of the DNA molecules. The complete sequence is then automatically assembled by the computer. In this project, DNA sequencing of plasmid DNA and PCR amplification products was carried out by commercial sequencing centers (MWG Biotech, Ebersberg, Germany and Genhunter Corporation, Nashville, TN, USA).

### 2.2.6 Plasmid DNA preparation

For high amount preparations, plasmid DNA was purified using the commercially available DNA Maxi Prep Kit from QIAGEN. Plasmids were isolated from E.coli DH5 $\alpha$  cultures grown in LB culture medium (10 g Tryptone, 5 g Yeast extract, 10 g NaCl, all from Sigma-Aldrich, - filled up with ddH<sub>2</sub>O to 1 liter). Bacteria cultures were grown for 12-14 hours (OD<sub>600</sub> of about 4.0) at 37°C under shaking (225 rpm) in the presence of the appropriate selective antibiotics (100  $\mu$ g/ml Ampicillin, or 50  $\mu$ g/ml Kanamycin – Sigma-Aldrich), based on the antibiotic resistance gene on the plasmid backbone. Overnight cultures for plasmid DNA Maxi Preps (100 ml total volume) were inoculated from frozen DH5 $\alpha$  15%-glycerol stocks (850  $\mu$ l E.coli suspension, 150  $\mu$ l glycerol – Sigma-Aldrich) containing the respective plasmid. The stocks were kept at -80°C for long-term storage. Alternatively, Maxi Prep cultures were inoculated with 200  $\mu$ l E.coli starter culture that was grown in LB medium for 8-9 hours from a single agar plate colony. After growth, E.coli Maxi Prep cultures were centrifuged for 20 min at 3000 g and 4°C to pellet the cells, and then subjected to plasmid isolation.

In the Maxi Prep, the plasmid DNA is purified through binding to an anion-exchange resin column, under low-salt and low-pH conditions. Lysis of bacteria is based on the alkaline lysis method of Birnboim and Doly, involving a NaOH/SDS (sodium dodecyl sulfate) buffer [201]. Subsequent purification involves the removal of RNA -that is fragmented by RNase digestion during the bacteria pellet resuspension - and other low-weight molecules through washing steps with medium-salt buffers (QIAGEN), that in turn allows the plasmid DNA to remain bound to the anion-exchange matrix. In a step that precedes the medium-salt buffer washes, the alkaline lysis is neutralized by potassium acetate, resulting into the precipitation of cell membrane bound genomic DNA, proteins and larger cellular debris.

After washing, elution of plasmid DNA from the column is facilitated by high-salt buffers (QIAGEN), followed by isopropanol precipitation, resulting into pure pelleted plasmid DNA that is re-dissolved in TE buffer (10 mM Tris-HCl pH 8.0, 1 mM EDTA – Sigma-Aldrich) and stored at -20°C for future use.

In accordance, Mini-Prep plasmid DNA purification during cloning procedures was carried out with the QIAprep Spin Miniprep Kit (QIAGEN), and cell lysis as well as plasmid DNA purification is based on analogous steps as described for the Maxi-Prep plasmid DNA purification (QIAprep Spin Miniprep Kit Handbook). E.coli cultures

for Mini Preps were inoculated by picking single colonies from freshly streaked LB agar plates (as described below), followed by growth for 12-14 hours at 37°C and 225 rpm shaking.

The optical density (OD) of E.coli suspensions was measured at a wavelength of 600 nm (OD<sub>600</sub>) using an Eppendorf BioPhotometer (Eppendorf Corporation).

### 2.2.7 Transformation of CaCl<sub>2</sub>-competent DH5α E.coli

Through transformation, foreign DNA can be introduced into bacteria cells that were rendered competent by exposure to calcium ions [202]. Uptake of plasmid DNA occurs during a heat-shock that enables the nucleic acid to efficiently penetrate the cells. To generate calcium competent E.coli cells, LB growth medium (200 ml) was inoculated with 3 ml of a DH5α overnight starter culture and grown to an OD<sub>600</sub> of 0.4 (early to mid-log phase) at 37°C, followed by a cooling step for 15 min on ice. The cells were pelleted by centrifugation (3000 g, 10 min, 4°C) and the pellet was resuspended in 80 ml of Tfb1 buffer (pH 5.8 - 30 mM KOAc, 100 mM RbCl<sub>2</sub>, 10 mM CaCl<sub>2</sub>, 50 mM MnCl<sub>2</sub>, 15 % Glycerin, all from Sigma-Aldrich) and incubated for 15 min on ice, followed by centrifugation. The pellet was then resuspended in 8 ml of TfbII buffer (pH 6.5 - 10 mM MOPS, 75 mM CaCl<sub>2</sub>, 10 mM RbCl<sub>2</sub>, 15% Glycerin), followed by another incubation step for 15 min on ice. The suspension was aliquoted (50 µl) into prechilled 1.5 ml tubes and frozen immediately at -80°C for future transformations.

Transformations were carried out with 50 µl aliquots of competent DH5α E.coli cells. In brief, the cells were thawed on ice and 0.1-0.5 µg of plasmid DNA was added to the thawed cell suspension, followed by an incubation step for 30 min on ice. E.coli cells were then heat-shocked at 42°C for 45 sec, followed by an immediate incubation on ice for 2 min. To grow, 900 µl of non-selective LB growth medium was added and the E.coli cells were incubated at 37°C for 1 hour under shaking (1200 rpm) to recover and to allow transcription and synthesis of antibiotic-resistance genes. Subsequently, 100 µl of the suspension was plated onto LB agar plates (2% agar, Sigma-Aldrich) containing the appropriate selective antibiotics (100 µg/ml Ampicillin or 50 µg/ml Kanamycin). The agar plates were grown inverted at 37°C for 12-14 hours and then checked for the presence of colonies.

### 2.2.8 DNA restriction digests

DNA restriction endonucleases (or restriction enzymes) are procaryotic enzymes that catalyze specific reactions on the DNA in a sequence-specific manner and protect the bacteria host cell from viral infections by degrading viral DNA [203]. Their discovery has marked a revolutionary change in molecular biology, and today, their use to cleave DNA at defined positions into specific fragments is one of the most common procedures in molecular biology and genetic engineering. The majority of restriction endonucleases used in molecular biology applications belong to the type II and most members of this type II recognize a short nucleotide sequence (4-6 nucleotides in length) on the DNA and cleave the double helix within the recognized sequence. The recognition sequence is mostly palindromic, i.e. the sequence on one DNA strand is the same in 5' to 3' direction as on the complementary strand. Different restriction endonucleases that recognize the same target sequence are referred to as isoschizomers. Other type II restriction endonucleases cleave the DNA outside of their recognition sequence on one side. The cleavage of the double helix results into 3'-hydroxyl on one side and a 5'-phosphate residue on the other side of the cut and some restriction endonucleases leave blunt ends after cleaving, whereas others cleave the double helix in a staggered manner, yielding cohesive ends with single-stranded 5' or 3' overhangs.

All restriction endonucleases were from NEB (New England Biolabs Incorporation, Ipswich, MA, USA) and were used according to the manufacturer's instructions. In general, restriction digests in this project were set up in a total volume of 20-50  $\mu$ l. The mixture contained purified template DNA dissolved in ddH<sub>2</sub>O or TE buffer, together with 5  $\mu$ l of the appropriate 10X enzyme buffer (containing MgCl<sub>2</sub> - NEB), 0.5  $\mu$ l of 100X bovine serum albumine solution (10 mg/ml - NEB) and an 5-fold excess of restriction enzyme units compared to  $\mu$ g of DNA (with enzyme volume not exceeding 10% of the total reaction volume). Reaction mixtures were incubated for 1 hour or longer at 37°C or the appropriate temperature for certain restriction endonucleases, according to the manufacturer's instructions.

### 2.2.9 DNA ligation

Whereas restriction endonucleases cleave the double helix, DNA ligases catalyze the ligation of two blunt- or cohesive-end DNA fragments through the formation of phosphodiester bonds between adjacent 5'-phosphate and 3'-hydroxyl termini in the double helix. Commonly, T4 DNA ligase – a product of the bacteriophage T4 - is used for molecular biology applications and catalyzes the formation of phosphodiester bonds by use of ATP as cofactor [204].

DNA ligation was carried out according to the manufacturer's instruction (NEB). Typically, the enzymatic reaction had a total volume of 20  $\mu$ l, containing 2  $\mu$ l of 10X enzyme buffer (0.5 M Tris-HCl pH 7.5, 0.1 M MgCl<sub>2</sub>, 10 mM ATP, 250  $\mu$ g/ml BSA - NEB), and 400 U of T4 DNA ligase (NEB). Ligation was carried out at 16°C for 12 hours, with a 10-fold molar excess of DNA insert fragment compared to plasmid DNA backbone to assure a high efficiency of insertion.

### 2.2.10 Plasmid Constructs

Foxc1, Foxc2 and Foxa2 expression plasmids (CMV-Foxc1, CMV-Foxc2, and CMV-Foxa2) are based on the pcDNA3 backbone (Invitrogen) and were kindly provided by Tom Kume (Vanderbilt University). The cloned cDNA sequences were as follows: Foxc1, +415 to +2779 based on ENSEMBL Genome Browser Transcript ID ENSMUST00000062292; Foxc2, +373 to +2704 based on Ensembl Genome Browser Transcript ID ENSMUST00000054691; Foxa2, +112 to +1970 based on Ensembl Genome Browser Transcript ID ENSMUST00000047315 (<http://www.ensembl.org>).

*Pecam-1* promoter-luciferase plasmids pGL2-mp (minimal promoter), pGL2-lpp, (long proximal promoter), pGL2-5'3.5kb/mp (distal 5'-flanking 3.5kb fragment and minimal promoter), and pGL2-l2-4.5kb/mp (2<sup>nd</sup> intron 4.5kb fragment and minimal promoter) were kindly provided by Dr. Scott Baldwin (Vanderbilt University – further description in RESULTS). The cloned genomic sequences (relative and absolute nucleotide numbers) were as follows: plasmid pGL2-mp - relative -88 to +57 / absolute 106,531,458 to 106,531,315; plasmid pGL2-lpp - relative -280 to +57 / absolute 106,531,651 to 106,531,315; plasmid pGL2-5'3.5kb/mp – relative -13,597 to -10,063



/ absolute 106,544,967 to 106,541,433 (distal 5'-flanking 3.5kb fragment); plasmid pGL2-I2-4.5kb/mp -relative +5,849 to +10,273 / absolute 106,525,521 - 106,521,098 (2<sup>nd</sup> intron 4.5kb fragment). For all promoter-luciferase plasmids, the relative nucleotide numbers refer to the transcription initiation site of mouse *Pecam-1*. Absolute nucleotide numbering was obtained from the UCSC Bioinformatics Database, with the transcription initiation site at nucleotide position 106,531,371 on chromosome 11 (descending nucleotide numbers).

Promoter-Luciferase-plasmids pGL2-5'1kb(A)/mp (distal 5'-flanking 1kb fragment and minimal promoter), pGL2-5'1kb(B)/mp (distal 5'-flanking 1kb fragment and minimal promoter), and pGL2-5'1.5kb/mp (distal 5'-flanking 1.5kb fragment and minimal promoter) were generated by PCR using pGL2-5'3.5kb/mp as DNA template. The PCR reaction contained 100 ng template DNA, 5 µl 10X Pfu buffer (Promega), 0.5 µl dNTPs (20 mM each dNTP – Amersham Biosciences), 2 µl primer mix (5 µM each primer), and 2 U *Pfu* Polymerase (Promega), all filled up with H<sub>2</sub>O to 50 µl. *Pfu* Polymerase is a DNA polymerase that has 3' to 5' exonuclease activity (proofreading), thus resulting into high fidelity amplification of the DNA template. Amplification was carried out as follows: initial denaturation (95°C – 2 min), 35 cycles (95°C – 30 sec, 60°C – 30 sec, 74°C – 2 min), final elongation (74°C – 5 min).

The cloned genomic sequences were as follows: plasmid pGL2-5'1kb(A)/mp– relative -13,597 to -12,547 / absolute 106,544,967 - 106,543,917 (distal 5'-flanking 1kb fragment); plasmid pGL2-5'1kb(B)/mp - relative -12,568 to -11,499 / absolute 106,543,939 - 106,542,870 (distal 5'-flanking 1kb fragment); pGL2-5'1.5kb/mp – relative -11,520 to -10,063 / absolute 106,542,891 – 106,541,433 (distal 5'-flanking 1.5kb fragment).

The primers were as follows: plasmid pGL2-5'1kb(A)/mp forward 5'-ggggtaccGAGCTCATGGTTTGGTTTCT-3', reverse 5'-cgacgcgtCACTTATAGTAAAACACCTG-3'; pGL2-5'1kb(B)/mp forward 5'-ggggtaccCAGGTGGTTTTACTATAAGTG-3', reverse 5'-cgacgcgtGTCAGTGTCCTGACTGATG-3'; pGL2-5'1.5kb/mp forward 5'-ggggtaccCATCAGTCAGGGACACTGAC-3', reverse 5'-cgacgcgtGAGCTCTCCTGAGCGTGAAG-3'; lower-case nucleotides indicate restriction sites added for cloning purposes. Fragments were cloned into pGL2-mp using *KpnI* (in the forward primer) and *MluI* (in the reverse primer).

Mutated promoter-luciferase-plasmids pGL2-5'1.5kbD1/mp, pGL2-5'1.5kbD2/mp, pGL2-5'1.5kbD3/mp, and pGL2-5'1.5kbD4/mp were generated by *in vitro* site-directed mutagenesis, using the QuikChange<sup>®</sup> II Site-Directed Mutagenesis Kit (Stratagene Corporation, La Jolla, CA, USA) and pGL2-5'1.5kb/mp as DNA template. Site-directed mutagenesis is a technique to selectively manipulate a nucleotide sequence by creating a mutation at a defined site on a DNA molecule [205]. Whereas conventional mutagenesis protocols require the presence of single-stranded DNA as template, the method used in this project allows to directly mutate supercoiled double-stranded plasmid DNA. The key of this technique lies in the use of two complementary oligodeoxynucleotide primers, that both carry the desired mutation and anneal to the same sequence on the opposite strands of the template plasmid DNA. The mutations in the primers can consist of single nucleotide point mutations or even larger insertions or deletions. In case of a deletion to be inserted into the plasmid, the primers consist of two “nucleotide arms” (around 20 bp in length) that represent the sequence on either side of the deletion. During amplification, the parental plasmid DNA forms a loop between the two “nucleotide arms” and is not integrated into the newly polymerized DNA, thus resulting into a deletion that is carried on during the amplification.

The protocols were according to the manufacturer's instructions (Stratagene). In brief, the template plasmid DNA was amplified by PCR consisting of an initial denaturation step (95°C - 1 min), 18 cycles (95°C - 50 sec; 60°C - 50 sec; 68°C - 7.5 min), and a final elongation step (68°C – 7 min). The PCR mixture contained 5 µl of 10X reaction buffer (Stratagene), 50 ng of template DNA, 125 ng of 5'- and 3'-PCR primer (described below), 1 µl of 20 mM dNTP Mix (Amersham Biosciences), 3 µl of QuickSolution (Stratagene), filled up with H<sub>2</sub>O to 50 µl total. PfuUltra HF DNA polymerase (2.5 U - Stratagene) was then added to the mixture and following amplification, the samples were cooled down on ice and incubated with 10 U/µl *DpnI* (Stratagene) for 1 hour at 37°C. *DpnI* is a restriction endonuclease that requires the presence of N<sup>6</sup>-methyladenine within its recognition sequence (5'-Gm<sup>6</sup>ATC-3') to cleave DNA [206]. Thus, it specifically digests the methylated parental DNA (pGL2-5'1.5kb/mp) derived from E.coli Maxi Preps but has no affinity for non-methylated DNA, which is generated during the mutagenesis PCR reaction. An aliquot of 45 µl

XL10-Gold competent *E. coli* cells (Stratagene) was incubated with 2  $\mu$ l  $\beta$ -Mercaptoethanol (Stratagene) for 10 min on ice and subsequently 2  $\mu$ l of the *DpnI*-treated DNA was added to the mixture, followed by 30 min incubation on ice and a 30 sec heat-shock at 42°C. After another 2 min incubation on ice, 500  $\mu$ l of NZY<sup>+</sup> broth (10 g NZ amine, 5 g yeast extract, 5 g NaCl, 12.5 ml 1 M MgCl<sub>2</sub>, 12.5 ml 1 M MgSO<sub>4</sub>, 10 ml 2 M glucose – ddH<sub>2</sub>O to 1 liter) was added and the cells were grown for 1 hour at 37°C under shaking (225 rpm), followed by plating on LB-agar plates (2% agar - 100  $\mu$ g/ml ampicillin) and grown until colonies were visible. Colonies were picked, grown in LB-medium, and subjected to plasmid DNA Mini Preps and DNA sequencing to check for the presence of the deletion.

Primers used for the individual deletions were as follows: plasmid pGL2-5'1.5kbD1/mp (deletion relative -11,495 to -11020; deletion absolute 106,542,865 to 106,542,390) 5'-caggacactgactttgCCTAGGATGGGCACC-3' and 5'-GGTGCCCATCCTAGGcaaagtcagtgtccctg-3'; plasmid pGL2-5'1.5kbD2/mp (deletion relative -11,495 to -10,884; deletion absolute 106,542,865 to 106,542,254) 5'-cagtcagggacactgactttgGTTTGTTAAATGTTC-3' and 5'-GAACATTTAACAAACcaaagtcagtgtccctgactg-3'; plasmid pGL2-5'1.5kbD3/mp (deletion relative -11,495 to -10,741; deletion absolute 106,542,865 to 106,542,111) 5'-cagggacactgactttgGTTAGTTAAATGTTCCC-3' and 5'-GGGAACATTTAACTAACcaaagtcagtgtccctg-3' ; plasmid pGL2-5'1.5kbD4/mp (deletion relative -11,495 to -10,458; deletion absolute 106,542,865 to 106,541,828) 5'-cagggacactgactttgGGTCTGATCCTCCTG-3' and 5'-CAGGAGGATCAGACCcaaagtcagtgtccctg-3'. The nucleotides in lower case letters indicate the "primer-arm" on one side of the deletion, whereas the upper-case letters indicate the "primer-arm" on the other side.

The complete sequences of the cloned promoter and cDNA inserts are given in the supplemental file 'plasmid\_sequences.pdf'.

### 2.2.11 Agarose gel electrophoresis

Agarose is a gelatinous polymer isolated from red algae and its use in agarose gel electrophoresis is an effective technique for the separation of nucleic acid fragments

of different sizes. During electrophoresis, the negatively charged nucleic acid molecules migrate toward the positive electrode of the electrophoresis unit and are separated according to their size, with smaller fragments migrating faster through the polymerized gel [207].

DNA amplification products from conventional PCR and LightCycler runs were separated in 1.5% agarose gels (ultraPURE agarose, Invitrogen), run in horizontal electrophoresis chambers (Bio-Rad Laboratories, Hercules, CA, USA) in 1X TBE electrophoresis buffer (0.089 M Tris-borate, 2 mM EDTA, 0.02% ethidium bromide - Sigma-Aldrich). The size of DNA fragments was determined using a 100 basepair ladder (Amersham Biosciences), which contains DNA fragments of known size, as molecular marker. After electrophoresis, the DNA bands were visualized under UV light at a wavelength of 254 nm and agarose gels were then photographed using a Polaroid camera or a Bio-Rad Gel Documentation system (Bio-Rad).

#### 2.2.12 Ethanol Precipitation of DNA

DNA was purified by Ethanol precipitation. For this purpose, sodium acetate pH 5.2 (Sigma-Aldrich) was added to a total volume of 10% to the DNA solution, together with 2 volumes of ice-cold 100% Ethanol and mixed thoroughly. Next, the mixture was incubated for 30 min at -20°C to precipitate the DNA and subsequently centrifuged at 15.000 g for 10 min. The DNA pellet was washed twice with ice-cold 70% ethanol, each time followed by a 5 min centrifugation step at 15.000 g. Following, the pellet was air-dried for 5 min at room temperature and subsequently dissolved in 20-30 µl ddH<sub>2</sub>O or TE buffer.

### **2.3 Quantitative Real-Time Amplification (qPCR)**

#### 2.3.1 LightCycler Real-Time PCR System

Embryonic EPC chromatin for chromatin immunoprecipitation (ChIP) analysis was amplified taking advantage of the Roche Advanced LightCycler<sup>®</sup> System (Roche

Diagnostics) using the LightCycler FastStart DNA Master SYBR Green I Kit and LightCycler glass capillaries as reaction vessel. The LightCycler System is a powerful tool that allows monitoring real-time amplification of reverse transcribed mRNA [208]. Compared with conventional PCR, real-time amplification is much more sensitive, since the amount of PCR amplicons is continuously monitored during every amplification cycle, allowing accurate quantification of PCR products. Furthermore, no agarose gels, which lack sensitivity, are necessary for quantification. A real-time PCR system is based upon the detection and quantification of a fluorescent reporter dye, e.g. SYBR Green I [209]. This dye is incorporated into the double stranded DNA helix and, upon intercalation, emits green fluorescence at a wavelength of 530 nm. Since unbound dye only emits minimal background fluorescence, the increased signal is in direct proportion to the amount of doubled-stranded PCR product in a reaction. In addition, the LightCycler System takes advantage of a thermostable recombinant Taq Polymerase, that does not display any activity below 75°C and allows to perform a hot-start PCR reaction, that avoids the creation of unspecific PCR amplification products.

The concentration of cDNA can be determined relatively to a standard curve. As an example, a cDNA pool that is known to contain a certain transcript was amplified with the respective primer pair at a high cycle number and at different temperatures to find optimal primer working conditions. Subsequently, 10 µl of amplified cDNA was taken out from every capillary and run on an agarose gel to verify the proper length of the amplification product and thus the specificity of the amplification reaction. In addition, a melting curve calculated by the LightCycler Software 3.0 (Roche Diagnostics) indicates the purity and specificity of the amplification as monitored in real-time. During melting curve analysis, the PCR reaction is slowly but continuously heated to 95°C, resulting into denaturation of the DNA double helix and decrease of the SYBR Green I fluorescence signal. The decrease in activity from the bound SYBR Green of each PCR amplicon is presented as a melting curve, and the presence of a single peak indicates the specific amplification of the desired PCR product, alongside with a specific band in an agarose gel. In turn, non-specific amplicons and primer dimers are indicated by multiple peaks in the melting curve analysis.

Amplified cDNA that shows the right length and a proper melting curve without minor peaks was then used for a dilution series. For this, 1:10<sup>3</sup> and 1:10<sup>5</sup> dilutions of amplified cDNA are prepared with RS2 RNA as carrier (Roche Diagnostics GmbH,

Mannheim, Germany) and 1:10<sup>7</sup> and 1:10<sup>9</sup> dilutions are prepared in autoclaved ddH<sub>2</sub>O. Carrier RNA avoids the adhesion of template cDNA to the wall of the reaction capillary, thus assuring a higher quality of the analysis. During the main amplification of all cDNA samples with a certain primer pair, the corresponding dilutions are re-amplified and their concentrations are set to a relative value in the LightCycler software before the amplification. E.g., the 10<sup>3</sup> dilution can be set to a value of 10<sup>6</sup>, the 10<sup>5</sup> dilution to a value of 10<sup>4</sup>, the 10<sup>7</sup> dilution to a value of 10<sup>2</sup> and the 10<sup>9</sup> dilution to a value of 1. On the basis of these four relative values, a standard curve is calculated by the LightCycler software and the relative cDNA concentrations from all samples are then referenced by the software to these standard curves.

### 2.3.2 iQ5 Real-Time PCR System

Real-time quantification of gene transcript levels was also carried out using the Bio-Rad iQ<sup>TM</sup>5 Real-Time PCR system and the iQ<sup>TM</sup> SYBR<sup>®</sup> Green Supermix (Bio-Rad Laboratories, Hercules, CA, USA). Like the LightCycler, this system as well uses the fluorescent dye SYBR green I and the key of the real-time quantification method is the same as the one described above for the LightCycler system.

In brief, 1 µl of cDNA was combined with 2 µl primer mix (5 µM each), 7 µl ddH<sub>2</sub>O and 10 µl iQ<sup>TM</sup> SYBR<sup>®</sup> Green Supermix (2X – containing 100 mM KCl, 40 mM Tris-HCl pH 8.4, 0.4 mM dNTPs, 50 U/ml iTaq Polymerase, 6 mM MgCl<sub>2</sub>, SYBR Green I, 20 nM fluorescein) to obtain a whole reaction volume of 20 µl. The quantitative real-time PCR (qPCR) reactions were carried out in 96-well twin.tec PCR plates (Eppendorf).

The relative gene expression levels obtained with the iQ5 qPCR system were calculated using the  $2^{-\Delta\Delta C_T}$  method [210]. In brief, the method is a way to calculate the relative amount of a gene transcript in a given sample as well as relative changes in gene expression without the need to create a standard curve. The amount of cDNA (mRNA) added to the reaction is normalized to an endogenous reference (internal control gene), typically a housekeeping gene such as *β-actin*, *Gapdh*, or *rRNA*. In addition, the transcript levels are presented as fold-change relative to an untreated control sample, also called the calibrator, which is arbitrarily chosen for each qPCR reaction. The C<sub>T</sub> value indicates the threshold cycle during the PCR reaction, i.e. the

number of cycles at which the target sequence is present as a certain copy number and reached a fixed threshold. The data analysis is based on the equation:

$$\Delta\Delta C_T = (C_{T, sample} - C_{T, internal-control})_{time/sampleX} - (C_{T, sample} - C_{T, internal-control})_{time/sample0}$$

The first part of the equation calculates the  $\Delta C_T$  value of a treated sample or a sample at a specific experimental time point by subtracting the corresponding  $C_T$  value of the internal control gene (i.e. *Gapdh*) from the  $C_T$  value of the specific gene of interest, giving  $\Delta C_{T, time/sampleX}$ . The second part of the equation gives the  $\Delta C_T$  value of the calibrator sample, e.g. an untreated control sample or a sample at time point zero in an experiment, giving  $\Delta C_{T, time/sample0}$ . The  $\Delta\Delta C_T$  value is obtained by subtracting  $\Delta C_{T, time/sample0}$  from  $\Delta C_{T, time/sampleX}$ . The amount of target gene transcript is then given by the term  $2^{-\Delta\Delta C_T}$ .

The  $2^{-\Delta\Delta C_T}$  value of the untreated control sample (calibrator) is 1, since  $\Delta\Delta C_T$  for the calibrator sample is 0 and  $2^0$  equals 1. All other samples are calculated relative to the arbitrary value of the untreated control sample. A detailed description of the mathematical derivation of the  $2^{-\Delta\Delta C_T}$  method and further applications have been described by Livak & Schmittgen [210].

The cDNA was amplified using the following primers: *β-actin* forward 5'-CTACGAGGGCTATGCTCTCCC-3', reverse 5'-CCGACTCATCGTACTCCTGC-3'; *Gapdh* forward 5'-CTCACTCAAGATTGTCAGCAATG-3', reverse 5'-GAGGGAGATGCTCAGTGTTGG-3'; *Cxcr4* forward 5'-GATTGGTCTTCCTGCCACCA-3', reverse 5'-CAGTAACAGGAGAGGATGACG-3'; *Icam-1* forward 5'-GGAGACGCAGAGGACCTTAACAG-3' reverse 5'-CATCTCCTGTTTGACAGACTTCACC-3'; *Pecam-1* 5'-forward AGACATGGAATACCAGTGCAAG-3', reverse 5'-ACAGGATGGAAATCACAACCTTCAT-3'.

The iQ5 qPCR parameters for all primers were as follows: heat-activation of the hot-start iTaq Polymerase (55°C – 2 min), initial denaturation of DNA (95°C – 3 min), 45 amplification cycles (94°C – 20 sec, 62°C – 30 sec, data collection and real-time analysis, 72°C - 1 min), denaturation (95°C - 1 min), incubation (55°C - 1 min), melting curve analysis (55°C to 94.5°C - 0.5°C increment - 15 sec each), final cooling (4°C). The data were analyzed with the iQ5 Optical System Software (Version 2.0 - Bio-Rad).

## **2.4 Fluorescence Activated Cell Sorting (FACS) Analysis**

FACS analysis is a technique for examining and counting cells in a suspension. For example, it is used to detect surface proteins on eukaryotic cells and to quantify their amount through the binding of primary antibodies – directed against a specific protein - that in turn are recognized by secondary fluorescently-labeled antibodies [211].

FACS analysis was performed using the BECTON DICKINSON Flow Cytometer FACSCalibur System (BD Biosciences, San Jose, USA). Data were analyzed with the CellQuest Software 3.3 (BD Biosciences). Primary antibodies recognizing mouse antigens were detected with red R-phycoerythrin-conjugated AffiniPure F(ab')<sub>2</sub> fragment donkey anti-rat IgG (Jackson Laboratories, Bar Harbor, ME, USA). The surface protein levels were quantified using two-dimensional dot plot analysis for double-stained eEPCs (red phycoerythrin and EGFP positive eEPCs). A dot plot is usually divided into four quadrants: lower left (LL), lower right (LR), upper left (UL) and upper right (UR). The settings in the software were chosen that the x-axis shows cells that emit a green fluorescence EGFP signal whereas the y-axis shows cells that are positive for red fluorescence phycoerythrin (PE), which is conjugated to the secondary antibody. Cells that are negative for both colors are located in the LL quadrant. Cells that only emit an EGFP signal accumulate in the LR quadrant. Only cells that are positive for both signals locate in the UR quadrants and indicate presence of the respective surface protein. Cells occasionally show only a red PE signal in the UL quadrant. These cells are eEPCs that express the gene of interest but lost EGFP expression. Summarizing the percentages of gated cells in the UL and UR leads to the total percentage of cells that express the protein of interest. By comparing this percentage to the control (stained with isotype antibody that does not bind to the cells) it is possible to conclude whether a protein is present on the cell surface.

For FACS analysis, eEPCs were plated at a density of  $2 \times 10^5$  cells/ml into 6-well tissue culture plates and transiently transfected with 8  $\mu$ g of Foxc1-expression plasmid or pcDNA3 as negative control. Additionally, 8  $\mu$ g of pBK-CMV-EGFP were transfected into the cells. After 24 hours, the cells were washed with 1X PBS and detached from plates by incubation with 5 mM EDTA (Sigma-Aldrich) at 37°C for 20-



30 min. After successful detaching, the suspension was centrifuged at 250 g for 2 min to pellet the cells, that were subsequently washed with 4 ml ice-cold FACS buffer (4% bovine serum albumin, ICN Biomedicals, Solon, OH, USA and 0.1% sodium azide, Sigma-Aldrich, both diluted in 1X PBS), centrifuged again and finally resuspended in 2 ml fresh ice-cold FACS buffer. About  $2 \times 10^5$  cells of this suspension were used for incubation with each primary antibody, at a final antibody concentration of 5  $\mu\text{g/ml}$ . Cells were incubated 30 min at 4°C with anti-mouse Pecam-1 rat-monoclonal (Mec 13.3), rat IgG Isotype, or anti-mouse Tie2 rat-monoclonal primary antibody (all BD Pharmingen, Heidelberg, Germany) and subsequently washed twice with 400  $\mu\text{l}$  ice-cold FACS buffer. R-phycoerythrin-conjugated donkey-anti-rat secondary antibody (Jackson Laboratories, Bar Harbor, ME, USA) was added to the cell suspension at a final concentration of 5  $\mu\text{g/ml}$  and incubated for 30 min at 4°C (protected from light), followed by two washing steps with 400  $\mu\text{l}$  ice-cold FACS buffer. Finally, the cells were fixed in 400  $\mu\text{l}$  1% paraformaldehyde (Sigma-Aldrich) and subjected to FACS analysis.

## **2.5 Microscopy and Fluorescence Microscopy**

Microscopy and fluorescence microscopy were carried out using a NIKON Eclipse TE2000-U Microscope (Nikon, Tokyo, Japan). Fluorescence emission by cells was observed by means of a NIKON Super High Pressure Mercury Lamp at a wavelength of 480 nm for excitation of EGFP and at 550 nm for Cy3. Cells were photographed using a NIKON F90X camera (Nikon, Tokyo, Japan).

## **2.6 Immunofluorescence**

Immunofluorescence is a way to detect proteins in tissue sections, based on the binding of primary monoclonal or polyclonal antibodies to their respective antigens. As in FACS analysis, secondary antibodies, conjugated with a fluorescence dye, bind to the primary antibodies. The fluorescence signal is observed using fluorescence microscopy.

Mouse tissues were cryopreserved in OCT Tissue Tek (Sakura Finetek, Torrance, CA, USA) and stored at -80°C for further work. Tissue sectioning was carried out with

a JUNG FRIGOCUT 2800E Cryostat (Leica Microsystem Vertrieb GmbH, Bensheim, Germany). All sections had a thickness of 10  $\mu\text{m}$ .

Prior to the antibody staining, the tissue sections were fixed in a 1:1 acetone/methanol solution (Sigma-Aldrich) at 4°C for 5 min. The sections were then surrounded with a PapPen (SCI Science Services, Munich, Germany) and washed 5x with 1X PBS for 10 min each, followed by a blocking step for 1 hour with blocking buffer (1% bovine serum albumin and 0.05% Saponin, Sigma-Aldrich, in 1X PBS) at room temperature to prevent unspecific antibody binding to the tissue sections. Rat anti-Pecam-1 monoclonal antibody (BD Biosciences Pharmingen, Heidelberg, Germany) was added to the sections at a concentration of 5  $\mu\text{g}/\text{ml}$  and incubated overnight at 4°C. After this step, the sections were washed 5x with 1X PBS for 10 min each and subsequently incubated with a Cy3-conjugated donkey anti-rat IgG secondary antibody (Jackson ImmunoResearch Laboratories Inc., West Grove, PA, USA) for 1 hour at room temperature. Finally, the sections were again washed 5x with 1X PBS for 10 min each, air-dried for a short time, mounted with VECTASHIELD Mounting Medium (Vector Laboratories, Burlingame, CA, USA) and photographed under fluorescence light at a wavelength of 550 nm. The sections were also sealed with nail polish for long-term storage.

## **2.7 Promoter-Luciferase Assays**

The Firefly luciferase gene is a molecular genetic tool to identify and study the presence and activity of regulatory elements in gene promoter areas, as well as to investigate their interaction with trans-regulatory factors. In general, luciferase reporter assays are commonly used to investigate the regulation of eukaryotic gene expression.

*Firefly* luciferase is a 61kDa monomeric protein synthesized by the firefly beetle. It catalyzes the oxidation of beetle luciferin into oxyluciferin in a reaction requiring the presence of  $\text{O}_2$ , ATP and  $\text{Mg}^{2+}$  ions. As a result, ATP is hydrolyzed into AMP and  $\text{PP}_i$ , and energy is emitted in the form of photons [212]. The key principle of the assay lies in the quantification of promoter activity through the amount of *luciferase*

mRNA transcribed, which is proportional to the luminescence that is emitted during the reaction catalyzed by translated luciferase protein. A certain promoter fragment is cloned in front of the *luciferase* gene that is part of a reporter plasmid. The construct is transfected into a cell line where the activity of the cloned promoter area is to be studied. This way, the intensity of the emitted luminescence is directly correlated to the activity of a genetic regulatory element cloned upstream of the luciferase gene. For the project, the Dual-Luciferase Reporter Assay System (Promega) was used. The system takes advantage of the simultaneous expression of two distinct reporter genes in the transfected cells. The activities of *Firefly* luciferase and of a second luciferase enzyme derived from the sea pansy (*Renilla Reniformis*) [213] are measured together from a single sample. *Renilla* luciferase is a 36kDa monomeric protein and catalyzes the oxidation of coelenterazine to coelenteramide with simultaneous emission of photons. The two luciferase enzymes use distinct substrates and emit different wavelength fluorescent light, allowing to measure sequentially the activity of either enzyme. The advantage of the co-expression of two reporter genes lies in its high accuracy, allowing to rule out variability such as differences in transfection efficiency, cell numbers, or cell lysis efficiency. The activity of the experimental reporter gene (*Firefly* luciferase under the control of a promoter area of interest) is thereby normalized to the activity of the *Renilla* luciferase reporter gene, which is under the control of the constitutively active Herpes Simplex Virus *thymidine kinase* (HSV-*tk*) promoter.

In this project, eEPCs, BAECs, MS1-ECs, Cos7, and ES cells were plated at a density of  $1 \times 10^5$ - $5 \times 10^5$  cells/ml into 24-well plates (Falcon) and subjected to transfection with 0.3  $\mu$ g pGL2 promoter-luciferase plasmid (section 2.2.10) and 0.03  $\mu$ g HSV-*tk*-*Renilla*-luciferase plasmid (Promega) to correct for experimental variabilities. For co-transfections, the cells were additionally transfected with 2.4  $\mu$ g Fox-expression plasmid (CMV-Foxc1, CMV-Foxc2, CMV-Foxa2) or basic pcDNA3 (Invitrogen) as control plasmid. After 24 hours, the growth medium was removed and the cells were washed with 1X PBS, followed by lysis using the 5X Passive Lysis buffer provided in the Dual Luciferase Kit (Promega). Per well, 100  $\mu$ l of diluted (1X) Passive Lysis buffer was added and the plates were shaken subsequently for 15 min at room temperature on an orbital shaker to assure efficient lysis. Following lysis, the luciferase activity was measured according to the manufacturer's instructions

(Promega). In brief, 20  $\mu$ l of cell lysate was combined with 20  $\mu$ l of luciferase assay reagent II containing the substrate for *Firefly* luciferase, followed by measuring of the luminescence, using a Monolight 2010 Luminometer. Afterwards, the firefly luminescence was quenched by adding Stop & Glo Reagent that simultaneously activates the *Renilla* luciferase activity. The *Firefly* luciferase values are then normalized to the *Renilla* luciferase values from the same sample. All luciferase assays were performed in triplicates and replicated at least twice to obtain a statistically significant data set.

## **2.8 Western Blot**

Western Blot is used to detect a specific protein in a cell or tissue homogenate (or extract) [214]. The principle of the method lies in the separation of denatured proteins, usually depending on their size (i.e., the length of the polypeptide chain), using gel electrophoresis and polyacrylamide gels under denaturing conditions. Initially, the protein extract is denatured and solubilized by SDS (sodium dodecylsulfate). Typically, SDS-PAGE (polyacrylamide gel-electrophoresis) is used to separate the proteins. It maintains them in a denatured state preventing formation of secondary and tertiary structures. In addition, the negatively charged SDS causes the proteins to adopt an overall negative net charge and thus allows their separation during electrophoresis, where they migrate toward the positive anode. Smaller proteins migrate faster through the polyacrylamide gel. Following, the proteins are electrophoretically transferred to a positively charged nitrocellulose membrane, causing irreversible binding. During transfer, the membrane is placed on the anode side of a transfer unit, resulting into a “pulling” of the negatively charged antigens onto the membrane. To prevent unspecific binding of antibodies during the subsequent stages, the membrane is blocked by a diluted protein solution – usually non-fat dry milk powder - that blocks binding sites on the membrane where no antigens are bound. The specific antigen of interest is detected by a primary antibody that in turn is recognized by a secondary antibody directed against the species-specific part of the primary antibody. The secondary antibody itself is conjugated to a reporter enzyme such as horseradish peroxidase that catalyzes a detectable

chemiluminescent reaction visualized on X-ray films. Alternatively, the secondary antibody can carry a radioactive label for detection purposes.

For Western Blots in this project, protein lysates were generated from embryonic EPCs using the NE-PER Nuclear and Cytoplasmic Extraction Reagents Kit (Pierce Biotechnology), according to the manufacturer's instructions. In brief, cytoplasmic contents are released by disruption of the cell membranes. In a next step, the intact nuclei are recovered from the cytoplasmic extract by centrifugation, and nuclear proteins are extracted through lysis of the nuclei. The use of pure nuclear extract without the presence of cytoplasmic components elevates the quality to study interactions of DNA and nuclear proteins. To assure the stability of the nuclear extract, a proteinase inhibitor cocktail tablet (Roche Diagnostics, Indianapolis, IN, USA) was added to the extraction reagents (provided by Pierce Biotechnology) and the nuclear and cytoplasmic extracts were stored at -80°C for further applications.

The total protein concentrations of the cell lysates were determined using the BCA Protein Assay Reagent Kit (Pierce Biotechnology). This assay allows colorimetric quantification of protein amounts by the reduction of  $\text{Cu}^{2+}$  to  $\text{Cu}^+$  by chelation of cupric ions through proteins in an alkaline environment (i.e. the biuret reaction or assay) [215]. The light blue to violet chelated complex absorbs light at 540 nm and the intensity of the colored signal is in proportion to the amount of peptides in the mixture, with four to six peptide bonds forming a complex with one cupric ion. For Western Blot, 3  $\mu\text{g}$  of protein lysate were incubated together with 4  $\mu\text{l}$  of 5X loading buffer (250 mM Tris-HCl pH 6.8, 500 mM DTT, 10% SDS, 20% Glycerin, 2% Bromphenol blue) in a total volume of 20  $\mu\text{l}$  for 10 min at 70°C to unfold the polypeptide chains, followed by electrophoresis using NUPage 4-12% Bis-Tris polyacryamide gels (Invitrogen) and a vertical gel electrophoresis unit (Hoefer Pharmacia Biotech Inc., San Francisco, CA, USA) at 85 V for 2 hours in running buffer (24 mM Tris-Base, 192 mM glycine, 3.4 mM SDS, pH 7.4) Next to the protein samples, a molecular weight ladder (SeeBlue Plus2 Prestained Standard - Invitrogen) was run. Following electrophoresis, a Hybond-ECL nitrocellulose membrane (Amersham Biosciences) was placed onto the gel and the complex was covered on both sides with blotting paper (VWR International, West Chester, PA, USA) and a transfer sponge on the outside (VWR). The whole complex was soaked in transfer buffer (48 mM Tris-Base, 39 mM glycine, 0.038% SDS, 20% methanol

pH 8 - Sigma-Aldrich) and placed into a transfer unit (Hoefer), followed by electrophoretic blotting at 60 V for 2 hours in transfer buffer. Subsequently, the membrane was incubated for 1 hour in 5% non-fat dry milk powder (Nestle Corporation) at room temperature under shaking at 100 rpm, followed by incubation with the primary antibody for 12 hours at 4°C or 1 hour at room temperature. The membrane was incubated with goat polyclonal anti-Foxc1 or goat polyclonal anti-Foxc2 (Abcam Incorporation, Cambridge, MA, USA – both at a concentration of 0.5 µg/ml, diluted in 5% non-fat dry milk powder) or mouse monoclonal anti-β-Actin (Santa Cruz Biotechnology, Santa Cruz, CA, USA). Following incubation, the membrane was washed 5x with PBST buffer (PBS, 0.05% Tween20 - Sigma-Aldrich) for 10 min each and subsequently incubated with a secondary antibody (0.2 µg/ml in 5% non-fat milk powder) directed against the F<sub>c</sub> part of mouse or goat antibodies and conjugated with horseradish peroxidase (Santa Cruz). After incubation for 2 h at room temperature under shaking at 100 rpm, the membrane was washed 5x with PBST buffer, followed by the development of chemiluminescent light reaction, using the ECL Western Blotting Analysis System (Amersham). This kit provides the substrate reagent and buffers for the horseradish peroxidase enzyme and allows to develop a light reaction that was subsequently detected using a X-ray film (CL-X Posure Film, Pierce Biotechnology).

Horseradish peroxidase catalyzes the oxidation of chemiluminescent substrates such as luminol in the presence of H<sub>2</sub>O<sub>2</sub> [216], and this enzymatic activity is then visualized on X-ray films.

## **2.9 Chromatin Immunoprecipitation**

Chromatin immunoprecipitation (ChIP) assay is a technique to study DNA-protein interactions in vivo [217]. Unlike plasmid promoter assays or band-shift experiments, where binding to synthetic DNA loci (e.g. plasmid DNA) is studied, ChIP allows to assess the binding of a protein to a DNA sequence on the chromosome. The principle of this method lies in a reversible cross-linking of all DNA-associated protein

to the chromatin, by the means of gentle formaldehyde fixation of cultured cells. The chromatin is then isolated through cell lysis, followed by nuclei purification and lysis. As a key step, the chromatin is fragmented by sonication into small pieces (around 200-1000 bp in length). The obtained DNA-protein complexes are then immunoprecipitated using antibodies directed against the proteins of interest, followed by purification of the DNA-protein-antibody complex using protein A or G agarose beads that bind the F<sub>c</sub> part of immunoglobulins. Thus, any DNA sequence that is specifically cross-linked to the protein of interest precipitates as part of the chromatin-protein complex. This immunoprecipitate complex is then purified and the cross-link is reversed, thus liberating the DNA. Finally, the identity of the isolated DNA fragments is uncovered by means of PCR. DNA regions that have associated with a specific protein are amplified, as indicated by a positive PCR signal.

For CHIP experiments in this project,  $4 \times 10^7$  eEPCs were transfected with 50 µg CMV-Foxc1 plasmid. Following transfection, the cells were washed 3x with 1X PBS 24 hours later and fixed for 10 min at 37°C in 1% formaldehyde, followed by 3 wash steps with ice-cold 1X PBS. The cells were then scratched from the plates using 500 µl ice-cold 1X PBS per 100 mm plate and spun down (1500 g, 5 min, 4°C). Hypotonic buffer Mendez A (10 mM Hepes pH 7.9, 10 mM KCl, 1.5 mM MgCl<sub>2</sub>, 0.34 M sucrose, 10% glycerin, Roche protease inhibitor cocktail tablet) was added to the pellet for resuspension. Lysis was carried out by addition of Triton-X (0.04% final concentration), followed by an incubation step for 10 min on ice. The samples were spun down (1300 g, 4 min, 4°C), resulting into separation of nuclear and cytoplasmic proteins. After two wash steps with ice-cold 1X PBS, the pellet was dissolved in 2.3 ml LSB (0.1M NaCl, 10 mM Tris-HCl pH 7.4, 0.1% NP-40, 1 mM EDTA – Sigma-Aldrich) and the nuclei were lysed by addition of 300 µl 20% Sarkosyl. Next, the chromatin was gently transferred onto a 40 ml LSB-sucrose cushion (100 mM sucrose) and centrifuged (2500 g, 10 min, 4°C) to separate soluble protein from chromatin bound protein. The supernatant was removed and the chromatin was resuspended in 2 ml TE buffer (containing a Roche protease inhibitor cocktail tablet), followed by sonication (Branson sonifier, Danbury, CT, USA - 250-D, 50% amplitude, 2 x 50 sec in 1 second intervals). Finally, the chromatin concentration was measured at OD<sub>260</sub>.

For immunoprecipitation, 10 µg of goat anti-Foxc1 polyclonal antibody (Abcam) or 10 µg of Goat Isotype IgG (Jacksons Laboratories) as control was added to 500 µg sonicated chromatin and incubated at 4°C for 12-16 hours. 50 µl of protein G agarose/salmon-sperm DNA beads (50 % slurry – Upstate Millipore Corporation, Billerica, MA, USA) were added and the mixture was incubated (2 hours, 4°C) followed by a quick spin to pellet the beads. The supernatant was removed and the beads were resuspended in RIPA buffer (150 mM NaCl, 0.1% SDS, 0.5% DOC, 1% NP-40, 50 mM Tris-HCl pH 8.0) and transferred to Poly-Prep chromatography columns (Bio-Rad) where they were rinsed with 20 ml RIPA buffer, 20 ml LiCl buffer (250 mM LiCl, 0.5% NP-40, 0.5% DOC, 1 mM EDTA, 10 mM Tris-HCl, pH 8.0), and 20 ml TE buffer. Subsequently, the columns were sealed and the beads were transferred with 1 ml TE buffer to a microfuge tube. Following a quick spin, the immunoprecipitated chromatin was eluted in 200 µl TE buffer / 10% SDS under shaking for 10 min at 37°C, followed by a second elution at room temperature. The supernatant was transferred into new tubes and 200 µl TE buffer was added to dilute the SDS. The mixture was incubated at 65°C for 2 hours to reverse-cross-link the immunoprecipitate, followed by Proteinase K (Roche Diagnostics) digest (45°C, overnight) to degrade the antibodies and proteins. Finally, the chromatin was purified by Phenol / Chloroform / Isoamylalcohol extraction and subsequent ethanol precipitation. All protocols for ChIP analysis were based on a protocol by Gerhardt *et al.* [218].

The purified eEPC chromatin was amplified with the following primers: Foxc1 binding sites forward 5'-CAGAGTCCTAAGTTTCACATCCCTA-3' , reverse 5'-GTCAGGAGGATCAGACCTTTAAAAC-3'; Negative control promoter site forward 5'-GCAGAGAACAACCTGAGTTGGT-3', reverse 5'-CTGACTTTGGTGGTCTTTTCTCGTT-3'. The amplifications were carried out using the LightCycler system (described in section 2.3.1). The amplification products were run on 1.5% agarose gels for evaluation without real-time quantification. The LightCycler PCR Mix for amplification of ChIP-derived chromatin contained 13.1 µl ddH<sub>2</sub>O, 2.4 µl 25 mM MgCl<sub>2</sub> (Roche Diagnostics), 0.5 µl primer Mix (5 µM each), 2 µl LightCycler Fast Start Enzyme (Roche Diagnostics), and 2 µl template DNA. The PCR parameters for Foxc1 binding site primers and negative control promoter primer were as follows: 50 amplification cycles (95°C - 10 sec, 5 cycles 62°C annealing, 5 cycles 60°C annealing, 40 cycles 58°C annealing - all 10 sec, 72°C - 45 sec).



Densitometric analysis of the ChIP-PCR agarose gel bands to quantitate the relative amount of amplicon was carried out with the Bio-Rad Gel Documentation System Software (Bio-Rad).

## **2.10 Online Databases and Bioinformatics Programs**

Sequence screening for individual transcription factor binding sites in selected genomic sequences was carried out with the MatInspector program from Genomatix (Genomatix Software Incorporation, Munich, Germany – <http://www.genomatix.de>), that allows the identification of cis-regulatory elements embedded in nucleotide motifs by means of a large library of weight matrices [219].

Alignment of the genomic sequence of the mouse *Pecam-1* locus with the corresponding human *Pecam-1* sequence was performed using the DiAlignTF program from Genomatix [220]. The program combines sequence alignments with the identification of conserved transcription factor binding sites within aligned orthologous sequences, thus achieving a higher degree of confidence regarding the biological functionality of identified transcription factor binding sites. The genomic sequences used for the MatInspector and DiAlignTF programs were derived from the NCBI Entrez Gene WebViewer (<http://www.ncbi.nlm.nih.gov/sites/entrez> - see RESULTS for details).

The nucleotide numbering used to indicate the relative position of the different genomic fragments of the mouse *Pecam-1* locus were calculated by alignment of those sequences with the genomic sequences from the UCSC Bioinformatics Database, which displays the positions in absolute nucleotide numbering on the respective chromosome. Alignments were performed with the Blat Search Genome tool from the UCSC Bioinformatics Database. The numbers were then calculated relative to the transcription initiation site of *Pecam-1*, as indicated by the UCSC Bioinformatics Database.

The nucleotide sequences of *Pecam-1* transcripts were obtained from the NCBI Nucleotide Database (<http://www.ncbi.nlm.nih.gov/>). The accession numbers for the mRNAs are mentioned in the RESULTS section. The nucleotide sequences from the

*Pecam-1* genomic areas cloned for promoter-luciferase assays were obtained from Dr. Scott Baldwin and coworkers (Vanderbilt University – personal communication). The display of homology areas between the mouse and human *Pecam-1* locus was based on the output parameters of the DiAlignTF program (Genomatix). The alignment of 20kb of the 5'-flanking genomic sequence was subdivided into 2,000 data points (each representing a block of 10 nucleotides) and the relative nucleotide homology within the sequence blocks was indicated according to the output value of the alignment, with '0' indicating no similarity and '10' representing maximal similarity of a pairwise nucleotide alignment.

### **3. RESULTS**

#### **3.1 Expression of Fox genes in eEPCs**

Previous *in vivo* studies in our laboratory showed that eEPCs possess the ability to migrate to areas of active tumor growth and contribute to the neovascularization process by incorporating into the endothelial layer and by forming microvascular sprouts [112]. Alongside with these events, eEPCs shift their phenotype to a more mature endothelial cell type. However, the rate of incorporation and overall contribution to the tumor's microvascular network was rather low (around 3% of the total tumor vessel density was composed of eEPCs). In order to understand the molecular controls behind the eEPC-differentiation and to genetically manipulate this process, we aimed at identifying transcriptional regulators that are involved in eEPC differentiation. Previous Affymetrix microarray analysis, comparing the transcriptome of eEPCs before and after cAMP/retinoic acid-mediated differentiation, had identified induction of *FoxC* genes. Specifically, the transcript levels of *Foxc1* and *Foxc2* increased 4-6 fold after cAMP-induced differentiation of eEPCs (data not shown). Based on this finding, we focused on the Forkhead transcription factor family members *Foxc1* and *Foxc2*, since these two genes had been previously implicated in the development of the cardiovascular system in the past [180].

As a first step, the transcript levels of *Foxc1* and *Foxc2* in eEPCs were evaluated directly by RT-PCR to gauge expression levels of the two genes. In agreement with the microarray data, I found that expression of both genes was induced after *in vitro* differentiation of eEPCs with 0.5 mM cyclic AMP (Fig. 1). Among further genes, cAMP induced the expression of the endothelial-specific genes *Flk-1* and *vWF* as well as of *E-selectin* and *P-selectin* (Fig. 1) two genes that are expressed on the endothelium and are involved in leukocyte migration [221]. The data showed that cAMP is capable of inducing the shift of eEPCs toward a more mature endothelial phenotype.

Since the two transcriptional regulators *Foxc1* and *Foxc2* belong to a wider family of transcription factors, the expression profile of 29 members of the mouse Fox gene

family was screened by RT-PCR in order to test if this effect is unique to members of the *FoxC* subfamily. As a positive control, the expression profile of the selected Fox genes was assessed in parallel using E12.5 whole embryo RNA including intraembryonic RNA as well as Yolk Sac RNA (E12.5).

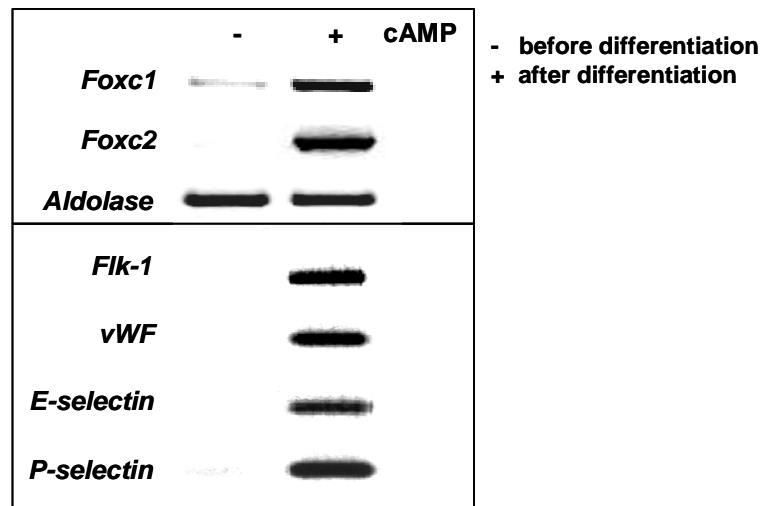


**Figure 1.** Induction of *FoxC* genes upon eEPC-differentiation. Embryonic EPCs were incubated with 0.5 mM cAMP for 24 hours. Untreated eEPCs were used as control. Total RNA was isolated from control (-) and cAMP-treated cells (+) and reverse transcribed into cDNA and amplified by PCR. The results show induction of *Foxc1* and *Foxc2* gene expression during cAMP-induced eEPC differentiation; cAMP also induces the expression of endothelial-genes such as *Flk-1* and *vWF*, as well as members of the selectin family, such as *E-selectin* and *P-selectin*. RT-PCR were carried out with RNA from 3 different experiments and repeated twice (n=9). Shown is a representative result.

Alongside, the expression profile of the orthologue human FOX genes was screened in human umbilical vein endothelial cells (HUVECs), which in contrast to eEPCs represent a mature endothelial line (Table 1). The number of active Fox genes in whole embryonic tissue (n=27) was much higher compared to eEPC (n=8) and HUVEC (n=6) lines (Table 1, Fig. 2). The number of active Fox genes in eEPCs was slightly higher as in HUVECs. However the expression of *FOXB2*, *FOXJ2*, and *FOXQ1* in HUVECs was not tested. The stimulation of eEPCs with cAMP induced the expression of 12 further members of the Fox gene family (Table 1 and Fig. 2), indicating that embryonic endothelial progenitors may employ Fox genes as important transcriptional regulators during and after the differentiation process. In turn, four Fox genes, namely *Foxf2*, *Foxj2*, *Foxo1*, and *Foxq1* had decreased gene expression levels after eEPCs were differentiated, indicating that some Fox genes may also have specialized functions during the undifferentiated progenitor cell state.

Fox Gene	E12.5 Embryo	eEPCs	eEPCs + cAMP	HUVECs
Foxa1	+	-	+	+
Foxa2	+	+	increased	-
Foxa3	+	-	-	-
Foxb1	+	-	+	-
Foxb2	+	-	+	not tested
Foxc1	+	-	+	+
Foxc2	+	-	+	-
Foxd1	+	-	+	-
Foxd2	+	-	-	-
Foxd4	+	-	+	-
Foxf1	+	-	+	-
Foxf2	+	+	decreased	-
Foxg1	+	-	+	-
Foxh1	+	-	-	-
Foxi1	+	-	-	-
Foxj1	+	-	-	-
Foxj2	+	+	decreased	not tested
Foxk1	+	-	-	+
Foxl1	+	-	+	-
Foxm1	+	-	+	-
Foxn1	-	-	-	-
Foxn2	+	+	+	+
Foxo1	+	+	decreased	-
Foxo3	+	+	+	+
Foxo4	+	+	increased	-
Foxp1	+	-	-	+
Foxp2	+	-	-	-
Foxp3	-	-	+	-
Foxq1	+	+	decreased	not tested
<b>Total</b>	<b>27</b>	<b>8</b>	<b>20</b>	<b>6</b>

**Table 1.** Expression analysis of Fox genes. Expression of 29 members of the mouse and human Fox transcription factor family was analyzed using RNA from E12.5 whole embryos, undifferentiated and cAMP-differentiated eEPCs as well as HUVECs. RNA was reverse transcribed into cDNA and amplified with gene-specific primers; (+) indicates detected transcript; (-) indicates no detected transcript; after differentiation of eEPCs, the expression levels of four Fox genes decreased and those of two Fox genes increased; twelve Fox gene family members were induced during eEPC-differentiation and the expression levels of two Fox genes was not affected; Gene expression analysis is based on agarose-gel electrophoresis. PCRs were carried out three times.

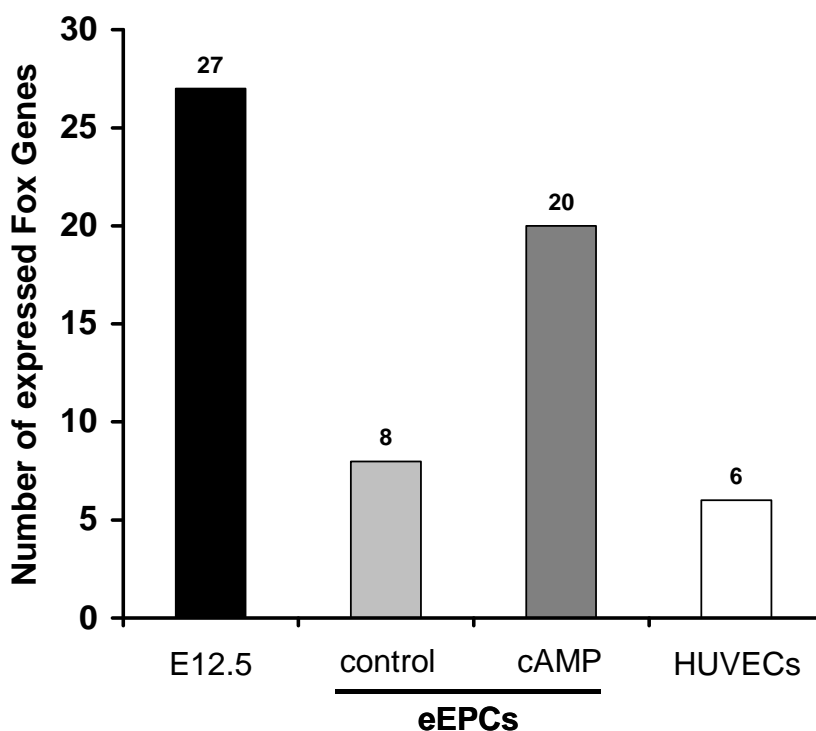


**Figure 2.** Fox gene expression. The chart shows the number of expressed Fox transcription factors in the different tissues and cell lines tested; cAMP-treatment of eEPCs strongly augments the number of expressed Fox genes.

### **3.2 Foxc1 and Foxc2 regulate expression of *Pecam-1* in eEPCs**

The upregulation of *FoxC* genes during differentiation of eEPCs suggested that they might play a role in the endothelial maturation process. To answer this question, *Foxc1*, *Foxc2*, and *Foxa2* (the last as a control) genes were over-expressed to monitor changes in the expression levels of known endothelial-specific genes. In this experiment, undifferentiated eEPCs were transfected with expression plasmids encoding either *Foxc1* or *Foxc2* full-length cDNAs under the control of the CMV promoter (CMV-*Foxc1* or CMV-*Foxc2*). To assure that *Foxc1* and *Foxc2* proteins were translated from the plasmid-encoded mRNA, Western Blot analysis was performed with nuclear protein extract from transfected eEPCs (Fig. 3). The assay showed high amounts of synthesized *FoxC* protein, confirming efficient over-expression of the transgenes.

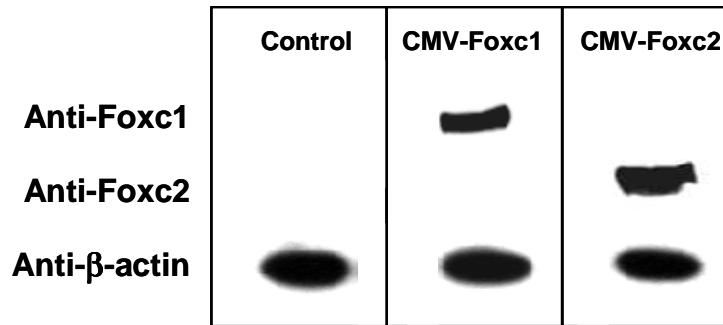


**Figure 3.** Western Blot with eEPC protein lysates showing high amounts of Foxc1 and Foxc2 proteins after transient transfection with CMV-Foxc1, CMV-Foxc2 or empty pcDNA3 (control);  $\beta$ -actin was used as internal control.

In a next step, the expression profiles of a variety of endothelial-specific effector genes (e.g., *Pecam-1*, *Icam-1*, *eNOS*, *vWF*), transcriptional regulators (e.g. Sox genes, Id genes, members of the Gata-family, KLF factors, Egr-1 and members of the Fox gene family), signaling ligands and their respective receptors (e.g., TGF $\beta$  family members, Ephrin/Eph family members, Integrins, Wnt family members, chemokines and chemokine receptors) as well as extracellular matrix molecules (matrix metalloproteinases and their inhibitors) were tested for potential responsiveness to FoxC genes by RT-PCR using gene-specific primers. A complete list of the examined genes is shown in the Supplemental Table at the end of the document. Whereas expression levels of most tested genes were not affected by Foxc1 or Foxc2, *Pecam-1* (Platelet Endothelial Cell Adhesion Molecule-1) was specifically induced by Foxc1, but not by Foxc2 (Fig. 4A). Another adhesion molecule, *Icam-1* (Intercellular Adhesion Molecule-1) responded to both FoxC proteins, an effect that was also seen for the chemokine receptor *Cxcr4* (Fig. 4A). Quantitative real-time PCR confirmed the gene induction in response to Foxc1. As shown in Figure 4B, *Pecam-1* transcript levels were elevated by 5.5-fold, and *Icam-1* and *Cxcr4* expression increased 3.5-fold and 6.5-fold, respectively. In contrast, the expression of genes expressed in the vascular system such as *Flk-1* and *Flt-1*, as well as members of the ephrin/Eph family (*ephrinB2* and *EphB4*), did not respond to overexpression of either Foxc1 or Foxc2 (Fig. 4A). These findings suggest that Foxc1 and Foxc2 may play a role in the genetic regulation of genes encoding for surface proteins that are involved in the recruitment of circulating cells during inflammatory conditions.

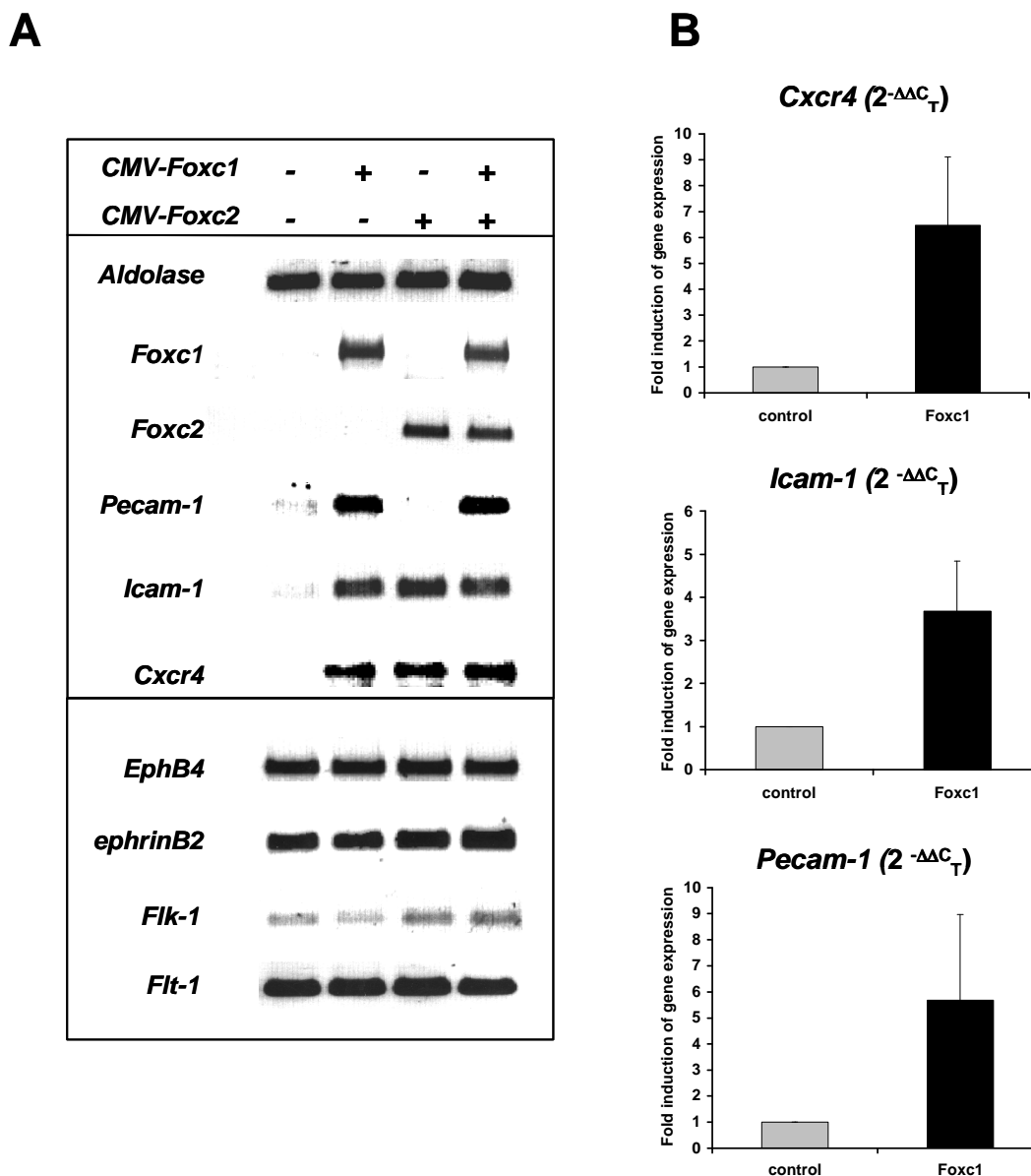


**Figure 4.** Embryonic EPC gene expression profile after transient *Foxc1* and *Foxc2* expression. **A)**  $5 \times 10^6$  cells were transiently transfected with *CMV-Foxc1* and/or *CMV-Foxc2* expression plasmids. Basic pcDNA3 vector was used as control. Total RNA was isolated 24 hours after transfection and subsequently reverse transcribed into cDNA and amplified by gene specific PCR primers. *Pecam-1* expression responses to *Foxc1*. *Icam-1* and *Cxcr4* transcript levels are induced by either FoxC protein. Vascular genes like *Flk-1* and *Flt-1* or *ephrinB2* and *EphB4* are not affected by *Foxc1* and *Foxc2*. *Aldolase* was used as normalization control. Transfections were repeated at least three times with RNA from at least two independent experiments. Shown is a representative result. **B)** Quantitative real-time PCR (qPCR) depicts the fold-induction of mRNA levels after expression of *Foxc1* in eEPCs. The transcript levels of *Cxcr4*, *Icam-1*, and *Pecam-1* show an about 6.5-fold, 3.5-fold, and 5.5-fold increase, respectively, in response to *Foxc1* (black bars). The relative mRNA levels were calculated using the  $2^{-\Delta\Delta C_T}$  method and normalized to  $\beta$ -actin expression as internal control; qPCRs were carried out in triplicates with mRNA from at least two independent experiments. ( $n > 6$ ). The expression levels in control cells (gray bars) was set to an arbitrary value of 1 and the fold induction of gene expression in response to *Foxc1* was calculated accordingly. The standard deviation is indicated for the *CMV-Foxc1* transfected samples (black bars).



To test if *Pecam-1* gene induction leads to higher levels of Pecam-1 protein on the eEPC cell membrane, we performed Fluorescence Activated Cell Sorting (FACS) using antibodies recognizing Pecam-1. I detected very low levels of *Pecam-1* protein on the surface of undifferentiated eEPCs, in accordance with the mRNA results (Fig. 5). In *Foxc1*-expressing eEPCs, Pecam-1 surface molecule quantity shows an approximately 6-fold increase (from 3% to 19% Pecam-1-positive cells), demonstrating that the *Foxc1*-induced *Pecam-1* mRNA expression in eEPCs leads to increased Pecam-1 protein levels (Fig. 5).

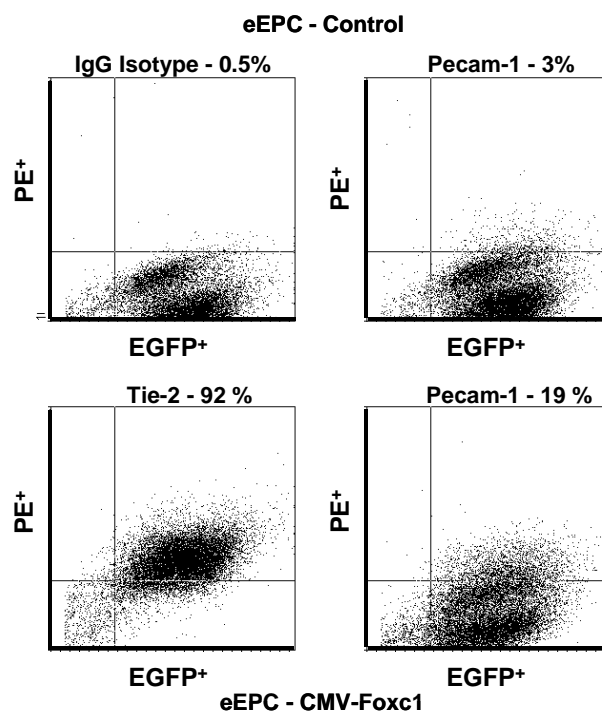


**Figure 5.** Two color dot plot FACS Analysis of EGFP-positive eEPCs, as described in Material and Methods.  $10 \times 10^5$  eEPCs were incubated with an anti-Pecam-1 rat monoclonal antibody and with an anti-Tie2 rat monoclonal antibody, and a rat IgG Isotype control. The endothelial-specific marker Tie2 served as the positive control; the signal from the Isotype IgG antibody was set as a negative control. Cells were labeled with a donkey anti-rat secondary antibody conjugated with the red dye Phycoerythrin. Cells in the upper row dot plots show control (pcDNA3 transfected) eEPCs. Bottom row dot plots indicate CMV-Foxc1 transiently transfected eEPCs. The total percentage of double-positive cells is indicated for each dot plot. Pecam-1 surface protein levels show an approximately 6-fold increase after *Foxc1* expression. Tie2 positive cells make up to 92% of the total counted eEPC population. X-axis shows EGFP-positive cells; y-axis indicates Phycoerythrin (PE)-positive cells.

### 3.3 *Pecam-1* as an endothelial target gene of *Foxc1*

*Pecam-1* is a 130kDa type I transmembrane surface protein that belongs to the immunoglobulin (Ig) superfamily of cell adhesion molecules [62]. Its expression is restricted to endothelial cells and certain hematopoietic cells and it has been implicated as a critical mediator of leukocyte transendothelial migration to sites of acute inflammation. In addition, it is found in the inner cell mass of the blastocyst, which gives rise to embryonic stem (ES) cells [222].

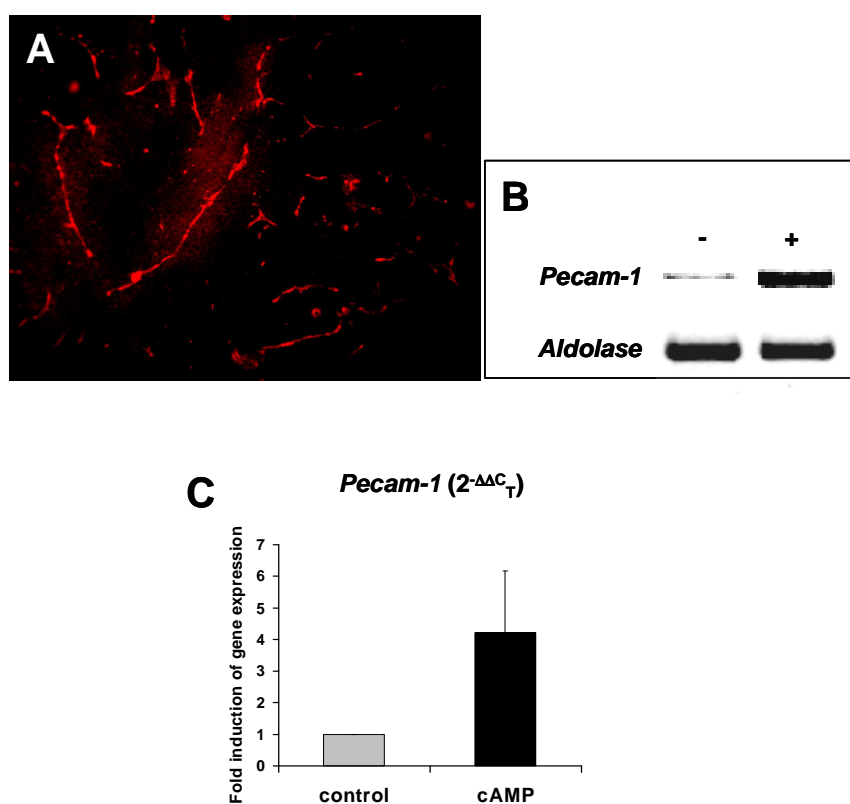


**Figure 6.** Expression of *Pecam-1*. **A)** 10  $\mu$ m mouse liver sections were stained with a rat anti-*Pecam-1* monoclonal antibody. Cy3-conjugated donkey-anti-rat antibody was used to detect bound primary anti-*Pecam-1* antibody on the tissue section. The liver microvasculature stains intensely for the endothelial marker *Pecam-1*. **B)** RT-PCR shows induction of *Pecam-1* expression during cAMP-induced *in vitro* differentiation of eEPCs. *Aldolase* was used for normalization. (-) control eEPCs; (+) cAMP-differentiated eEPCs (0.5 mM cAMP). **C)** Quantitative real-time PCR (qPCR) indicates an about 4-fold increase in *Pecam-1* transcript levels after cAMP-induced eEPC-differentiation (black bar). The relative mRNA levels were calculated using the  $2^{-\Delta\Delta C_T}$  method and normalized to *Gapdh* expression as internal control; qPCRs were carried out in triplicates with mRNA from three independent experiments. (n = 9). The expression levels in control cells (gray bar) was set to an arbitrary value of 1 and the fold induction of gene expression in response to cAMP was calculated accordingly. The standard deviation is indicated for the cAMP-treated sample (black bar).

Because of its high expression in the endothelium, *Pecam-1* is widely used as marker for endothelial cells (Fig. 6A). In addition, like *Foxc1* and *Foxc2*, *Pecam-1* expression is induced during *in vitro* differentiation by cAMP, indicating an involvement during the maturation toward a differentiated endothelial phenotype (Fig. 6B). The level of *Pecam-1* induction was about 4-fold, as quantified by qPCR (Fig. 6C), and thus similar to that seen after *Foxc1* expression in eEPCs (Fig. 4B).

The results described above show that *Pecam-1* expression is specifically upregulated after *Foxc1* expression in eEPCs (Fig. 4). To test if *Pecam-1* is a direct target of *Foxc1* and in order to identify the putative transcriptional regulatory elements, we undertook a detailed analysis of the *Pecam-1* promoter response to FoxC factors in eEPCs and mature endothelial cells.

### **3.4 Cis-regulatory areas of the *Pecam-1* promoter**

The mouse *Pecam-1* gene is located on band qE1 of chromosome 11, spanning a range of almost 60kb (based on Ensembl Genome Browser – <http://www.ensembl.org>). In an attempt to identify genomic areas of the *Pecam-1* locus that are bound by *Foxc1*, this study took advantage of *Pecam-1*-promoter-luciferase plasmids kindly provided by Dr. Scott Baldwin and co-workers (Vanderbilt University). In the past, proximal and distal, as well as intronic areas, of the mouse *Pecam-1* locus have been analyzed for the presence of *cis*-regulatory elements by the group of Dr. Baldwin (unpublished data in preparation). Among others, four different genomic fragments of the *Pecam-1* locus were subcloned into the pGL2 promoter firefly-luciferase plasmids.

These four constructs are: 1) the minimal promoter elements derived from the transcriptional start site of mouse *Pecam-1* (pGL2-mp; -88 to +57); 2) the long proximal promoter sequences (pGL2-lpp; -280 to +57); 3) a distal 5'-flanking 3.5kb-fragment (-13,597 to -10,063) in combination with the minimal promoter (pGL2-5'-3.5kb/mp); and 4) a 4.5kb fragment from the second intron (+10,273 to +5,849) in combination with the minimal promoter (pGL2-l2-4.5kb/mp) (Fig. 7,8) (see Material

and Methods for further details). The latter two fragments showed the highest transcriptional activity regarding 5'-flanking and intronic sequences, respectively, in isolated endothelial cells and transient transgenic mouse embryos (Dr. Baldwin, personal communication).

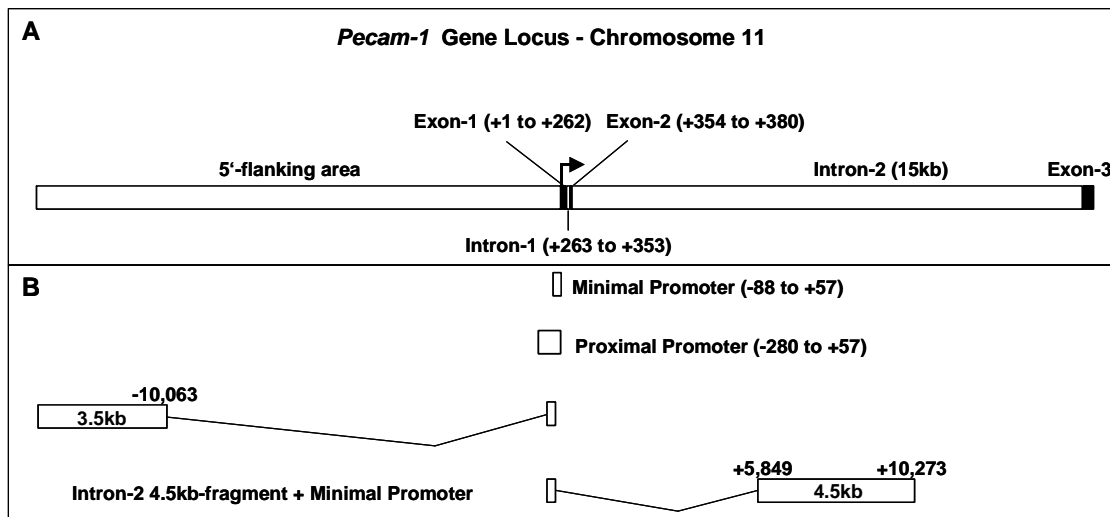


**Figure 7.** Mouse *Pecam-1* gene locus. **A)** Schematic overview of the 5'-flanking region and exons 1-3 of the mouse *Pecam-1* locus on band qE1 of chromosome 11. The transcription initiation site (TIS) is at +1. **B)** *Pecam-1* promoter constructs. Overview of areas of the *Pecam-1* locus (in alignment with the diagram in A) that were cloned for promoter analysis and the identification of putative Foxc1-response elements. The location of the selected areas are directly upstream of the transcription start (minimal promoter sequence from -88 to +57), long proximal promoter sequence (from -280 to +57) as well as a 3.5kb fragment located distal in the 5' flanking area of *Pecam-1* (-13,597 to -10,063) and a 4.5kb fragment located within the second intron (+5,849 to +10,273). All nucleotide numbering is relative to the TIS (+1) and is based on the UCSC Genome Bioinformatics Database (<http://www.genome.ucsc.edu>).

### **3.5 *Pecam-1* promoter and enhancer analysis in different cell lines**

As a first step, the four promoter plasmids (Fig. 8) were analyzed for their ability to drive *Pecam-1* expression in eEPCs and mature endothelial lines as well as in non-endothelial cells. In parallel to the *Pecam-1* promoter studies, *Pecam-1* expression levels were evaluated by conventional RT-PCR to obtain an overview of endogenous *Pecam-1* gene expression in the corresponding cell lines.

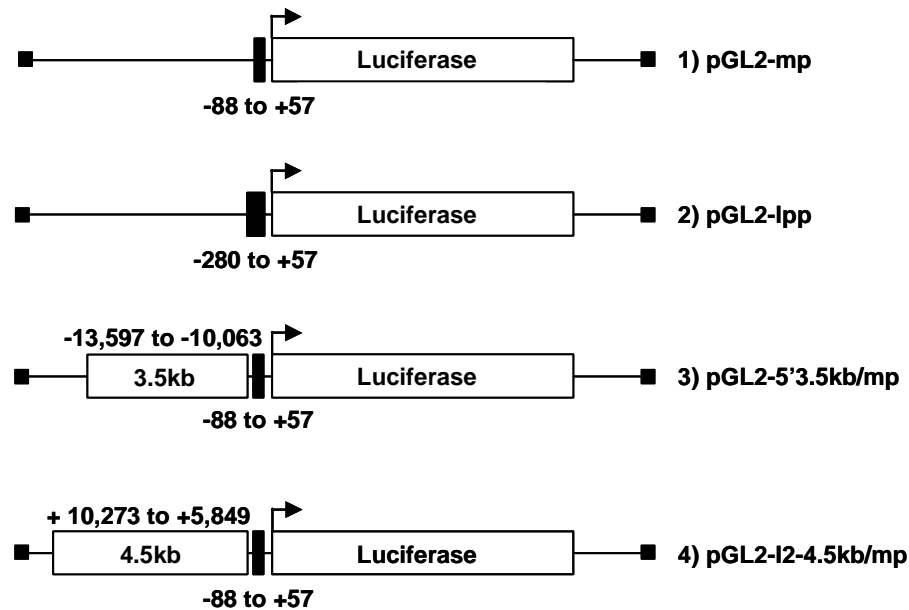


**Figure 8.** Outline of *Pecam-1* promoter plasmids. Schematic structure of the four *Pecam-1* promoter plasmids cloned in front of the Firefly Luciferase gene inside the pGL2 vector. The plasmids contain the 1) minimal promoter sequence (pGL2-mp / -88 to +57); 2) long proximal promoter sequence (pGL2-lpp / -280 to +57); 3) distal 5'-3.5kb fragment + minimal promoter (pGL2-5'3.5kb/mp / -13,597 to -10,063); 4) 2<sup>nd</sup> intron 4.5kb-fragment + minimal promoter (pGL2-l2-4.5kb/mp / +10,273 to +5,849). The nucleotide numbering is relative to the transcription initiation site (+1) and is based on the UCSC Genome Bioinformatics Database (<http://www.genome.ucsc.edu>).

As shown, *Pecam-1* transcripts are detectable at high levels in mature pancreatic endothelial cells (MS1-ECs), cardiac endothelial cells (H5V-ECs) and bovine aortic endothelial cells (BAECs) but not in undifferentiated eEPCs, mouse fibroblasts (3T3) and Cos7 cells. As reported previously [222], we detected that undifferentiated embryonic stem (ES) cells express *Pecam-1* (Fig. 9B).

These results show that *Pecam-1* is specifically expressed in mature endothelial cells and embryonic stem cells. To test which genomic area drives *Pecam-1* expression and to assess if all areas are equally active in *Pecam-1*-expressing cells, *Pecam-1* promoter activity in eEPCs, MS1-ECs, and BAECs as well as in ES cells and Cos7 cells was measured after transient transfection with the *Pecam-1* promoter reporter plasmids (Fig. 9A). The minimal promoter (pGL2-mp) showed low activity only in BAECs, whereas the long proximal promoter (pGL2-lpp) drove reporter activity in BAECs and ES cells.

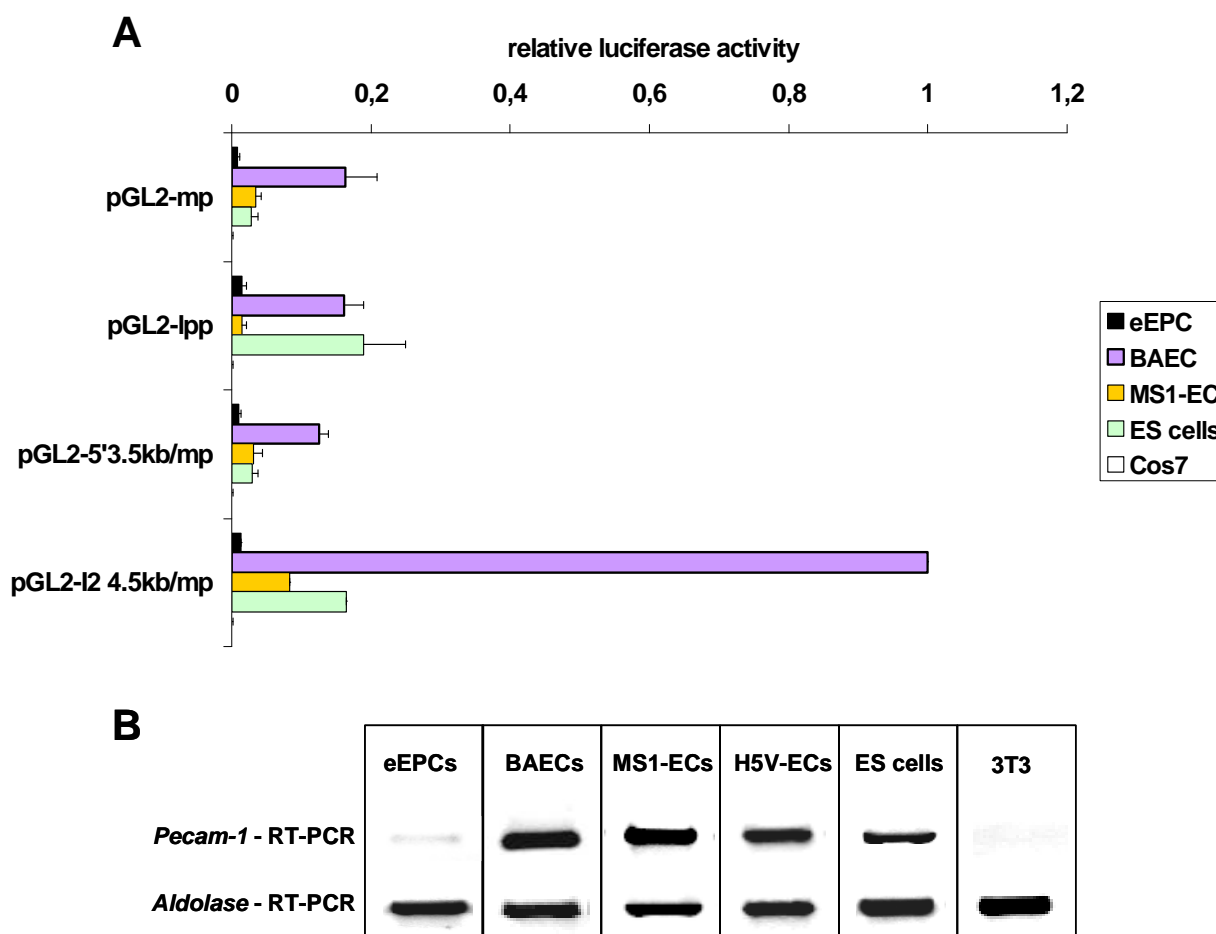


**Figure 9. *Pecam-1* expression analysis** **A)** For promoter analysis, eEPCs, BAECs, MS1-ECs, ES cells, and Cos7 cells were transiently transfected with 0.3  $\mu$ g of *Pecam-1* promoter plasmids (outline in Fig. 7). Ten ng of the HSV-*tk-Renilla* plasmid were co-transfected for normalization, as described in Material and Methods. Luciferase activity was measured 24 hours after transfection. The luciferase activity derived from pGL2-I2-4.5kb/mp in BAECs was set to an arbitrary value of 1 and all other values were normalized accordingly. *Pecam-1* expression is driven by pGL2-I2-4.5kb/mp in BAECs (purple bars), MS1-ECs (orange bars), and ES cells (green bars). Embryonic EPCs (black bars) and Cos7 (white bars) cells do not display promoter activity. Luciferase assays were carried out in triplicates and repeated at least once and bars represent average values ( $n > 6$ ). The standard deviation is indicated for each bar. **B)** RT-PCR analysis shows expression of *Pecam-1* in BAECs, MS1-ECs, H5V-ECs, and ES cells but not in eEPCs and 3T3 fibroblasts. RNA was isolated from at least three different experiments and PCR was repeated at least twice. Aldolase was used as normalization control. Shown is a representative result.

The enhancer from the 2<sup>nd</sup> intron (pGL2-I2-4.5kb/mp) displayed high activity in BAECs, and moderate activity in ES cells and pancreatic microvascular endothelial cells (MS1-ECs), thus suggesting that this regulatory element might be primary responsible to drive *Pecam-1* expression in endothelial cells of larger vessels. The distal 5'-flanking enhancer (pGL2-5'3.5kb/mp) did not display extra activity. In accordance with endogenous *Pecam-1* expression levels, no reporter gene activity

was seen in immature eEPCs and Cos7 cells, for all four reporter plasmid (Fig. 9A). Taken together, the data suggest that different genomic areas contribute in the transcriptional regulation of *Pecam-1* expression, depending on the origin of the cell lines.

### **3.6 Foxc1 activates transcription through the 5'-flanking 3.5kb-fragment**

The results showed that no promoter/enhancer fragment was active in undifferentiated eEPCs.

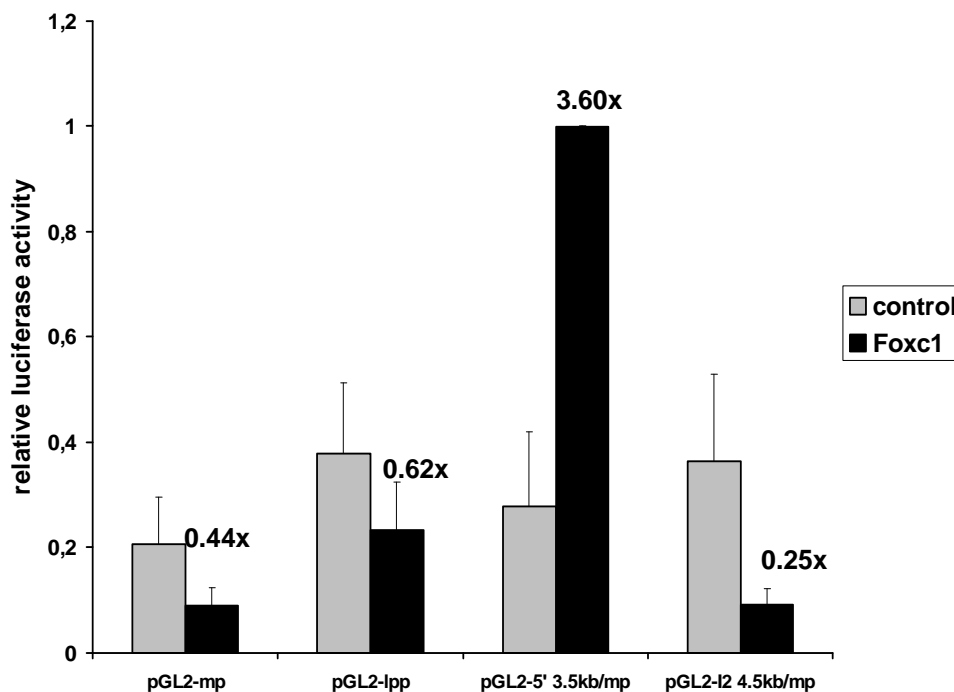


**Figure 10.** *Pecam-1* promoter activation in eEPCs by Foxc1.  $5 \times 10^5$  eEPCs were transiently transfected with 2.4  $\mu\text{g}$  of CMV-Foxc1 (black bars) or pcDNA3 (gray bars) together with 0.3  $\mu\text{g}$  of *Pecam-1* promoter plasmids and 10 ng of HSV-*tk-Renilla* to normalize, as described in Material and Methods. Luciferase activity was measured 24 hours after transfection. Luciferase activity derived from the co-transfections with pGL2-5'3.5kb/mp and CMV-Foxc1 was set to an arbitrary value of 1 and the values derived from the other co-transfections were normalized accordingly. Foxc1 activates the *Pecam-1* promoter through pGL2-5'3.5kb/mp. Fold increase or decrease in response to Foxc1 is shown for each bar. Luciferase assays were carried out in triplicates and repeated at least twice and bars represent average values ( $n > 9$ ). The standard deviation is indicated for each bar.

To test if the putative Foxc1-responsive elements reside within the tested genomic areas, the cells were co-transfected with the promoter plasmids and a Foxc1-expression (CMV-Foxc1) plasmid. As shown in Figure 10, a strong activation of reporter gene transcription through the 5'-flanking 3.5kb-fragment (pGL2-5'3.5kb/mp) was observed after Foxc1 expression, showing a 3.6-fold higher activity compared to control, empty-vector transfected eEPCs that do not express Foxc1 (Fig. 10). Transcriptional activation of the reporter gene by Foxc1 was neither seen for the proximal (pGL2-lpp) and minimal promoter area (pGL2-mp) nor with the intronic 4.5kb-fragment (pGL2-l2-4.5kb/mp), where the background activity even dropped about 4-fold after Foxc1 expression in the cell. Similar, a drop of the relative reporter activity was seen in the promoter plasmids containing the proximal and minimal promoter sequences (about 2-fold in each case). Since the effect is not seen with the empty vector transfection, it is ruled out that this suppression is due to competition for a limited pool of transcription factors between co-transfected plasmids. Instead, it appears that Foxc1 protein overexpression might be interfering with the general transcriptional machinery. The around 3.5-fold induction after Foxc1 binding is in accordance with the increase in *Pecam-1* mRNA and protein levels after Foxc1 expression in eEPCs (Fig 4B, 5). Additionally, *Pecam-1* levels increase about the same fold after eEPCs are induced to differentiate with cAMP and retinoic acid. In conclusion, these data support the notion that a cis-acting regulatory site within the 5'-flanking 3.5kb-fragment is driving *Pecam-1* expression after *Foxc1* expression in eEPCs.

### **3.7 The distal 5'-flanking 3.5kb-fragment responds specifically to Foxc1**

To test if the transactivation of *Pecam-1* in eEPCs through the distal upstream element is specific to Foxc1, the cells were co-transfected with the pGL2-5'3.5kb/mp promoter plasmid and pGL2-mp as control, together with the CMV-Foxc1, CMV-Foxc2, or CMV-Foxa2 expression plasmids. Gain of function studies showed that *Pecam-1* expression in eEPCs was specifically activated by Foxc1 but not by the



closely related transcription factor Foxc2 or the family member Foxa2 after transient transfection of eEPCs. (Fig. 11A). Thus, the ability of these three Fox transcription factors to activate target gene expression through the 5'-flanking 3.5kb-fragment was compared.

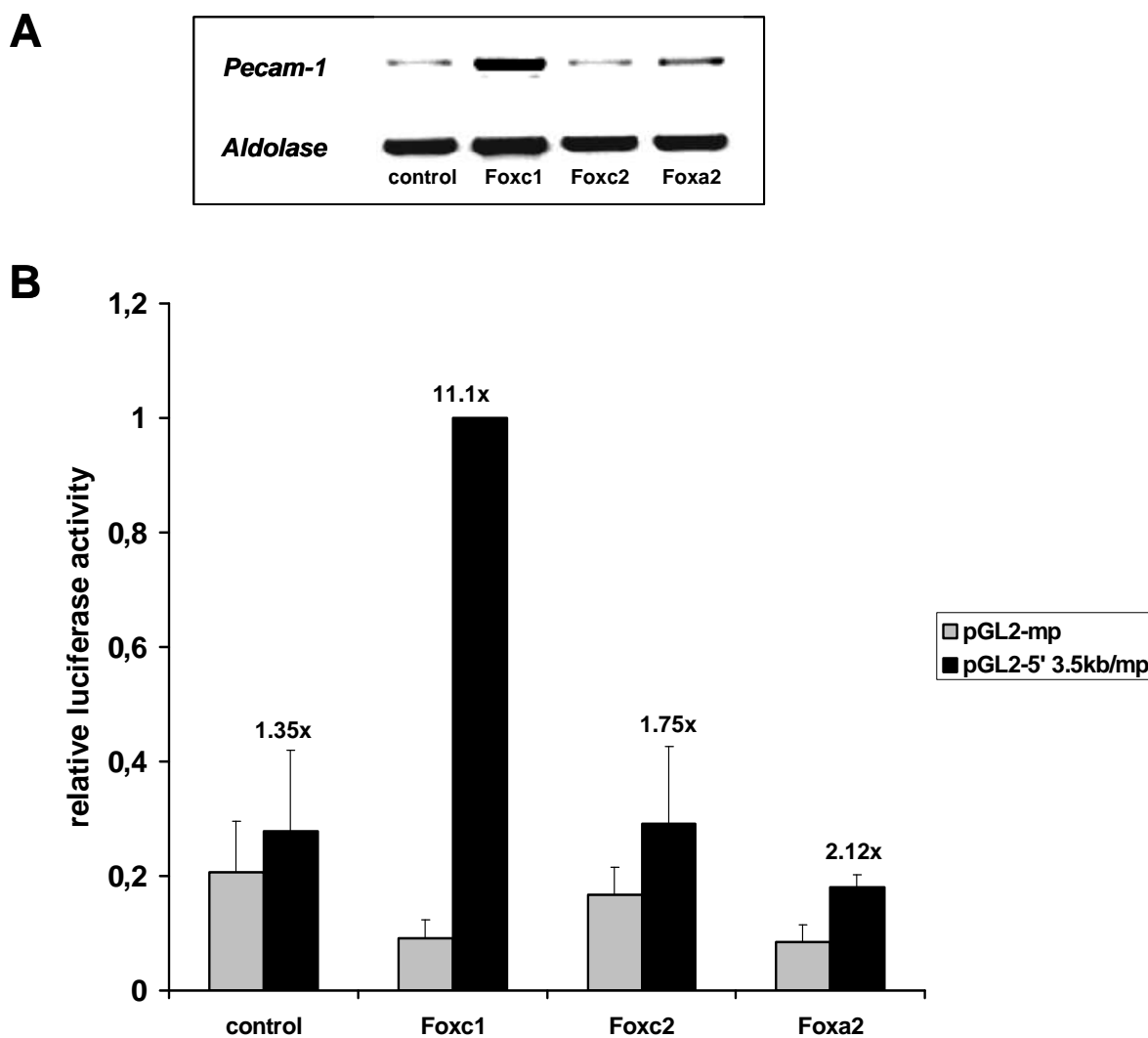


**Figure 11.** *Pecam-1* induction is specific for Foxc1. **A)**  $5 \times 10^6$  eEPCs were transiently transfected with 8  $\mu\text{g}$  of CMV-Foxc1, CMV-Foxc2, CMV-Foxa2, or pcDNA3 (control) followed by RNA isolation after 24 hours and RT-PCR. Foxc1, but not Foxc2 and Foxa2 activates expression of *Pecam-1* in eEPCs. *Aldolase* is shown as normalization control. **B)** eEPCs were transiently transfected with 2.4  $\mu\text{g}$  of CMV-Foxc1, CMV-Foxc2, CMV-Foxa2, or pcDNA3, together with 0.3  $\mu\text{g}$  of pGL2-mp (gray bars) or pGL2-5'3.5kb/mp (black bars) and 10 ng of HSV-*tk-Renilla* to normalize, followed by luciferase assays after 24 hours. Luciferase activity derived from the co-transfections with pGL2-5'3.5kb/mp and CMV-Foxc1 was set to an arbitrary value of 1 and all other luciferase values were normalized accordingly. The fold activity of reporter expression from pGL2-5'3.5kb/mp compared to pGL2-mp is shown for each co-transfection. The 3.5kb fragment (pGL2-5'3.5kb/mp) is induced by Foxc1. Luciferase assays were carried out in triplicates and repeated at least twice and bars represent average values ( $n > 9$ ). The standard deviation is indicated for each bar.

As shown, the transcriptional activation was specific for Foxc1 (11-fold over the minimal promoter), since both Foxc2 (1.75-fold over minimal promoter) and Foxa2 (2.12-fold over minimal promoter) had a minimal effect (Fig. 11B), thus not reaching a significant induction, similar as in control eEPCs (pcDNA3 transfected). These data confirmed the RT-PCR studies that showed induction of endogenous *Pecam-1* expression in eEPCs only through Foxc1.

### **3.8 Foxc1 activates transcription specifically in eEPCs**

In eEPCs, the induction of *Pecam-1* after Foxc1 expression is regulated through the 5'-flanking 3.5kb-fragment (pGL2-5'3.5kb/mp). The response of this putative control element to Foxc1 was also investigated in BAECs as well as in non-endothelial cells (ES cells and Cos7 cells) (Fig. 12A). After transient co-transfections of CMV-Foxc1 plasmid and *Pecam-1* promoter plasmids, I found that Foxc1 did not trans-activate reporter gene expression in BAECs and Cos7 cells (Fig. 12A), showing that the transcriptional activation through Foxc1 specifically takes place in eEPCs (about 3.5-fold induction compared to control cells – Fig. 10). This suggests that the effect of Foxc1 on *Pecam-1* expression might be cell-context specific (Fig. 12A). The basal signal of pGL2-5'3.5kb/mp was even lowered in BAECs (about 11-fold), ES cells (about 5-fold) and in Cos7 cells (about 1.5-fold) after expression of Foxc1, compared to control (pcDNA3 transfected) cells. Lowered reporter activity was seen for all promoter plasmids in response to Foxc1 expression in these cells (data not shown), possibly indicating a general suppression activity of the basic *Pecam-1* promoter.

In accordance, *Pecam-1* transcript levels were decreased in response to Foxc1-overexpression in mature pancreatic endothelial cells (about 4-fold) and ES cells (about 2-fold), as shown by qPCR (Fig. 12B).

In addition, attempts to assess reporter gene activation through pGL2-5'3.5kb/mp upon *Foxc1* expression in pancreatic (MS1-ECs) and cardiac (H5V-ECs) endothelial cells did not work well, possibly because these cells are hard to transfect efficiently, especially with a combination of several plasmids. A number of different techniques

did not result into the desired transfection efficiency that would have allowed the monitoring of the *Pecam-1* promoter plasmid activity after co-transfection with the CMV-Fox expression plasmids.

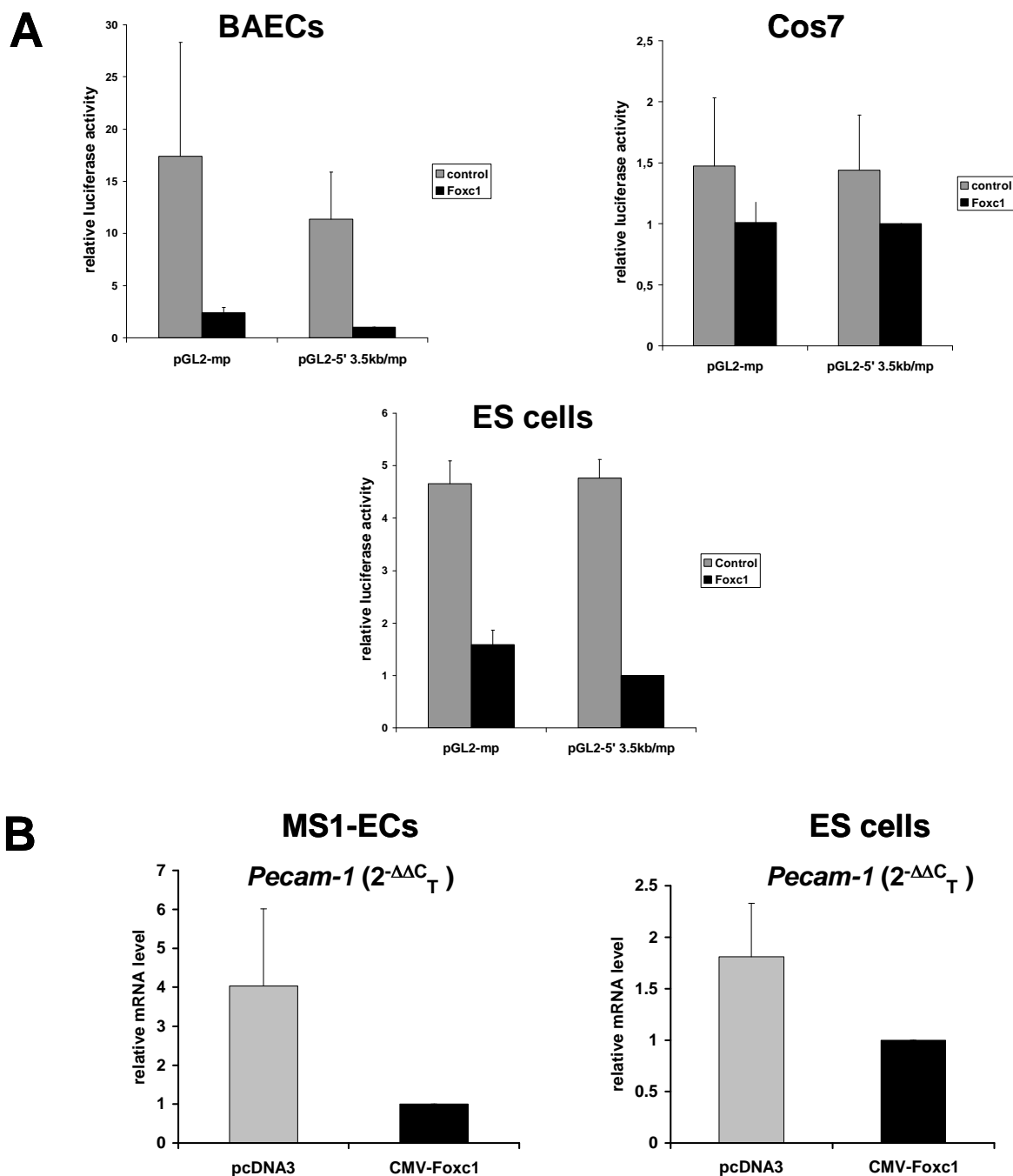


Figure 12. Legend next page

**Figure 12. A)** *Pecam-1* transactivation by *Foxc1* is specific for eEPCs.  $1 \times 10^5$  BAECs, ES cells, or Cos7 cells were transiently transfected with 2.4  $\mu\text{g}$  of CMV-*Foxc1* (black bars) or pcDNA3 (gray bars) together with 0.3  $\mu\text{g}$  of pGL2-mp or pGL2-5'3.5kb/mp and 10 ng of HSV-*tk-Renilla* to normalize, followed by luciferase assays after 24 hours. Luciferase activity derived from the co-transfections with pGL2-5' 3.5kb/mp and CMV-*Foxc1* was set to an arbitrary value of 1 and all other luciferase values were normalized accordingly. Note that luciferase values are normalized independently for each cell line and values in the charts do not represent absolute luciferase units. BAECs, ES cells, or Cos7 cells do not activate reporter expression through pGL2-5'3.5kb/mp in response to *Foxc1* (black bars). Luciferase assays were carried out in triplicates and repeated at least twice and bars represent average values ( $n > 9$ ). The standard deviation is indicated for each bar. **B)** Quantitative Real-Time PCR (qPCR) shows a decrease in endogenous *Pecam-1* mRNA levels in MS1-ECs and ES cells after overexpression of *Foxc1*.  $5 \times 10^6$  MS1-ECs or ES cells were transiently transfected with 8  $\mu\text{g}$  of CMV-*Foxc1* plasmid (black bars) or pcDNA3 as control (gray bars). Cells were lysed 24 hours after transfection and total RNA was subjected to RT-PCR, followed by qPCR. Endogenous *Pecam-1* mRNA levels decrease about 4-fold (MS1-ECs) or about 2-fold (ES cells) in response to *Foxc1* expression. The mRNA level in CMV-*Foxc1*-transfected cells was set to an arbitrary value of 1 and the mRNA level in control cells was normalized accordingly for each cell line. The relative mRNA levels for each sample were calculated using the  $2^{-\Delta\Delta C_T}$  method and normalized to  $\beta$ -*actin* expression; qPCRs were carried out in triplicates with mRNA from two independent experiments. ( $n = 6$ ). The standard deviation is indicated for the control samples (gray bars).

### **3.9 Endogenous *Pecam-1* RNA analysis matches promoter activation studies**

To corroborate the promoter studies, activation of endogenous *Pecam-1* expression in response to *Foxc1* was studied. Figure 13 summarizes the data, showing that *Pecam-1* transcript levels are elevated only in eEPCs after *Foxc1* expression.

In contrast, mature endothelial lines (MS1-ECs, H5V-ECs, BAECs), which express constitutively high levels of *Pecam-1*, do not upregulate *Pecam-1* expression after transient transfection of CMV-*Foxc1* plasmid. Undifferentiated ES cells express *Pecam-1*, but - like in mature endothelial cells - transcript levels are not influenced by the presence of *Foxc1* in the cells (Fig. 13). Non-endothelial lines such as Cos7 cells and 3T3 mouse fibroblasts do not express *Pecam-1*, and no de novo activation is seen after *Foxc1* expression is induced. Thus, it appears that endogenous upregulation of *Pecam-1* after *Foxc1* induction is confined to embryonic EPCs indicating that the *Pecam-1* response is cell-context specific.

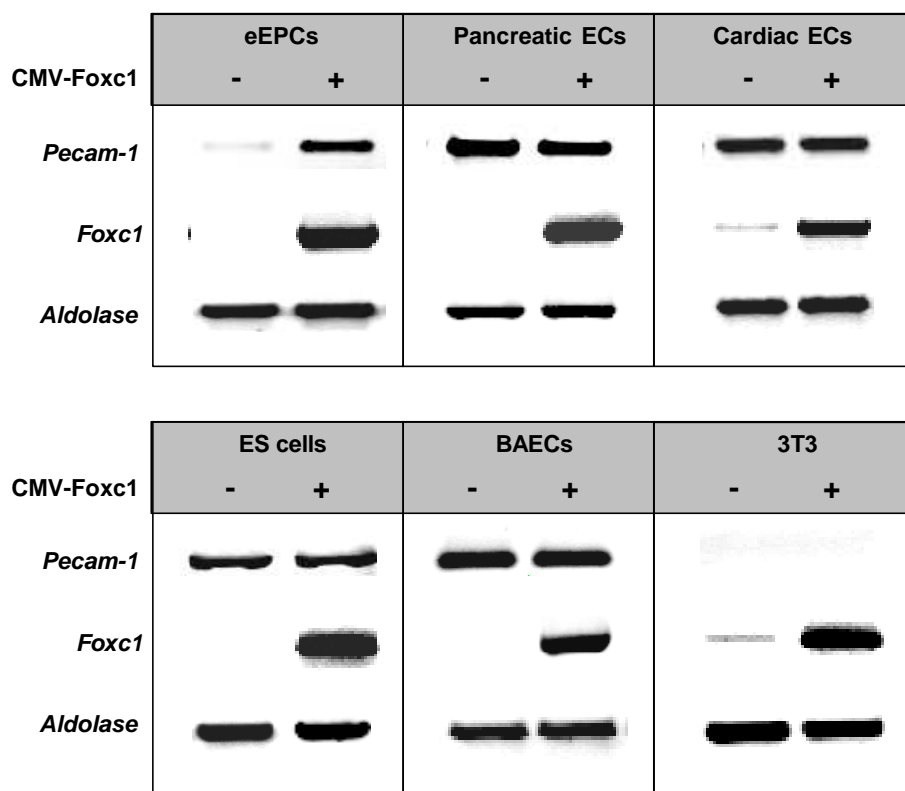


**Figure 13.** Foxc1 induction of the endogenous *Pecam-1* gene is restricted to eEPCs.  $5 \times 10^6$  eEPCs, MS1-ECs, H5V-ECs, ES cells, BAECs, or 3T3 fibroblasts were transiently transfected with 8  $\mu$ g of CMV-Foxc1 (+) or pcDNA3. (-). Cells were lysed 24 hours after transfection and total RNA was subjected to RT-PCR. Foxc1 activates *Pecam-1* expression only in undifferentiated eEPCs. BAECs, MS1-ECs, H5V-ECs, and ES cells express high *Pecam-1* and the expression levels are not elevated in response to Foxc1. Fibroblasts (3T3) do not express *Pecam-1*. Aldolase is shown as normalization control. RNA was isolated from at least three different experiments and PCR was repeated at least twice. Shown is a representative result.

### **3.10 Dose-dependent activation of the *Pecam-1* promoter by Foxc1**

In a new round of transfection experiments in eEPCs, a stepwise decrease of the amount of Foxc1-expression vector – from a 4-fold molar excess compared to reporter plasmid pGL2-5'3.5kb/mp, to a 2-fold molar excess and to an equimolar amount - resulted in a consistent drop of the reporter gene activity from 100% to 76% and to 35%, respectively (Fig. 14). Thus, the activation of reporter expression through the 5'-flanking 3.5kb-fragment in response to Foxc1 is dose-dependent and

requiring relatively high Foxc1 expression levels. This result suggests that Foxc1, or an intermediate, might act through a weak binding site.

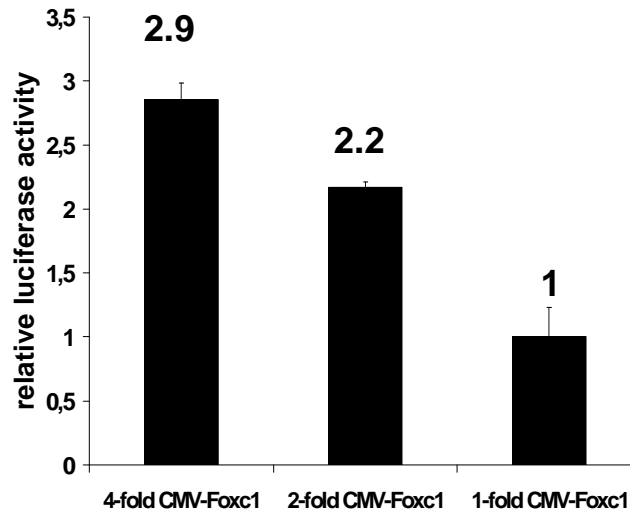


**Figure 14.** Responsiveness of pGL2-5'3.5kb/mp to Foxc1 in eEPCs is dose dependent.  $5 \times 10^5$  eEPCs were transiently transfected with 0.3  $\mu\text{g}$  of pGL2-5'3.5kb/mp and 10 ng of HSV-*tk-Renilla* to normalize, together with CMV-Foxc1 at 4-fold, 2-fold and equal molar amounts, followed by luciferase assays after 24 hours. Luciferase activity derived from the co-transfections with CMV-Foxc1 in an equimolar amount was set to an arbitrary value of 1 and all other luciferase values were normalized accordingly. The reporter gene activity decreases in correlation with lowered CMV-Foxc1 amounts. The relative luciferase values are shown above each bar. Luciferase assays were carried out in triplicates and repeated once with bars representing average values ( $n = 6$ ). The standard deviation is indicated for each bar.

### **3.11 Activation of the *Pecam-1* promoter takes place in multiple, independently isolated eEPC clones**

Embryonic EPCs are primary cell lines isolated from single or pools of mouse E7.5 embryos. To ensure that the observed induction of *Pecam-1* by Foxc1 does not depend on the cell isolation, the promoter/enhancer analysis was performed in three independently isolated eEPC lines, namely T17b, T19b and FT4b. After transient transfection with the *Pecam-1* promoter plasmids (outlined above in Fig. 8) and CMV-Foxc1, reporter gene activation through pGL2-5'3.5kb/mp was seen in all three different eEPC clones, resulting into a 3,67, 3,72 and 4,01-fold induction after Foxc1 expression as compared to control eEPCs (pcDNA3 transfected; Fig. 15). The results

showed that *Pecam-1* upregulation in response to Foxc1 is taking place at comparable levels in independently isolated eEPC lines.

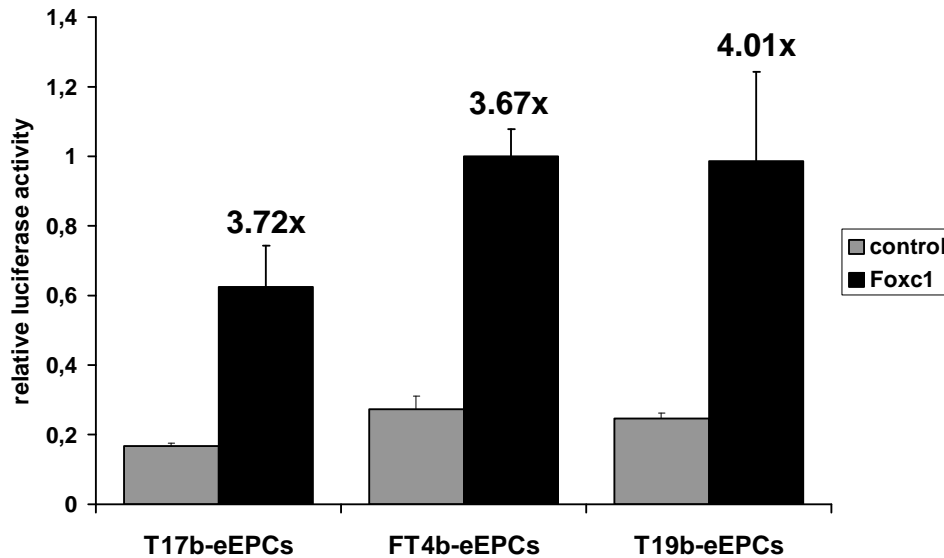


**Figure 15.** *Pecam-1* activation by Foxc1 takes place in different eEPC clones.  $5 \times 10^5$  cells from three independent eEPC clones (T17b, FT4b, T19b) were transiently transfected with 2.4  $\mu$ g of CMV-Foxc1 (black bars) or pcDNA3 (gray bars) together with 0.3  $\mu$ g of pGL2-5'3.5kb/mp and 10 ng of HSV-*tk-Renilla* to normalize, followed by luciferase assays after 24 hours. Luciferase activity derived from the co-transfections with pGL2-5'3.5kb/mp and CMV-Foxc1 was set to an arbitrary value of 1 for each clone and corresponding control luciferase values were normalized accordingly. The fold activation of reporter expression through pGL2-5'3.5kb/mp in response to Foxc1 is indicated for each clone. Luciferase assays were carried out in triplicates and repeated once, and bars represent average values ( $n = 6$ ). The standard deviation is indicated for each bar.

### **3.12 *Pecam-1* promoter activity – Summary**

In summary, Foxc1 activates a 3.5kb-fragment located in the distal 5'-flanking area of *Pecam-1* and induces transcription in embryonic endothelial progenitor cells (Fig. 16). In contrast, mature endothelial lines, such as bovine aortic cells, pancreatic ECs and cardiac ECs drive high endogenous levels of *Pecam-1* expression through regulatory sequences located within the 4.5kb-intronic fragment. Exogenous Foxc1 protein does not affect expression in mature endothelial cells. ES cells display moderate activity of the proximal promoter located directly upstream of the *Pecam-1*

transcription start and, as with mature endothelial cells, gain of *Foxc1* function does not increase *Pecam-1* expression nor does it induce luciferase activity of the promoter/enhancer constructs. The promoter elements have no activity in Cos7 cells, regardless of *Foxc1*, in accordance with the fact that Cos7 cells represent a *Pecam-1* negative non-endothelial cell population [223].

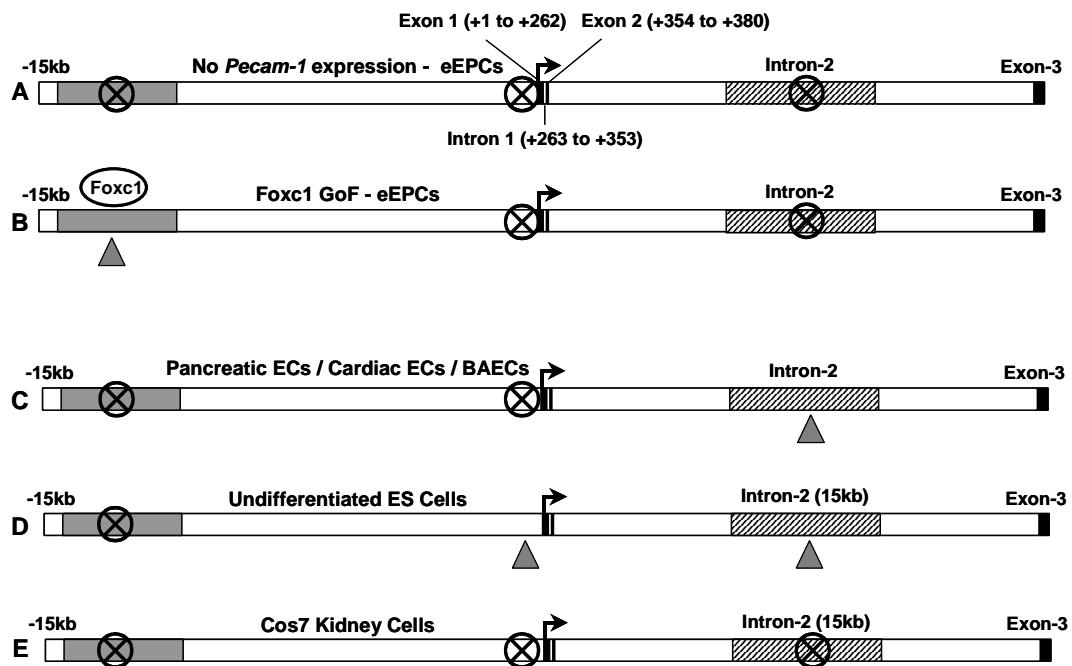


**Figure 16.** Summary of *Pecam-1* Promoter regulation in different cell types. **A)** Undifferentiated eEPCs do not show cis-regulatory activity of the distal 5'-flanking 3.5kb fragment (gray box), the proximal promoter areas (around Exon-1), or the 4.5kb fragment (black-white striped box) in the second intron. **B)** Gene transcription is activated through the distal 5'-flanking 3.5kb fragment after *Foxc1* expression **C)** Mature endothelial cells (pancreatic ECs, cardiac ECs, bovine aortic ECs) have high endogenous *Pecam-1* expression driven by the 4.5kb fragment located within the second intron (gray triangle). The activity of the intronic enhancer is independent of *Foxc1*. **D)** Undifferentiated ES cells drive *Pecam-1* expression through the proximal promoter area as well as through the intronic 4.5kb fragment (gray triangles). **E)** Cos7 kidney cells do not express *Pecam-1* and display no activity of the different promoter elements, regardless of *Foxc1* expression. All inactive promoter elements are indicated by a black circled X; GoF = Gain of Function.

### 3.13 Localization of *Foxc1*-responsive sites

Next, the 5'-flanking 3.5kb-fragment (-13,597 to -10,063) was scrutinized for putative sites responding directly or indirectly to *Foxc1*. Using PCR amplification, the whole 3.5kb-fragment was separated into three pieces (-13,597 to -12,547; -12,568 to -



11,499; -11,520 to -10,063), which were sub-cloned into the luciferase reporter vector upstream from minimal promoter regulatory sequences (-88 to +57), yielding the promoter plasmids pGL2-5'1kb(A)/mp (-13,597 to -12,547), pGL2-5'1kb(B)/mp (-12,568 to -11,499), and pGL2-5'1.5kb/mp (-11,520 to -10,063) (Fig. 17A).

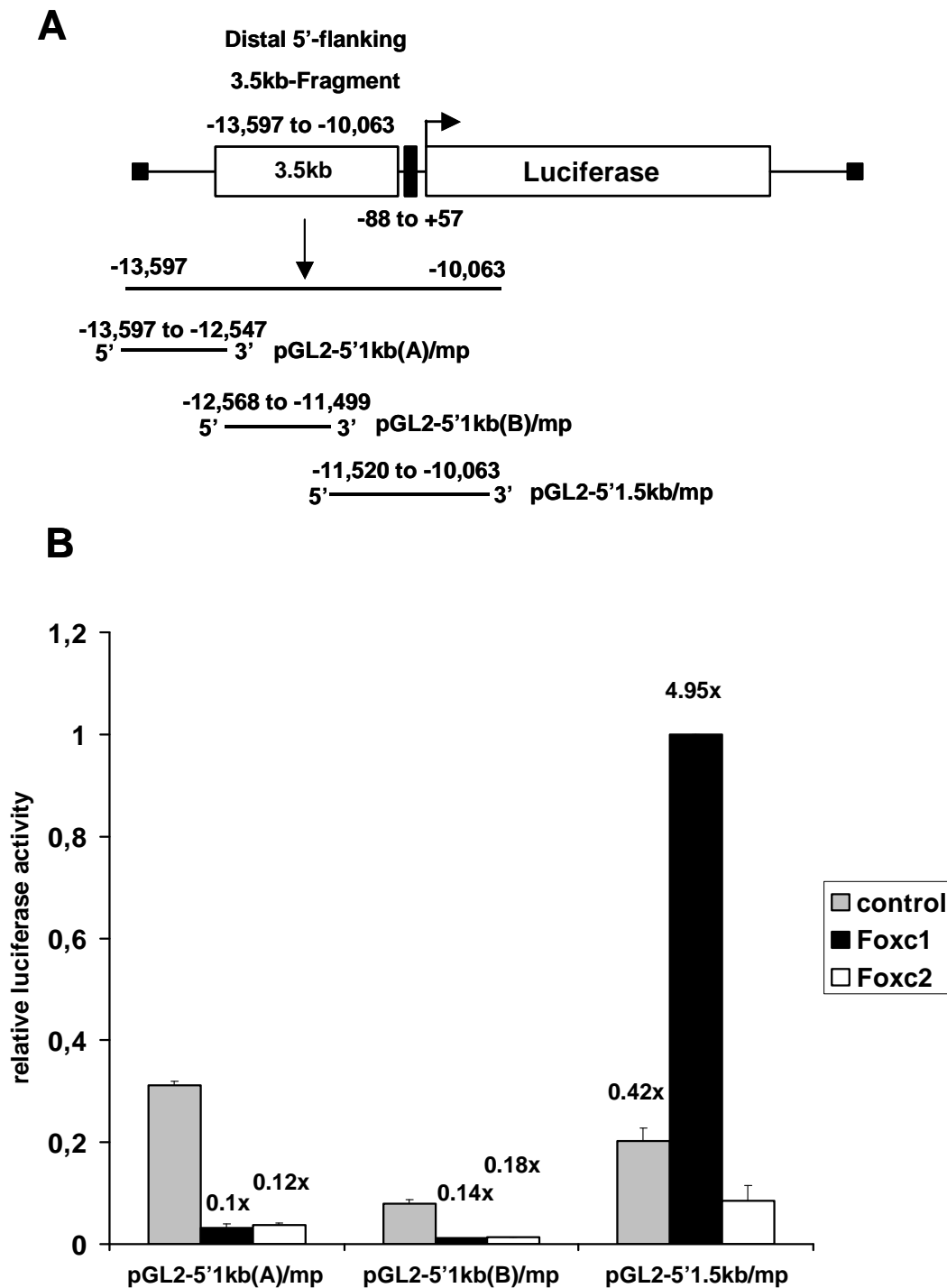


Figure 17. Legend next page

**Figure 17.** Localization of Foxc1 binding sites within the 3.5kb upstream element. **A)** The distal 5'-flanking 3.5kb-fragment inside pGL2-5'3.5kb/mp was divided into three fragments, followed by sub-cloning into pGL2-mp, yielding promoter plasmids pGL2-5'1kb(A)/mp (-13,597 to -12,547), pGL2-5'1kb(B)/mp (-12,568 to -11,499) and pGL2-5'1.5kb/mp (-11,520 to 10,063). Details are described in Material and Methods. **B)**  $5 \times 10^5$  eEPCs were transiently transfected with 2.4  $\mu\text{g}$  of CMV-Foxc1 (black bars), CMV-Foxc2 (white bars), or pcDNA3 (gray bars), together with 0.3  $\mu\text{g}$  of pGL2-5'1kb(A)/mp, pGL2-5'1kb(B)/mp, and pGL2-5'1.5kb/mp and 10 ng HSV-*tk-Renilla* to normalize. Luciferase activity derived from the co-transfections with pGL2-5'1.5kb/mp and CMV-Foxc1 was set to an arbitrary value of 1 and all other luciferase values were normalized accordingly. pGL2-5'1.5kb/mp responds to Foxc1 and drives reporter gene expression. No reporter transcription through pGL2-5'1.5kb/mp is seen in CMV-Foxc2 or pcDNA3 transfected cells. The fold-change in response to Foxc1 or Foxc2 is indicated for each bar. Luciferase assays were carried out in triplicates and repeated at least three times and bars represent average values ( $n > 9$ ). The standard deviation is indicated for each bar. All nucleotide numbering is relative to the transcription initiation site (+1) and is based on the numbering system of the UCSC Genome Bioinformatics Database (<http://www.genome.ucsc.edu>).

We then tested the ability of Foxc1 to induce the activity of the three sub-fragments in eEPCs. The results showed that the ca. 1.5kb-long sequence derived from the 3'-part of the 3.5kb-fragment (pGL2-5'1.5kb/mp) - distal to the *Pecam-1* transcription start - responded to Foxc1 leading to about 5-fold increase in luciferase activity compared to control, empty vector-transfected, cells (Fig. 17B). In contrast, the remaining 2kb-long sequence, which is sub-divided into two fragments about 1kb in length (pGL2-5'1kb(A)/mp and pGL2-5'1kb(B)/mp), does not respond to Foxc1, and reporter gene activity even drops about 10- and 7-fold, respectively, compared to control cells. The data indicate that putative Foxc1 regulatory elements are located within the 1.5kb-fragment. As with the intact 3.5kb fragment, activation of reporter gene expression through pGL2-5'1.5kb/mp was only seen in response to Foxc1, but not to Foxc2 (which led to approximately 2-fold decrease in activity compared to control cells) (Fig. 17B).

### **3.14 Analysis of the *Pecam-1* promoter using Bioinformatic Tools**

The responsiveness of the 1.5kb-sub-fragment within the distal element raised the possibility that this might be due to direct binding in this area. To test this idea, I analyzed the nucleotide sequence using the NCBI Nucleotide database (<http://www.ncbi.nlm.nih.gov/>) as well as the UCSC Bioinformatics Database (<http://www.genome.ucsc.edu/>) for putative, consensus Fox binding sites.

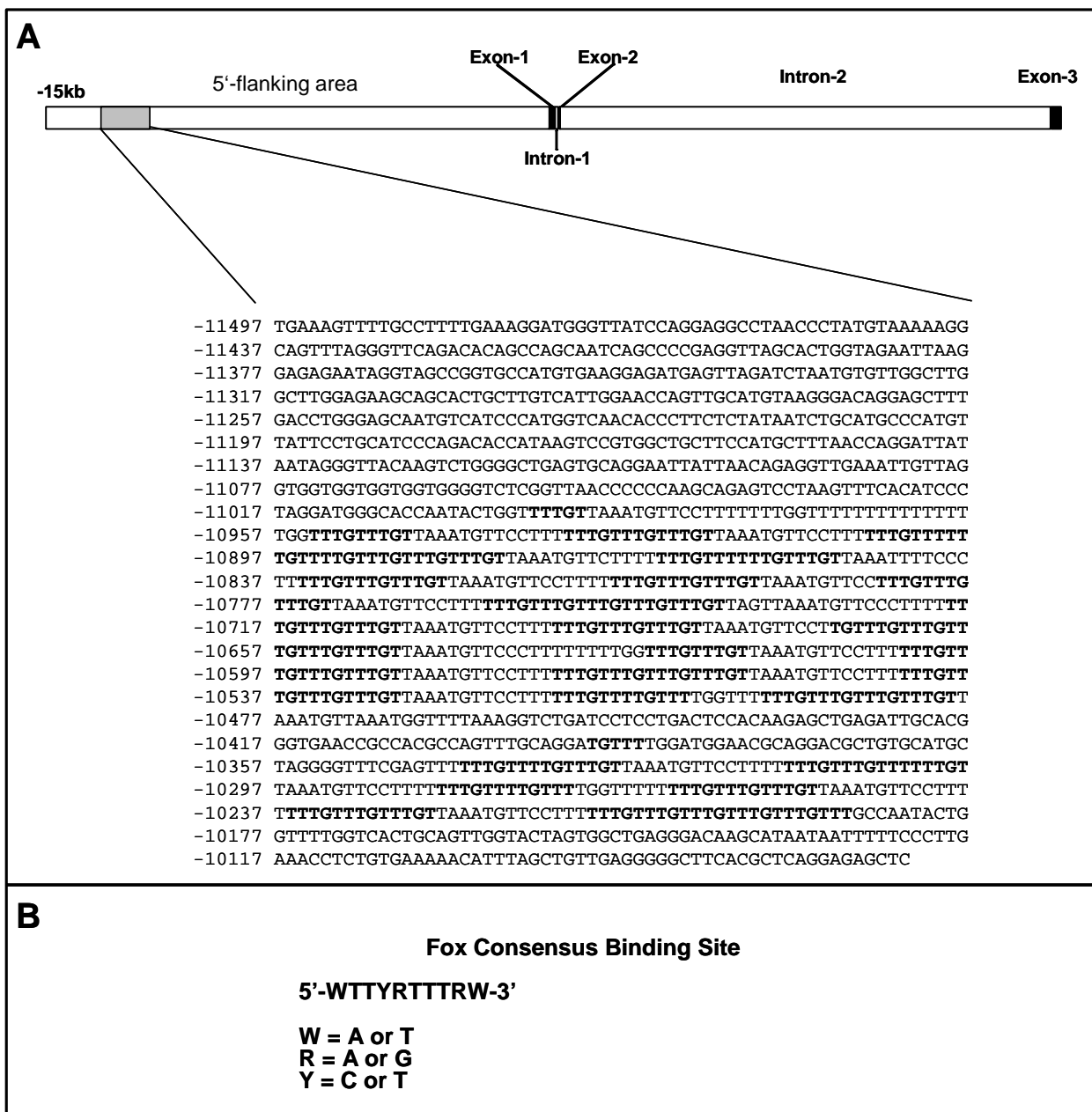


**Figure 18.** The Foxc1-response element contains multiple Foxc1 “core” binding sites. **A)** The distal 5'-flanking 1.5kb-fragment (-11,520 to -10,063 - gray box) of mouse *Pecam-1* contains a block of 61 ‘TTTGT’ pentanucleotide repeats , spanning from -10,995 to -10,478. A second, shorter block of 20 ‘TTTGT’ pentanucleotide repeats is located immediately downstream and spans from -10,390 to -10,188. Shown is the nucleotide sequence from -11,497 to -10,063. All nucleotide numbering is relative to the transcription initiation site (+1) of *Pecam-1* (<http://www.genome.ucsc.edu>). The pentanucleotide repeats are shown in bold and are separated by short stretches of nucleotides. **B)** Consensus Fox binding site (see text for details). The pentanucleotide ‘TTTGT’ is part of the consensus sequence.

This analysis showed that the genomic 1.5kb-fragment (-11,520 to -10,063) contains two non-connected stretches of ‘TTTGT’ pentanucleotide repeats (‘ACAAA’ in

reverse orientation), spanning from -10,995 to -10,478 and -10,390 to -10,188 (Fig. 18A). Interestingly, the pentanucleotide sequence 'TTTGT' is the core of the Fox transcription factor binding site consensus sequence, which is defined as 5'-WTTYRTTTRW-3' (W = A or T; R = A or G; Y = C or T) [224]. Within the repetitive blocks found within the *Pecam-1* distal element, the single 'TTTGT' repeats are separated by short stretches of nucleotides. The presence of a microsatellite repeat containing the core sequence of the Fox binding site raised the possibility that this (TTTGT)<sub>n</sub> microsatellite repeat motif could function as a remote cis-regulatory site that is able to bind the transcription factor Foxc1 and take part in the transcriptional activation of the *Pecam-1* gene.

### **3.15 The (TTTGT)<sub>n</sub> motif is found at the human *PECAM-1* locus**

The unusual sequence arrangement within the mouse *Pecam-1* distal element prompted us to search if the microsatellite repeat motif is found in other species besides mouse. To this end, the sequence of the 1.5kb-fragment embracing the repeat motif was further analyzed with bioinformatics tools.

Using the Genomatix DiAlignTF software [220], an alignment of 20kb of the 5'-flanking sequence of the mouse *Pecam-1* gene displays several areas of cross species homology with the corresponding human genomic sequence of *Pecam-1*. The area that contains the (TTTGT)<sub>n</sub> motif within the mouse genomic sequence only aligns over a short distance with that of the human sequence (Fig. 19), indicating that a sequence block (-10,231 to -10,193) of the mouse (TTTGT)<sub>n</sub> microsatellite repeat displays moderate cross-species homology to a TG-rich sequence around 16kb upstream of the human *PECAM-1* gene (Fig 19). A second homology peak within the area of the microsatellite motif (-10,440 to -10,402) indicates a low cross-species homology stretch that is located between the major and minor block of 'TTTGT' repeats. However, the major parts of the two sequence blocks containing the (TTTGT)<sub>n</sub> repeat motif are not conserved between mouse and human, as seen by the absence of a homology histogram (Fig. 19). In contrast, the proximal promoter areas located directly upstream of the transcriptional start site of *Pecam-1* are strongly

conserved between the orthologue sequences (Fig. 19). In addition, various histograms indicating moderate to high homology can be found throughout the 20kb 5'-flanking sequence and - in addition to the proximal promoter areas - an area displaying very high cross-species homology to the human sequence is found around 19kb upstream of the mouse *Pecam-1* transcription initiation site (Fig. 19).

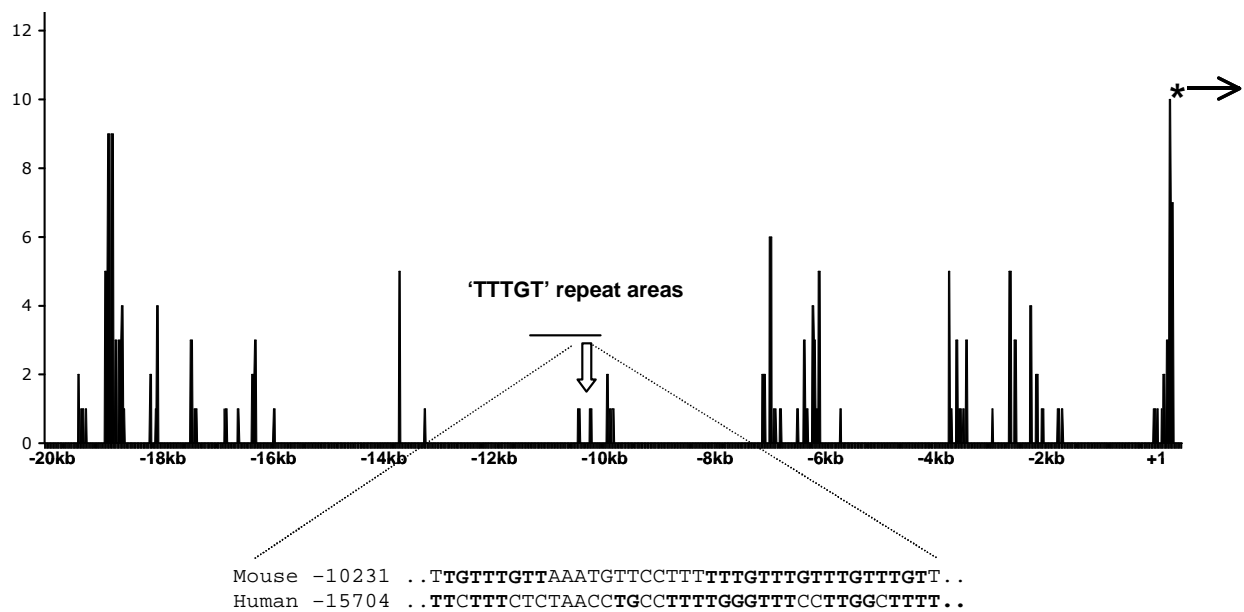


**Figure 19.** Cross Species homology upstream of the *Pecam-1* locus. Alignment of the respective *Pecam-1* genomic sequence of mouse and human. Homology areas between the two species are indicated by the histograms. The area containing the two blocks of 'TTTGT' repeats (-10,995 to -10,478 and -10,390 to -10,188) at the mouse 5'-flanking locus is indicated by the horizontal bar. A short stretch of low cross-species homology is seen in the area of the mouse 'TTTGT' microsatellite repeat (-10,231 to -10,193 - 'TTTGT' repeats in bold) as indicated by the vertical empty arrow. The neighbouring homology peak to the immediate left (-10,440 to -10,402) indicates a low cross-species homology area that is positioned between the major and minor block of 'TTTGT' repeats. The 'TTTGT' repeats are not conserved at the human *Pecam-1* locus, but rather represented by a TG-rich sequence motif, as indicated by the alignment below the graphic ('T' and 'G' in italic and underlined). The asterisk and the horizontal arrow indicate the start of transcription (+1) of the mouse *Pecam-1* gene - strong cross-species sequence homology is found in the area surrounding the transcription initiation site, and various homology areas of different intensity are present throughout the 20kb 5'-flanking area. The alignment was performed by means of the genomatix "DiAlignTF" Tool (<http://www.genomatix.de>), using the nucleotide sequences derived from the NCBI Entrez Gene MapViewer (<http://www.ncbi.nlm.nih.gov/sites/entrez>). The relative degree of cross-species homology is indicated on the y-axis and is based on the output of the DiAlignTF sequence alignment, ranging from '0' (no homology) to '10' (very high homology). The overall nucleotide similarity of the two aligned sequences was calculated as 7% by the DiAlignTF program. All nucleotide numbering is relative to the transcription initiation site (+1) of the mouse *Pecam-1* gene and is based on the NCBI Entrez Gene MapViewer sequence.

Although we did not attempt to further analyze potential transcription factor binding sites, it is very well possible that these homology areas contain cis-regulatory motifs that may partake in the activation or repression of *Pecam-1* expression.

Using the MatInspector software [219], the 40kb 5'-flanking genomic sequence of the human *PECAM-1* locus was screened for the presence of potential Foxc1 binding sites and/or 'TTTGT' repeat motifs, as found at the mouse *Pecam-1* locus. As shown in Figure 20, the analysis picked several areas at the human locus that contain blocks of 'TTTGT' repeats, ranging from two up to six repeat units.

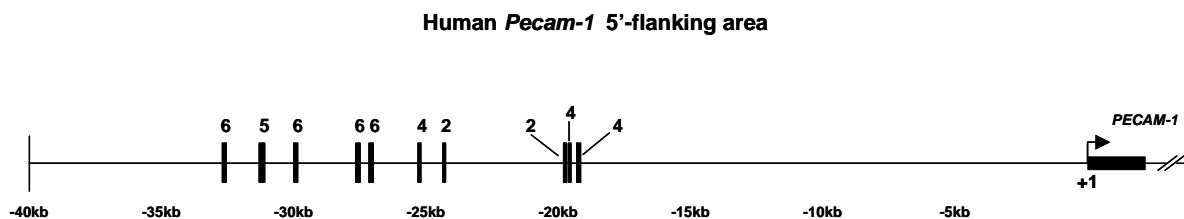


**Figure 20.** The human *PECAM-1* locus contains various short (TTTGT)<sub>n</sub> repeat motifs. **A)** The 5'-flanking sequence (40kb) of the human *PECAM-1* gene was screened for putative Forkhead Transcription Factor binding sites using the genomatix MatInspector Software (<http://www.genomatix.de>). The schematic graphic depicts areas containing 'TTTGT' repeats (black boxes) that were identified by the software as Forkhead binding sites. The upstream area between -33kb and -19kb contains several blocks of 'TTTGT' repeats. The number of single repeat units of each block is shown above the boxes, indicating a total of 45 identified repeat units. The width of the boxes reflects the total length of the sequence stretch embracing the repeats units.

The MatInspector analysis identified those repeats as Forkhead binding site with 'CAA' (reverse for 'TTTG') as core sequence. Likewise, the major block of 'TTTGT' repeats in the mouse sequence is identified by the software to contain numerous Forkhead binding sites with the same core sequence, thus allowing us to make the claim that the identified repeats in the human locus may serve as regulatory motifs and potential Foxc1 binding sites during human *PECAM-1* expression.

The number of repeat units was lower at the human locus than at the mouse locus. Our analysis showed that the human *PECAM-1* 5'-flanking area contains an overall of nine short blocks of 'TTTGT' repeats identified by the software, indicating a total of 45 'TTTGT' repeat units. However the repeat blocks were distributed over a range of 14kb (from around -33kb to -19kb) in the 5'-flanking area of the human *PECAM-1* gene. All identified 'TTTGT' sequence repeats and their corresponding nucleotide positions in relation to the human *PECAM-1* transcription initiation site are listed in Table 2.

Repeat Units	Position
6	-32,941
5	-31,569
6	-30,221
6	27,885
6	-27,372
4	-25,541
2	-24,720
2	-20,005
4	-19,884
4	-19,435

**Table 2.** Listing of 'TTTGT' repeats in the distal 5'-flanking area of the human *PECAM-1* gene. The left column shows the number of single repeat units; right column indicates the first nucleotide position of each repeat motif.

To further verify the possibility that the (TTTGT)<sub>n</sub> repeat motifs serve as putative cis-regulatory sites at the human *PECAM-1* locus, an experimentally verified Foxc1 binding site at the mouse *Tbx1* locus that was shown to be involved as cis-regulatory element in the expression of *Tbx1* [195], was identified by the MatInspector software as Forkhead binding site with 'CAAA' as core binding site (data not shown), as seen for the (TTTGT)<sub>n</sub> repeat motifs at the mouse and human *Pecam-1* locus. This strengthened our assumption that, like in the mouse, transcriptional control of the human *PECAM-1* gene may involve the randomly distributed (TTTGT)<sub>n</sub> repeat motifs (Fig. 20).

### **3.16 Deletion of the repeat motif abolishes promoter activity**

To test the notion that the (TTTGT)<sub>n</sub> repeat motif has cis-acting regulatory activity, the 1.5kb-fragment (pGL2-5'1.5kb/mp) containing the microsatellite sequence was deleted stepwise from the 5'-end using site-directed PCR mutagenesis, as described in Material and Methods. Figure 21 summarizes the obtained data, showing that a decrease in reporter gene activity correlated with a stepwise deletion of the (TTTGT)<sub>n</sub> repeats. A deletion of 612bp (-11,495 to -10,884) from the 1.5kb fragment encompassing 10 'TTTGT' repeats (promoter plasmid pGL2-5'1.5kbD2/mp) or 755bp (-11,495 to -10,741) with 28 'TTTGT' repeats (promoter plasmid pGL2-

5'1.5kbD3/mp), or 1038bp (-11,495 to -10,458) covering the major block of 61 'TTTGT' repeats (promoter plasmid pGL2-5'1.5kbD4/mp) led to a decrease of reporter activity of 20% and 49% and 73%, respectively.

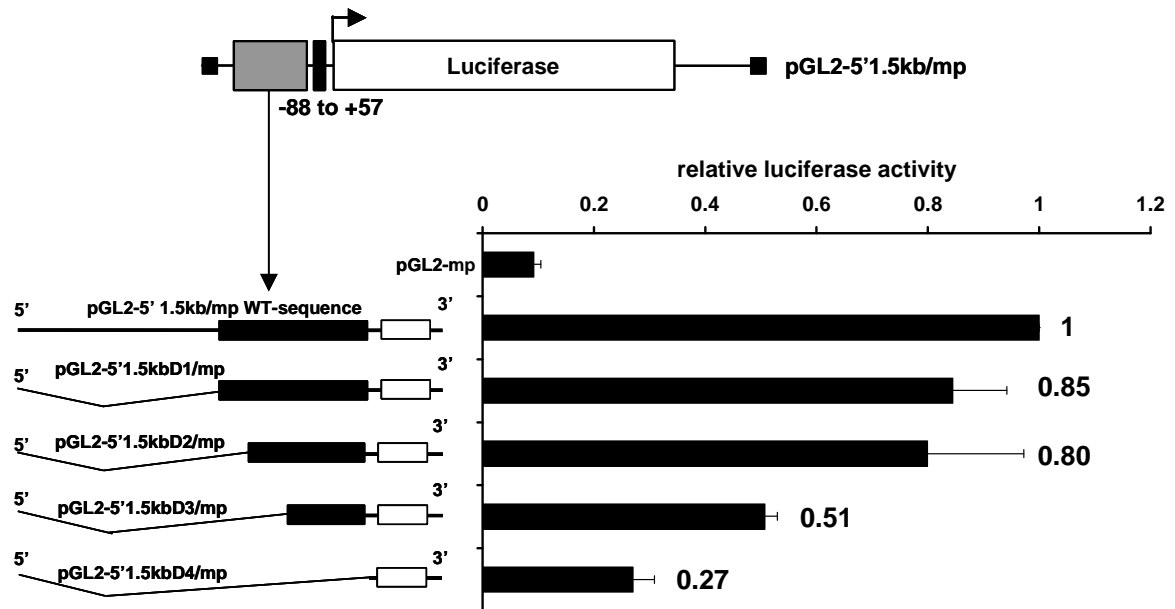


**Figure 21.** Deletion analysis of the Foxc1-responsive repetitive element. The (TTTGT)<sub>n</sub> repeat motif was deleted stepwise as described in Materials and Methods, using pGL2-5'1.5kb/mp (-11,520 to -10,063) as DNA template. 5x10<sup>5</sup> eEPCs were transfected with 0.3 µg of pGL2-5'1.5kb/mp, pGL2-5'1.5kbD1/mp (deletion -11,495 to -11,020 - no TTTGT repeats), pGL2-5'1.5kbD2/mp (deletion -11,495 to -10,884 - 10 TTTGT repeats), pGL2-5'1.5kbD3/mp (deletion -11,495 to -10,741 - 28 TTTGT repeats), pGL2-5'1.5kbD4/mp (deletion -11,495 to -10,458 - all 61 TTTGT repeats) or pGL2-mp, together with 2.4 µg of CMV-Foxc1 (black bars) or pcDNA3 (data not shown). Sequential deletion of the (TTTGT)<sub>n</sub> repeats results into a stepwise decrease of 20%, 49% or 73% of reporter gene activity in response to Foxc1. Deletion of the sequence upstream of the (TTTGT)<sub>n</sub> repeat motif results into a decrease of 15% of reporter gene activity. pGL2-mp was used as control. The black boxes indicate the major block of 'TTTGT' repeats (-10,995 to -10,478). The white box indicates the minor 'TTTGT' repeat block (-10,390 to -10,118) that was not deleted. The luciferase signal derived from the co-transfections of CMV-Foxc1 with pGL2-5'1.5kb/mp was set to an arbitrary value of 1 and all others values were normalized accordingly. Luciferase assays were carried out in triplicates and repeated twice and bars represent average values (n = 9). The standard deviation is indicated for each bar.

Still, an activity of 27% of the original pGL2-5'1.5kb/mp promoter plasmid remained after the major block of 'TTTGT' repeats was deleted. The minor second block containing 20 'TTTGT' repeats (-10,390 to -10,188) appears to be able to drive transcriptional activity compared to the minimal promoter alone (pGL2-mp) (Fig. 21). In addition, a deletion comprising 476bp (-11,495 to -11,020) of the sequence



upstream of the (TTTGT)<sub>n</sub> repeat motif (promoter plasmid pGL2-5'1.5kbD1/mp) leads to a decrease of 15% of the luciferase activity, possibly caused by the removal of positive regulatory elements in that area which may respond to eEPC-nuclear protein. In brief, the data show that the (TTTGT)<sub>n</sub> repeat motif is responsible of driving reporter gene transcription in response to Foxc1 expression and has cis-acting regulatory activity.

### **3.17 Foxc1 binds the (TTTGT)<sub>n</sub> motif on native chromatin**

In the previous experiments, Foxc1 protein was shown to bind the (TTTGT)<sub>n</sub> repeat motif on a promoter plasmid *in vitro*. To examine if this interaction can take place *in vivo*, the binding of Foxc1 protein at the chromosomal *Pecam-1* locus was analyzed using chromatin immunoprecipitation (ChIP) analysis. As shown in Figure 22, PCR primers were used to amplify a 599bp fragment (-11,039 to -10,441) that contains the major block of the 61 'TTTGT' repeats (-10,995 to -10,478) in the distal 5'-flanking area of mouse *Pecam-1* (Fig. 22A). The primers amplified sonicated eEPC chromatin that was precipitated with an anti-Foxc1 goat polyclonal antibody (Fig. 22B), but no amplification took place on chromatin precipitated with a goat Isotype IgG control antibody. The Input DNA sample (sonicated total eEPC chromatin) showed a positive control signal, whereas the PCR reaction with no template chromatin (H<sub>2</sub>O) was negative and proved the specificity of the PCR reaction. In addition, eEPC chromatin was amplified with a primer pair that spans a 171bp sequence upstream of the repeat motif (-13,021 to -12,851) and served as negative non-binding control site for Foxc1 in the distal 5'-flanking area of *Pecam-1*. No amplification of anti-Foxc1 goat polyclonal antibody-precipitated chromatin was seen in the PCR with these primers (Fig. 22B).

In addition, goat Isotype IgG antibody-precipitated chromatin and Input DNA showed no PCR signal and a positive signal, respectively. Finally, control PCR (no template chromatin) did not yield a PCR product, indicating the specificity of the observed

amplicons. In order to increase the interpretation of the experiment, the PCR bands were evaluated by means of agarose gel densitometry.

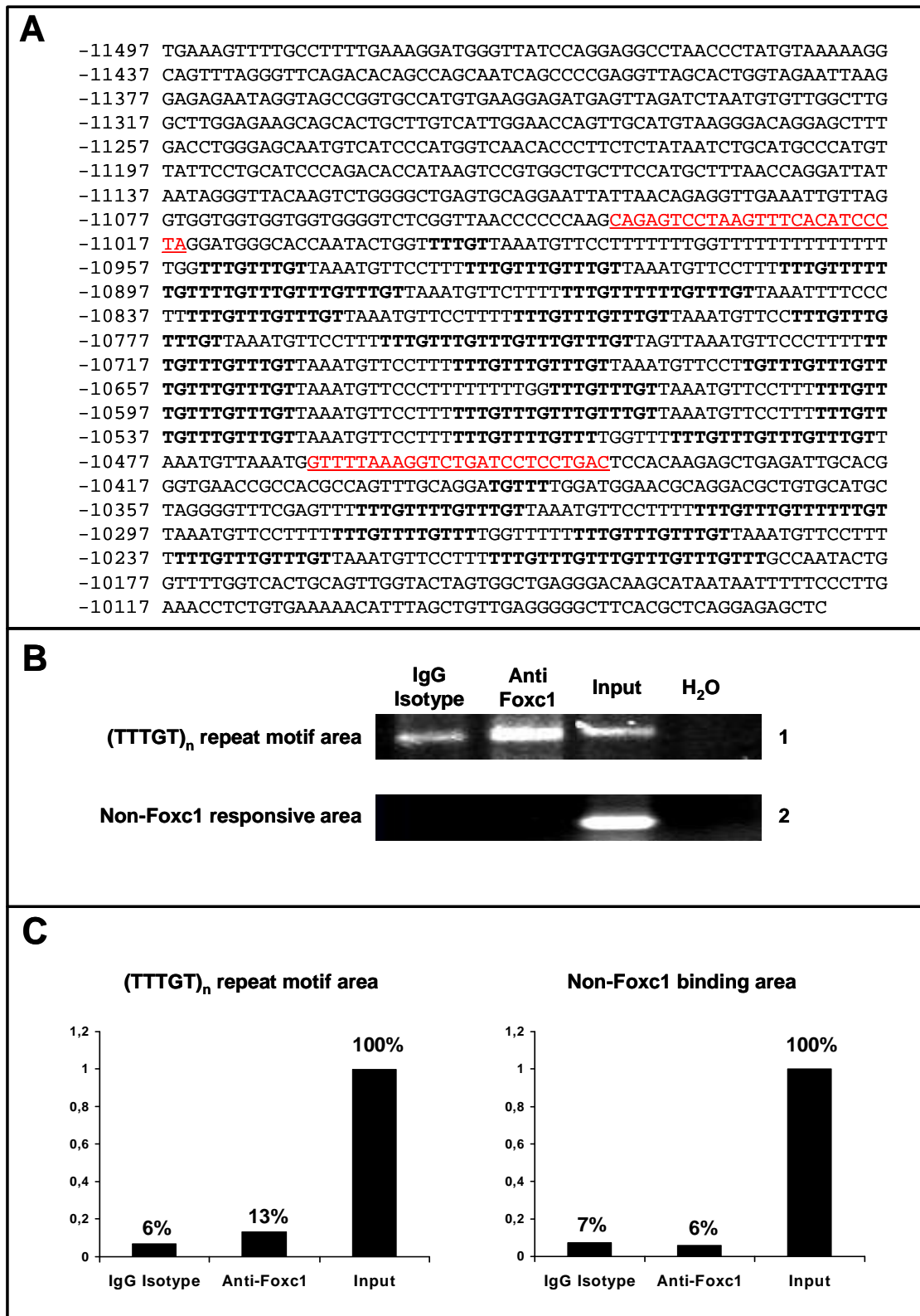


Figure 22. Legend next page

**Figure 22.** Chromatin Immunoprecipitation (ChIP) to assess Foxc1 binding to the repetitive (TTTGT)<sub>n</sub> element *in vivo*. **A)** Distal 5'-flanking sequence (-11,497 to -10,063) of the mouse *Pecam-1* locus containing the two blocks of 'TTTGT' pentanucleotide repeats (-10,995 to -10,478 and -10,390 to -10,188). Underlined red nucleotides point out the binding sites for the primers used to amplify immunoprecipitated eEPC chromatin. The primers amplify a 599bp fragment (-11,039 to -10,441) that contains the larger block of 'TTTGT' pentanucleotide repeats. **B)** For chromatin immunoprecipitation, 4x10<sup>7</sup> eEPCs were transiently transfected with 20 µg of CMV-Foxc1, followed by chromatin purification and immunoprecipitation with goat IgG Isotype as a negative control and anti-Foxc1 goat polyclonal. Sonicated total eEPC chromatin (Input) was used as positive PCR control. Chromatin was amplified by (1) PCR primers that span the major stretch of the (TTTGT)<sub>n</sub> repeat motif area in the distal 5'-flanking area of *Pecam-1* (as described in A); (2) PCR primers that amplify a 171bp fragment located in the 5'-flanking area of *Pecam-1* and upstream of the (TTTGT)<sub>n</sub> repeat motif (-13,021 to -12,851) and served as negative control non-binding site. H<sub>2</sub>O was also used as negative control. Foxc1 binds to the (TTTGT)<sub>n</sub> repeat motif, as indicated by the PCR-signal observed with anti-Foxc1 precipitated chromatin (1). The negative control primer do not amplify anti-Foxc1 precipitated chromatin, indicated by the missing PCR signal (2). Input chromatin is amplified by both PCR primers - Input chromatin was diluted to 10% in PCR-reaction (1). **C)** Quantification of PCR bands by means of gel densitometry. The intensity of the PCR signal from the Input was calculated for undiluted chromatin and set to an arbitrary value of 100%. All other values were normalized accordingly. ChIPs were performed twice. All nucleotide numbering is relative to the transcription initiation site (+1) and is based on the UCSC Genome Bioinformatics Database (<http://www.genome.ucsc.edu>).

The analysis showed that after amplification of the (TTTGT)<sub>n</sub> repeat motif area, the amount of chromatin precipitated with the anti-Foxc1 antibody is twice as high as IgG-precipitated chromatin (6% and 13% compared to the Input, Fig. 22C). In contrast, when the Non-Foxc1 binding area is amplified on the chromatin, no difference between anti-Foxc1- and IgG-precipitated chromatin was observed (Fig. 22C).

In brief, ChIP analysis confirmed binding of Foxc1 protein at the (TTTGT)<sub>n</sub> repeat motif on the chromatin in support of the reporter studies. It is noteworthy to mention that I also tried to analyze Foxc1 binding to the 'TTTGT' repeats by means of electrophoretic mobility shift assays (EMSA). Although we were able to induce a shift of a biotin-labeled probe consisting of four 'TTTGT' repeats with nuclear extract from Foxc1-expressing eEPCs, we could not definitively show that the shift was caused specifically by Foxc1 protein.

Thus, we took the *in vivo* promoter analysis one step further and attempted to study the specificity of this transcriptional mechanism in transgenic mice. To this end, LacZ *Pecam-1*-promoter constructs were cloned and used for pro-nucleus injections. However, attempts to create transient transgenic mouse embryos carrying the 5'-

flanking 1.5kb fragment (-11,520 to -10,063) in combination with the minimal promoter (-88 to +57) cloned in front of the LacZ reporter gene were not successful, thus not allowing further conclusions about the specificity and activity of the *Pecam-1* distal element transcriptional mechanism.

### **3.18 Results – Summary**

The data presented in this Ph.D. project have identified *Pecam-1* as a direct target of Foxc1 in embryonic endothelial progenitor cells. Promoter deletion analysis identified a fragment around 11kb upstream of the transcription initiation site that contains a Foxc1 responsive element. Sequence analysis identified a microsatellite sequence consisting of a (TTTGT)<sub>n</sub> pentanucleotide repeat motif that is arranged in two neighboring blocks. A stepwise deletion of this repeat motif causes a stepwise decrease in the ability of Foxc1 to drive reporter gene expression. Bioinformatics analysis revealed that this microsatellite sequence is also found randomly distributed in short blocks in the distal 5'-flanking area of the human *PECAM-1* gene. In accordance with the promoter activity assays, ChIP analysis showed that Foxc1 transcription factor binds to the (TTTGT)<sub>n</sub> repeat motif upstream of mouse *Pecam-1* on the chromosome *in vivo*. It is noteworthy that this molecular interaction was not observed in mature endothelial lines, such as mouse pancreatic and cardiac ECs, as well as bovine aortic ECs, nor in undifferentiated ES cells and Cos7 kidney cells, suggesting a specific role in the early stages of endothelial cell differentiation.

## **4. DISCUSSION**

Vascular development is a highly organized sequence of events requiring the spatial and temporal expression of specific genes. Endothelial differentiation from pluripotent stem cells through committed endothelial progenitors is one of the initial steps during blood vessel formation. Thereby, the expression of endothelial specific marker genes such as *Pecam-1* and *VE-cadherin* is associated with the differentiation process toward the endothelial lineage. In addition, recruitment and incorporation of EPCs at sites of adult neo-vascularization takes place as a multi-step process consisting of attraction, adherence, transendothelial migration and eventually differentiation.

In the last years, the identification of genomic regulatory sites of vascular specific genes has progressed the understanding about the transcriptional mechanisms required for vascular specific gene expression, although the mechanisms governing the transition from endothelial progenitor cells to endothelial cells are not well understood. In order to identify new molecular players during endothelial gene expression and differentiation, this Ph.D. thesis took advantage of embryonic EPC lines to study the involvement of the Forkhead transcription factor *Foxc1* in the EPC-differentiation process. The characterization of a *Foxc1* binding site embedded within a 'TTTGT' pentanucleotide microsatellite motif that drives endothelial-specific transcription of the *Pecam-1* gene preferentially in eEPCs is described herein and discussed below.

### **4.1 *Pecam-1* basal promoter activity reflects endogenous transcript levels**

*Pecam-1* promoter activity was driven by a 4.5kb-intronic fragment combined with the minimal promoter in mature aortic ECs, as well as at lower levels in pancreatic endothelial cells (MS1-ECs) and ES cells (Fig. 9A). Vascular-specific genes such as *Flk-1* and *Tie2* were shown to require an intronic enhancer for their endothelial-directed expression [87, 225], and *Pecam-1* may represent another example for this type of endothelial-specific gene expression regulation. The strong transcriptional activity of the 4.5kb intronic fragment is consistent with the high endogenous *Pecam-1* expression levels in BAECs, MS1-ECs and ES cells, whereas expression is

not seen in kidney cells and immature eEPCs, paralleled by a lack of activity of all four promoter plasmids (Fig. 9A,B). Further, reporter gene expression and endogenous *Pecam-1* activity are in accordance with *Pecam-1* expression being restricted primarily to the vascular endothelium and certain types of blood cells in adult life, whereas it is not expressed on the surface of epithelial cells, muscle cells, and fibroblasts, as well as other non-vascular cell lineages [62].

ES cells, which are derived from the inner cell mass of day 3.5 mouse embryos [222] express *Pecam-1* and, in addition to the intronic 4.5kb fragment, the long proximal promoter areas also drove reporter gene activity (Fig. 9A). Since pluripotent ES cells and terminally differentiated endothelial lineages represent different developmental stages, it is not unexpected that they may use different combinations of gene regulatory elements to drive stage-specific expression of *Pecam-1*. Overall, it is possible that the proximal promoter sequences and also the distal 5'-flanking 3.5kb-fragment are capable to drive expression during eEPC differentiation, but the strong cis-active elements that regulate transcription in mature endothelium are located within the intronic 4.5kb-fragment.

#### **4.2 Foxc1 induced *Pecam-1* expression reflects an eEPC-specific mechanism**

Transcriptional activation through the genomic 5'-3.5kb element might represent a stage-specific mechanism through a remote regulatory site in embryonic EPCs where Foxc1 is required to activate de novo *Pecam-1* expression. Consistent with this proposition, alterations in endogenous *Pecam-1* transcript levels in response to Foxc1 gain-of-function are only seen in eEPCs, but not in aortic, pancreatic and cardiac ECs, as well as undifferentiated ES cells (Fig. 13). It is also in agreement with the lack of significant Foxc1 expression in these cell types.

In general, gene expression is regulated by genomic sites that are located in close proximity of the transcription initiation site (TIS) of a gene, such as cis-active elements in the core promoter region. In addition, gene expression is also controlled by enhancer/silencer elements, which can be located within introns and upstream or downstream of the transcript and at great distances of up to one megabase from the TIS [226, 227]. It is possible that Foxc1 transcription factor plays a more significant

role activating gene transcription through enhancer regulatory sequences rather than being bound by regulatory elements within the core promoter of a target gene. Support of this suggestion comes from recent publications that identified Foxc1 binding sites at remote DNA loci upstream of the T-box transcription factor *Tbx1* or the Notch-ligand Delta-like 4 (*Dll4*) gene [181, 195].

In general, genes are expressed in different tissues or during distinct stages of development. In addition, gene expression can be activated in response to various external stimuli under normal or pathophysiological conditions. Extensive studies of how gene expression is regulated have established the model that the combined activity of multiple regulatory sites controls gene expression in a temporal and spatial manner [228, 229]. The identified Foxc1 binding site might represent such a tissue- and time-specific regulatory element that allows *Pecam-1* induction in early embryonic angioblasts (eEPCs). This would indicate an analogous situation as with the transcriptional control of *Tbx1* through Foxc1 and Foxc2, which exclusively drive its expression in the head mesenchyme and the pharyngeal endoderm of the embryo [195].

Moreover, cellular heterogeneity is an important factor of endothelial function. The vasculature has to adopt organ and tissue-specific characteristics, since every organ shares a specific interaction with the blood vessel system to meet its local requirements [14]. The phenotypic endothelial heterogeneity is mediated in part by temporal and spatial differences in gene expression and regulation [4], and also depends on the vascular bed the cells originate from. For example, lung, kidney and brain ECs were shown to have specific patterns of cell surface proteins [230, 231]. This molecular diversity is also regulated at the transcriptional level through tissue-specific regulatory elements [4].

### **4.3 *Pecam-1* expression is controlled by multiple factors**

Past studies showed that specific elements of the human *PECAM-1* promoter are capable to drive cell-line specific transcription of a reporter gene *in vitro*. For instance, a 1.3kb proximal 5'-flanking sequence of the human *PECAM-1* gene is lacking consensus TATA or CAAT binding elements, but contains multiple consensus

binding sites for different trans-acting factors, such as 2 NF- $\kappa$ B-sites, 4 Ets-sites, 3 Sp1-sites, 2 E-box-domains, 2 tandem GATA-associated sites, 4 GATA elements and 3 shear-stress responsive elements (SSRE) [94]. In addition, two retinoic-acid responsive elements are located in the core promoter and might be involved during transcriptional regulation. *In vitro* studies showed that NF- $\kappa$ B is involved in regulating *PECAM-1* expression in human myeloid cells, such as human promonocytic U937 cells and macrophages. TNF $\alpha$  elevated human *PECAM-1* promoter activity by 2.5-fold, and NF- $\kappa$ B was shown to function as downstream activator of this process in promonocytic cells. [232]. In turn, the transcription factor GATA-2 binds to a cis-acting GATA element at position -24 in the human *PECAM-1* promoter and drives optimal lineage specific expression in the megakaryocytic lines HEL and Dami [94]. Although activity of this core promoter element was described in megakaryocytes, it remained elusive if the same cis-regulatory elements are capable to drive human *PECAM-1* expression in endothelial cells and cells of the myeloid precursor lineage. Regardless, the studies showed that different transcription factors are responsible for *Pecam-1* expression in different lineages, showing that the tight restriction of *Pecam-1* gene expression to endothelial cells and certain leukocytes is most likely regulated on multiple levels and depends on the action of a multitude of trans-acting regulatory factors. This notion is further supported by transgenic mouse studies, which showed that the majority of endothelial-specific gene promoter constructs direct transcription of reporter genes to endothelial subpopulations in specific vascular beds. For example, short pieces of the promoter of *vWF* or *Tie2* only have the capacity to drive reporter gene expression in limited endothelial subpopulations [233, 234], whereas longer fragments of the 5'-or 3'-flanking loci extend the expression patterns to wider areas of the vascular tree [225, 235]. In that respect, the distal 5'-flanking *Foxc1* binding site could be required to regulate de novo *Pecam-1* expression in angioblasts during vasculogenesis.

#### **4.4 Expression of *Pecam-1* in isolated embryonic angioblasts requires a specific upstream regulatory element**

Depending on the cell type, *Pecam-1* is expressed constitutively – as in mature



endothelial cells - or requires the presence of special signals for inducible expression, as in monocytes, where *Pecam-1* expression is regulated during the maturation and differentiation to macrophages [236-238]. During *PECAM-1* activation in human myeloid cells, specific transcription factors, e.g. NF- $\kappa$ B in this case, account for its directed expression within the promonocytic lineage. This inducible expression most likely has a different type of molecular regulation than the constitutive expression found in mature endothelial cells [232]. In accordance, eEPCs may require the controlled activity of trans-acting factors such as *Foxc1* to initiate *Pecam-1* expression transiently in eEPCs during the transition from an undifferentiated to a differentiated cell stage, but this type of regulation is no longer required in mature endothelium of blood vessels. In mature endothelial cells constitutive *Pecam-1* expression appears to be driven by *Foxc1*-independent mechanisms (Fig. 12 and Fig. 13), involving cis-regulatory elements that are located within the minimal promoter and in the 4.5kb intronic enhancer (Fig. 9A) that do not require bound *Foxc1* protein for their activity. However, since mature endothelial lines – mouse and bovine alike - used in this project had *Pecam-1* expression driven through the intronic 4.5kb-fragment element, it is reasonable to speculate that human endothelial cells, such as human umbilical vein endothelial cells (HUVECs) would regulate *PECAM-1* expression by the same active promoter elements as mouse and bovine lines. Nevertheless, it appears that *Foxc1* might have an opposite role in mature endothelial cells since down-regulation of both endogenous *Pecam-1* expression, as well as reporter gene expression through *Pecam-1* promoter constructs, was observed after *Foxc1* expression.

In addition, *Pecam-1* expression is insulin regulated [239] and *Foxc2* has been implicated in insulin regulated PAI-1 expression [240]. Thus, it will be interestingly to test if *FoxC* genes are regulating *Pecam-1* levels in hyperglycemia.

To address these issues, we attempted to knock-down endogenous *FOXC1* expression in HUVECs by the means of sequence-specific siRNA molecules but without succes, likely because of the poor transfection efficiency of HUVECs cells, thus not allowing to assess a possible role of *FOXC1* at the human *PECAM-1* promoter. Likewise, our attempts to knock-down *Foxc1* expression during eEPC-differentiation by means of siRNA were not realized, thus not allowing to observe a

direct effect of lacking endogenous Foxc1 activity on *Pecam-1* activation in differentiated eEPCs. Alternative future approaches using viral vectors and shRNA (small-hairpin RNA) could overcome this problem and allow us to draw conclusions about this particular transcriptional mechanism.

#### **4.5 Loss of Foxc1 does not affect pan-endothelial *Pecam-1* expression**

A stage and/or temporal specific function of Foxc1 at the *Pecam-1* locus or a role under pathological conditions such as diabetes, might also explain why the vasculature of *Foxc1*<sup>-/-</sup> embryos still expresses *Pecam-1* [180]. Because of the endothelial heterogeneity and the complex regulation of *Pecam-1* expression, absence of one specific trans-factor might not result into an overall lack of gene expression. This notion gains further support by the fact that, although Gata-2 was implicated in *Pecam-1* regulation in megakaryocytes and NF- $\kappa$ B is involved in *Pecam-1* expression in cells of the monocytic lineage, *Pecam-1* expression in endothelial cells is not affected by loss of either of these two genes. Studies in female *Gata-2* +/- knock out mice showed that the vasculature of the placenta of *Gata-2* <sup>-/-</sup> embryos still stains positive for Pecam-1, when compared with the placenta of wild-type embryos [241]. In addition, mice lacking *Ikk1* and *Ikk2*, two genes encoding critical I $\kappa$ B kinases required to activate NF- $\kappa$ B, still display regular *Pecam-1* staining of the embryonic vasculature, although NF- $\kappa$ B activity is absent [242]. Alongside, one could argue that loss of Foxc1 alleles in embryos does not affect the overall expression of *Pecam-1* in the pan-vascular bed, because this transcriptional mechanism rather has specificity for an early endothelial progenitor population.

Besides, transcriptional activation of vascular genes is considered to be under the control of a combinatorial interaction of different classes of transcription factors that might provide the molecular basis for the endothelial cell-specificity [84], as it has been shown for the e.g. *Tie2* gene [243]. This might further explain why the absence of one trans-factor, i.e. Foxc1 in this case, might not lead to an overall loss of pan-endothelial *Pecam-1* expression, even if Foxc1 was required for *Pecam-1* activity in mature vascular beds. Additionally, as mentioned in the Introduction, FoxC proteins

were shown to activate the arterial marker Delta-Like 4 (*Dll4*), a Notch ligand, through a Fox binding site around 3.5kb upstream of the transcription start site. However, the authors showed that mutations in the Fox binding site do not result into a complete loss of promoter activity, suggesting that further transcription factors account for the activation of *Dll4* in arterial endothelium [181]. Likewise, loss of *Foxc1* might be compensated by other transcription factors whose interaction with the *Pecam-1* regulatory sites might still be sufficient to drive *Pecam-1* in mature endothelium.

In addition, the presence of co-factors could support the specificity of a transcription factor thus allowing its activity at a certain promoter to be restricted to the vasculature or certain endothelial sub-compartments [4, 84].

In that light, the molecular basis for the eEPC-specificity of *Foxc1* induced *Pecam-1* expression could be defined by a combination of *Foxc1* and other transcription factors and/or co-activators, which in turn might be unavailable in ES cells and mature endothelial cells. For example, the transcriptional adaptor proteins p300 and CREB-binding protein (CBP) form a multiprotein/DNA complex with HIF1 $\alpha$  while binding the *VEGF* gene, thus activating transcription in response to hypoxia [244], and FoxO transcription factors were shown to interact with CBP/p300 in mediating transcriptional activity [245]. However, an interaction of *Foxc1* protein with CBP/p300 during *Pecam-1* activation in eEPCs was not seen (data not shown) and further putative co-activators of *Foxc1* at the *Pecam-1* locus were not identified in the frame of this Ph.D. project.

#### **4.6 Foxc1 binds a microsatellite repeat in the 5'-area of the mouse *Pecam-1* gene**

The *Foxc1* binding site was identified within a microsatellite element that is comprised of a 'TTTGT' pentanucleotide repeat. Microsatellites, also called simple sequence repeats (SSR), consist of tandem repeats of up to six very short nucleotide motifs [246], that in many cases show multiallelic polymorphism. In eukaryotic genomes, SSRs are widely dispersed in non-coding regions, and coding regions of mammalian genomes often include trinucleotide SSRs [247]. They are thought to

represent a source of quantitative genetic variation. Their polymorphic nature, due to variations in the number of the tandem repeat units caused by mutations in the DNA through slippage-like events during replication [248, 249], makes them suitable markers for genetic mapping and kinship studies [250, 251]. Next to coding sequences of genes, SSRs have been found within introns as well as 5'-and 3'-UTRs where they can serve as regulatory elements of transcription. This is especially true for upstream promoter elements, where SSRs were shown to be involved in gene regulation.

Specifically, the human epidermal growth factor receptor (*EGF-R*) gene contains two blocks of (TCC)<sub>3</sub> repeats in its upstream promoter elements that were suggested to bind Sp1 and to be involved in regulation of *EGF-R* transcription [252]. Likewise, a motif of seven 'TCCC' repeats in the human proto-oncogene *c-Ki-ras* promoter [253] is involved in transcriptional regulation, and the transcription factor p53 was described to activate the expression of the tumor-suppressor gene *PIG3* through binding to a (TGYCC)<sub>n</sub> (Y= C or T) pentanucleotide repeat sequence within the human *PIG3* promoter [254]. Another polymorphic (CCT)<sub>n</sub> trinucleotide repeat, located around 100 nucleotides upstream of the major transcription initiation site of the human paired box gene-7 (*PAX7*) gene, was shown to confer high transcriptional efficiency to the *PAX7* promoter [255]. Those studies and others (reviewed in [256]) underscore the capability of repeated short sequence motifs to direct gene transcription.

Additional support comes from a recent publication that aimed at identifying transcription factor binding sites within microsatellite sequences across the entire human genome [251]. Iglesias and co-workers investigated the functionality of microsatellites located near the transcription initiation site (TIS - around the first exon) and the first intron of all annotated genes of the human genome and assessed their effect on gene expression as cis-regulatory elements. Among others, the pentanucleotide 'AAACA' (reverse sequence of 'TTTGT') was found in 12 polymorphic microsatellites in the human genome. It was shown that the 'TTTGT' repeats have the capacity to bind DNA associated proteins in band shift assays, indicating that this repeat-motif sequence can indeed serve as a binding-site and cis-regulatory element in gene promoters [251]. Although this study did not further investigate the precise nature of putative DNA binding proteins at the 'AAACA'

microsatellite repeat, we propose that Foxc1 might be among the group of yet to be identified proteins that has the ability to bind at 'AAACA' repeats on the chromatin and induce transcription of neighbouring genes. We found a similar scenario in band shift assays by using a biotin-labeled probe comprising four 'TTTGT' repeats that is shifted in presence of eEPC nuclear extract (data not shown), arguing that this pentanucleotide repeat is able to act as Fox protein binding site. However, the data obtained in these assays require further evaluation before being presented in a final conclusive form.

Further, it is plausible that the promoter activation through the repeat motif has biological relevance, since, if there was unspecific binding of ectopically expressed Foxc1 to the (TTTGT)<sub>n</sub> repeat motifs, it would likely occur in all the co-transfection experiments with the different cell lines included in this study. Alongside, the decreased *Pecam-1* mRNA levels in mature pancreatic endothelial cells (MS1-ECs) and ES cells in response to Foxc1 (Fig. 12B) indicate that the transcriptional effect of Foxc1 at the *Pecam-1* promoter may be biphasic. Foxc1 could carry out a repressional effect in mature endothelial cells and ES cells, whereas a potential specific function as transcriptional activator specifically takes place in eEPCs (Fig. 13). This is in accordance with the general notion that Fox transcription factors can act as trans-activators and trans-repressors [116].

#### **4.7 The activity of the upstream element depends on the number of microsatellite repeat motifs**

Consistent with the observed drop in reporter expression after the (TTTGT)<sub>n</sub> motif is shortened, Iglesias *et al.* showed that protein binding capacity increased with higher numbers of AAACA repeats, with 7 repeats displaying about twice the binding capacity as four repeats [251]. In this respect, the 'TGYCC' repeat-motif in the human *PIG3* promoter displays polymorphism in 117 human individuals, with four different motif lengths consisting of either 10,15,16, or 17 repeats [254]. Decreased numbers of 'TGYCC' repeats derived from the *PIG3* promoter of different human individuals conferred a decreased degree of responsiveness to p53 when combined with a minimal promoter. Parallel overexpression of *p53* showed that a motif comprising of

17 repeats confers an about 4-fold higher promoter activity compared to the allele containing only 10 repeats [254].

Moreover, the binding affinity of the transcription factor Sp1 for (CCT)<sub>n</sub>-repeats in the human *PAX7* promoter directly correlated with the repeat numbers of different alleles [255]. Genotype analysis showed that the polymorphic (CCT)<sub>n</sub>-repeat in the human *PAX7* promoter has length variation in a Western European population and consists of three different alleles with 8, 10, or 11 repeats in close proximity to the TIS and as for the 'TTTGT' and 'TGYCC' repeat motifs, alleles with a higher repeat number, in this case 11 repeats, drove higher reporter gene expression in rhabdomyosarcoma cells than alleles containing 8 or 10 repeats [255]. In similar fashion, I found that increasing numbers of 'TTTGT' repeats drive higher reporter activity *in vitro* in the *Pecam-1* reporter gene studies.

#### **4.8 The repeat number compensates the loss of the consensus motif**

Despite its low similarity to the p53 consensus binding sequence, the 'TGYCC' repeat motif in the human *PIG3* promoter was shown to be necessary and sufficient to activate *PIG3* expression in response to p53 [254].

Alongside, Fox proteins were also shown to bind DNA motifs with only partial homology to the consensus core sequence and the efficient binding of Fox protein to their target DNA also depends on the flanking sequences of the core [116, 155]. In that respect, the 'TTTGT' pentanucleotide repeat might represent a sub-optimal recognition site, which is yet able to bind Foxc1 protein. However, the lower binding affinity could explain why high Foxc1 levels were necessary to induce promoter activity in the reporter gene assays. The same was true in the case of p53, where high amounts of p53 expression plasmid were required to induce a higher activation of the *PIG3* promoter through binding to the (TGYCC)<sub>n</sub> repeats in the study of Contente and co-workers, compared to gene activation through a p53-consensus promoter site [254, 257].

Next to requiring higher amounts of transcription factor, the deviation from the consensus sequence might be compensated by the large number of 'TTTGT' motif repeats, as found in the mouse *Pecam-1* 5'-flanking area, thus allowing to pass a

threshold level to initiate gene expression. This would also explain that a large number of repeat units has to be deleted to significantly decrease reporter gene expression, with each single repeat unit contributing weakly to the overall activity.

#### **4.9 Fox proteins can bind low-affinity sites**

*FoxC* expression levels are regarded as a key factor during the precise temporal and spatial control of target gene expression, e.g. the progressive loss of functional *FoxC* alleles in embryos is associated with an increasing lateralization of paraxial and somite mesoderm, showing a dose-dependent function of the proteins at the DNA regulatory sites [192]. Thus, it is speculated that suboptimal Fox binding sites, such as the 'TTTGT' repeats in our case, need high levels of endogenous Foxc1 protein for binding in order to be functionally active.

Further support for a crucial dose dependent regulation of target genes by Fox transcription factors comes from *in vivo* studies in *C.elegans*. During development, the *FoxA* orthologue *pha-4* controls pharyngeal development and the concentration of Pha-4 protein increases during development, thus activating target genes with low-affinity binding site in their promoters, whereas during the onset of *pha-4* transcription, low protein concentrations are only able to activate target genes with high affinity binding sites within their regulatory sequences [258]. If target gene expression depends on a fine balanced level of Fox protein under certain circumstances, the presence of low-affinity sites such as the 'TTTGT' repeat motif described herein may allow a mechanism by which *Pecam-1* transcript levels depend on the intracellular concentration of Foxc1 protein, thus allowing a dose-dependent control of gene expression.

#### **4.10 Microsatellite repeats represent species-specific transcriptional elements**

The lack of a similar arrangement of the (TTTGT)<sub>n</sub> repeat motif at the human locus makes the two blocks of repeat units a unique feature of the mouse *Pecam-1* locus

(Fig. 19). However, a total of 45 'TTTGT' repeat units was identified further upstream of the transcriptional start site of human *PECAM-1* (Fig. 20). Unlike in the mouse, those repeats were shown to be distributed more randomly in shorter blocks of up to 6 repeat units. As a general rule, microsatellite repeats are considered to have evolved differently between closely related species, e.g., the human genome contains more and longer polymorphic repeats (especially dinucleotides), compared to the genome of chimpanzees or other related primates [259]. Thus, it is unlikely to expect a similar microsatellite motif – consisting of a comparable number and arrangement of 'TTTGT' pentanucleotides – directly at the corresponding genomic locus in orthologue species. Further support for a cis-regulatory role of the (TTTGT)<sub>n</sub> repeat motif comes from our Bioinformatics analysis, that identified an experimentally verified *Foxc1* binding site at the *Tbx1* locus [195], containing the same 'TTTG' core sequence that was also as identified by the software within the 'TTTGT' repeats at the mouse and human *Pecam-1* locus (Fig. 18, Fig. 20). Hence, we suggest that this microsatellite motif is involved in regulating the transcriptional activity of mouse and human *Pecam-1*.

Functional conservation of a transcriptional regulatory activity of a microsatellite repeat sequence has also been described for the human *PAX7* promoter, where the microsatellite shows a high conservation to the orthologue sequence in the mouse, which, interestingly, does not consist of a (CCT)<sub>n</sub> repeat motif, but rather a C/T rich sequence that might serve as a Sp1 binding site in vitro [255].

As a general assumption, mutational processes that lead to the diversity of simple sequence repeats include replication slippage, point mutation, and recombination. If DNA changes are not corrected by the DNA mismatch repair system, then new alleles at the microsatellite loci are generated and eventually result into alternate phenotypes and contribute to the species specificity of microsatellites. This kind of divergence has been proposed to be responsible, at least in part, for temporal and quantitative differences in gene expression between species [251].

In conclusion, we speculate that a cis-regulatory potential of a sequence repeat motif can be contained between related species, although there might be differences and variations on the nucleotide level or the position of the microsatellite repeat relative to the transcription initiation site of a gene.



#### **4.11 Variation in transcription factor binding sites across species**

In general, binding sites for highly conserved transcription factors can vary significantly between mouse and human, as shown in a recent study that used custom DNA microarrays which analyzed 10kb of sequences surrounding the known transcription start sites of 4000 orthologue gene pairs from mouse and human [260]. The DNA was precipitated from primary mouse and human hepatocytes using antibodies against liver-specific transcription factors, since hepatocytes and the transcription factors that control their development and function are highly conserved among mammals [261]. Interestingly, the study showed that up to 89% of orthologue promoter regions bound by a protein in one species were not recognized by the same protein in the second species, depending on the individual factor. For example only 26% of orthologue genes bound by hepatocyte nuclear factor 6 (HNF6) in human hepatocytes were recognized by this transcription factor in mouse hepatocytes. Moreover, the location of binding events varied widely between the two species, e.g. the binding of HNF6 at a certain locus was shifted about 4 kb from the promoter region in human DNA to the first intron in the mouse DNA [260]. Furthermore, 41 orthologue pairs were bound by the related transcription factor HNF1A in both species, but only 20 binding events occurred in sequences that were aligned between mouse and human. This high mobility was regarded to account for the most notable feature of the divergent transcription factor binding sites.

Generally, comparison of mouse and human genomic regulatory regions is used to identify putative binding sites for different classes of transcription factors. And conservation of sequence motifs suggests that a family of transcription factors might be important in regulating the e.g. vascular-specific expression of a certain gene [84]. However, bioinformatics studies suggest that comparative genomics may not always be sufficient to decode putative regulatory elements in promoter areas. Smith *et al.* showed that fewer than 10% of orthologue promoter pairs from mouse and human retain significant conservation, suggesting that tissue-specific sites would be difficult to identify by relying purely on traditional cross-species analysis through co-linear promoter alignment, which may result into high false-negative detection rates [229, 260]. In order to identify putative Foxc1 binding sites at the human *PECAM-1* locus

that might not match with the mouse sequence in co-linear alignments, we took advantage of the MatInspector and DiAlign Tools [219, 220]. In accordance with the above mentioned study [260], we suggest that the identified dispersed (TTTGT)<sub>n</sub> repeat motifs upstream of the human *PECAM-1* gene might present another example of a transcription factor binding site that has a shifted position at the human locus, as compared to the mouse locus.

In addition, it cannot be excluded that the human *PECAM-1* locus contains Foxc1 binding motifs, which might be embedded inside regular consensus sequences that are not in alignment with the repeat motif in the mouse genome and were not identified by the bioinformatics analysis applied in this study. Besides this notion, it is possible that further (TTTGT)<sub>n</sub> repeat motifs, other 'TG'-rich sequences or regular Foxc1 consensus binding sites are located in genomic areas of the human locus that were not analyzed at all for the presence of such sites, e.g. areas far upstream of the transcription initiation site, as well as downstream of the *PECAM-1* gene or within intronic regions. This is making it hard to speculate about the possible existence of further Foxc1 sites with reasonable accuracy.

In conclusion, the lack of identified Foxc1 binding sites in areas of the human locus that correspond to the microsatellite in the mouse sequence, does not rule out the possibility that putative functional Foxc1 sites, such as the already identified 'TTTGT' repeats in the human sequence, are present in distinct areas of the human *PECAM-1* locus.

#### **4.12 Difference between Foxc1 and Foxc2 functions**

Although the biological functions of the two closely related members of the FoxC subfamily are often conserved during evolution, their activities differ in some instances. For example, the congenital hydrocephalus phenotype in *Foxc1* <sup>-/-</sup> mice is not seen in *Foxc2* <sup>-/-</sup> mice [187, 189]. In turn, Foxc2 was shown to have stronger transcriptional activity in the cardiovascular system than Foxc1. [181, 190, 240]. For instance, the formation of the cardiac outflow tract, the right ventricle and the inflow tract is severely impaired in compound *Foxc1*<sup>+/-</sup>; *Foxc2*<sup>-/-</sup> and *Foxc1*<sup>-/-</sup>; *Foxc2*<sup>-/-</sup>

embryos, whereas compound *Foxc1*<sup>-/-</sup>;*Foxc2*<sup>+/-</sup> embryos do not display this kind of developmental abnormalities [190]. Moreover, *Foxc2*, but not *Foxc1*, was shown to bind and transactivate the promoter of the plasminogen activator inhibitor-1 (*PAI-1*) gene in endothelial cells [240].

Although *Foxc1* and *Foxc2* differ considerably in their sequence, the DNA binding domains are almost 100% identical [116]. In this respect, it is surprising that only *Foxc1* leads to transcriptional activation of the endogenous *Pecam-1* gene as well as of the upstream 5'-flanking 3.5kb element in the reporter construct. This likely occurs because *Foxc1* might be able to bind to other proteins within the transcriptional complex forming on the *Pecam-1* promoter, but *Foxc2* does not. This in turn would not be surprising since the two FoxC homologues differ extensively in the non-DNA binding domains [116]. This selective activation of *Pecam-1* through *Foxc1* likely represents another example of a functional difference between the closely related FoxC proteins, leading to gene target specificity under certain conditions; this in turn is consistent with the fact that the two genes cannot compensate for each other in many developmental stages.

#### **4.13 Foxc1 as regulator of vascular adhesion molecules?**

Myeloid cells regulate *Pecam-1* activity through involvement of the transcriptional regulator NF- $\kappa$ B (Nuclear Factor-kappa B), which has also been implicated in the transcriptional regulation of other members of the Ig (Immunoglobuline) superfamily, such as *Icam-1* (Intercellular Adhesion Molecule-1) and *Vcam-1* (Vascular Cell Adhesion Molecule-1) [262, 263], that are both implicated in endothelial-leukocyte adhesion during pathological conditions. These findings suggest a broad role of NF- $\kappa$ B in regulating the expression of cell adhesion molecules on the endothelium in response to environmental stimuli such as those occurring during inflammation. In accordance, in the frame of this project, *Foxc1* and *Foxc2* were shown to induce expression of *Icam-1* and the chemokine receptor *Cxcr4* (Fig. 4) in mouse eEPCs. Others have shown the induction of *Cxcr4* by FoxC proteins in endothelial cells (Tom

Kume, personal communication) and *Vcam-1* was identified as a target gene of *Foxc1* and *Foxc2* (Tom Kume, unpublished observations). As for NF- $\kappa$ B, our findings of *Pecam-1* as well as *Icam-1* and *Cxcr4* as target genes could indicate a role of FoxC transcription factors in regulating the expression of genes encoding for surface proteins that typically are involved in the recruitment and adhesion of bone marrow-derived peripheral blood cells of the leukocytic lineage to target organ sites during pathological conditions such as inflammation. However, further studies such as gain of function analysis in endothelial cell cultures or *in vivo* studies using FoxC knock-out animal models will be necessary to verify this hypothesis.

#### **4.14 Conclusion**

In summary, transgenic overexpression of the transcription factor *Foxc1* in eEPCs identified a transcriptional mechanism that up-regulates mouse *Pecam-1* expression in undifferentiated embryonic endothelial progenitor cells, which represent an early angioblast population [108]. Most likely, *Foxc1*-induced *Pecam-1* expression is active as a stage-specific mechanism in eEPCs as part of the molecular endothelial heterogeneity and may not reflect a general pan-endothelial transcriptional mechanism of *Pecam-1* in mature vascular beds. Alternatively, *Foxc1* might play a role in suppressing *Pecam-1* expression under special circumstances like during inflammatory conditions or hyperglycemia. It was shown that the induction of *Pecam-1* expression by *Foxc1* is direct, thus suggesting that *Foxc1* may be involved in the initial control of endothelial differentiation by inducing *Pecam-1*. The results presented here indicate that *Foxc1* regulates *Pecam-1* induction through a distal 5'-flanking binding site composed of a tandem repeated 'TTTGT' microsatellite motif that reflects the core-pentanucleotide of the Fox consensus binding site [224]. Microsatellites repeats have gained increasing importance as regulatory elements in gene expression and in human genetic diseases [251]. Yet, it is not entirely clear how they function during transcriptional regulation compared to single transcription factor binding sites with strong affinities. The data herein provide a new model of gene expression regulation involving a cis-active microsatellite repeat. In the future, it will be of interest to study the dispersed (TTTGT)<sub>n</sub> repeat motifs upstream of the human

*PECAM-1* gene for cis-regulatory activity by an experimental approach *in vitro* and *in vivo*, through e.g. ChIP analysis. This will add further data about a role of this repeat motif in endothelial gene regulation.

The presented data provide new insight into the regulation of vascular-specific gene expression. Identifying additional targets of Foxc1 and also Foxc2 in endothelial cells will also extend our understanding of the role of these transcription factors during cardiovascular development and disease.

**REFERENCES**

- [1] Hatzopoulos AK, Rosenberg RD. Embryonic development of the vascular system: Oxford University Press; 1999.
- [2] Cines DB, Pollak ES, Buck CA, et al. Endothelial cells in physiology and in the pathophysiology of vascular disorders. *Blood*. 1998;91:3527-3561.
- [3] Weibel ER, Palade GE. New Cytoplasmic Components in Arterial Endothelia. *J Cell Biol*. 1964;23:101-112.
- [4] Minami T, Aird WC. Endothelial cell gene regulation. *Trends Cardiovasc Med*. 2005;15:174-184.
- [5] Risau W, Flamme I. Vasculogenesis. *Annu Rev Cell Dev Biol*. 1995;11:73-91.
- [6] Drake CJ, Fleming PA. Vasculogenesis in the day 6.5 to 9.5 mouse embryo. *Blood*. 2000;95:1671-1679.
- [7] DeRuiter MC, Poelmann RE, VanderPlas-de Vries I, Mentink MM, Gittenberger-de Groot AC. The development of the myocardium and endocardium in mouse embryos. Fusion of two heart tubes? *Anat Embryol (Berl)*. 1992;185:461-473.
- [8] Noden DM. Embryonic origins and assembly of blood vessels. *Am Rev Respir Dis*. 1989;140:1097-1103.
- [9] Sabin FR. Studies on the origin of blood-vessels and of red blood-corpuscles as seen in the living blastoderm of chicks during the second day of incubation. *Contrib Embryol Carnegie Inst Publ Wash*. 1920;9:213-262.
- [10] Murray PDF. The Development in vitro of the blood of the early chick embryo. *Proc R Soc Lond [Biol]*. 1932;11:497-521.
- [11] Risau W. Vasculogenesis, angiogenesis and endothelial cell differentiation during embryonic development. Basel: Karger; 1991.
- [12] Carmeliet P. Angiogenesis in health and disease. *Nat Med*. 2003;9:653-660.
- [13] Pardanaud L, Yassine F, Dieterlen-Lievre F. Relationship between vasculogenesis, angiogenesis and haemopoiesis during avian ontogeny. *Development (Cambridge, England)*. 1989;105:473-485.
- [14] Ribatti D. Genetic and epigenetic mechanisms in the early development of the vascular system. *J Anat*. 2006;208:139-152.
- [15] Augustin HG. Tubes, branches, and pillars: the many ways of forming a new vasculature. *Circ Res*. 2001;89:645-647.

- [16] Burri PH, Djonov V. Intussusceptive angiogenesis--the alternative to capillary sprouting. *Mol Aspects Med.* 2002;23:S1-27.
- [17] Baldwin HS. Early embryonic vascular development. *Cardiovasc Res.* 1996;31 Spec No:E34-45.
- [18] Carmeliet P. Mechanisms of angiogenesis and arteriogenesis. *Nat Med.* 2000;6:389-395.
- [19] Gittenberger-de Groot AC, DeRuiter MC, Bergwerff M, Poelmann RE. Smooth muscle cell origin and its relation to heterogeneity in development and disease. *Arteriosclerosis, thrombosis, and vascular biology.* 1999;19:1589-1594.
- [20] Reynolds LP, Killilea SD, Redmer DA. Angiogenesis in the female reproductive system. *Faseb J.* 1992;6:886-892.
- [21] Augustin HG, Braun K, Telemenakis I, Modlich U, Kuhn W. Ovarian angiogenesis. Phenotypic characterization of endothelial cells in a physiological model of blood vessel growth and regression. *Am J Pathol.* 1995;147:339-351.
- [22] Carmeliet P, Jain RK. Angiogenesis in cancer and other diseases. *Nature.* 2000;407:249-257.
- [23] Boulton AJ, Malik RA. Diabetic neuropathy. *Med Clin North Am.* 1998;82:909-929.
- [24] Ross R. Cell biology of atherosclerosis. *Annu Rev Physiol.* 1995;57:791-804.
- [25] Folkman J. Angiogenesis in cancer, vascular, rheumatoid and other disease. *Nat Med.* 1995;1:27-31.
- [26] Rafii S, Lyden D. Therapeutic stem and progenitor cell transplantation for organ vascularization and regeneration. *Nat Med.* 2003;9:702-712.
- [27] Urbich C, Dimmeler S. Endothelial progenitor cells: characterization and role in vascular biology. *Circ Res.* 2004;95:343-353.
- [28] Peichev M, Naiyer AJ, Pereira D, et al. Expression of VEGFR-2 and AC133 by circulating human CD34(+) cells identifies a population of functional endothelial precursors. *Blood.* 2000;95:952-958.
- [29] Quirici N, Soligo D, Caneva L, Servida F, Bossolasco P, Deliliers GL. Differentiation and expansion of endothelial cells from human bone marrow CD133(+) cells. *Br J Haematol.* 2001;115:186-194.
- [30] Gehling UM, Ergun S, Schumacher U, et al. In vitro differentiation of endothelial cells from AC133-positive progenitor cells. *Blood.* 2000;95:3106-3112.
- [31] Yin AH, Miraglia S, Zanjani ED, et al. AC133, a novel marker for human hematopoietic stem and progenitor cells. *Blood.* 1997;90:5002-5012.

- [32] Miraglia S, Godfrey W, Yin AH, et al. A novel five-transmembrane hematopoietic stem cell antigen: isolation, characterization, and molecular cloning. *Blood*. 1997;90:5013-5021.
- [33] Kalka C, Masuda H, Takahashi T, et al. Transplantation of ex vivo expanded endothelial progenitor cells for therapeutic neovascularization. *Proceedings of the National Academy of Sciences of the United States of America*. 2000;97:3422-3427.
- [34] Asahara T, Masuda H, Takahashi T, et al. Bone marrow origin of endothelial progenitor cells responsible for postnatal vasculogenesis in physiological and pathological neovascularization. *Circ Res*. 1999;85:221-228.
- [35] Asahara T, Takahashi T, Masuda H, et al. VEGF contributes to postnatal neovascularization by mobilizing bone marrow-derived endothelial progenitor cells. *Embo J*. 1999;18:3964-3972.
- [36] Lin Y, Weisdorf DJ, Solovey A, Hebbel RP. Origins of circulating endothelial cells and endothelial outgrowth from blood. *J Clin Invest*. 2000;105:71-77.
- [37] Orlic D, Kajstura J, Chimenti S, et al. Bone marrow cells regenerate infarcted myocardium. *Nature*. 2001;410:701-705.
- [38] Orlic D, Kajstura J, Chimenti S, et al. Mobilized bone marrow cells repair the infarcted heart, improving function and survival. *Proceedings of the National Academy of Sciences of the United States of America*. 2001;98:10344-10349.
- [39] Kocher AA, Schuster MD, Szabolcs MJ, et al. Neovascularization of ischemic myocardium by human bone-marrow-derived angioblasts prevents cardiomyocyte apoptosis, reduces remodeling and improves cardiac function. *Nat Med*. 2001;7:430-436.
- [40] Asahara T, Murohara T, Sullivan A, et al. Isolation of putative progenitor endothelial cells for angiogenesis. *Science (New York, NY)*. 1997;275:964-967.
- [41] Takahashi T, Kalka C, Masuda H, et al. Ischemia- and cytokine-induced mobilization of bone marrow-derived endothelial progenitor cells for neovascularization. *Nat Med*. 1999;5:434-438.
- [42] Zhang ZG, Zhang L, Jiang Q, Chopp M. Bone marrow-derived endothelial progenitor cells participate in cerebral neovascularization after focal cerebral ischemia in the adult mouse. *Circ Res*. 2002;90:284-288.
- [43] Davidoff AM, Ng CY, Brown P, et al. Bone marrow-derived cells contribute to tumor neovasculature and, when modified to express an angiogenesis inhibitor, can restrict tumor growth in mice. *Clin Cancer Res*. 2001;7:2870-2879.
- [44] Lyden D, Hattori K, Dias S, et al. Impaired recruitment of bone-marrow-derived endothelial and hematopoietic precursor cells blocks tumor angiogenesis and growth. *Nat Med*. 2001;7:1194-1201.
- [45] Conway EM, Collen D, Carmeliet P. Molecular mechanisms of blood vessel growth. *Cardiovasc Res*. 2001;49:507-521.



- [46] Jain RK. Molecular regulation of vessel maturation. *Nat Med.* 2003;9:685-693.
- [47] Flamme I, Risau W. Induction of vasculogenesis and hematopoiesis in vitro. *Development (Cambridge, England).* 1992;116:435-439.
- [48] Breier G, Albrecht U, Sterrer S, Risau W. Expression of vascular endothelial growth factor during embryonic angiogenesis and endothelial cell differentiation. *Development (Cambridge, England).* 1992;114:521-532.
- [49] Veikkola T, Karkkainen M, Claesson-Welsh L, Alitalo K. Regulation of angiogenesis via vascular endothelial growth factor receptors. *Cancer Res.* 2000;60:203-212.
- [50] Thurston G. Role of Angiopoietins and Tie receptor tyrosine kinases in angiogenesis and lymphangiogenesis. *Cell Tissue Res.* 2003;314:61-68.
- [51] Yancopoulos GD, Davis S, Gale NW, Rudge JS, Wiegand SJ, Holash J. Vascular-specific growth factors and blood vessel formation. *Nature.* 2000;407:242-248.
- [52] Kukk E, Lymboussaki A, Taira S, et al. VEGF-C receptor binding and pattern of expression with VEGFR-3 suggests a role in lymphatic vascular development. *Development (Cambridge, England).* 1996;122:3829-3837.
- [53] Gale NW, Yancopoulos GD. Growth factors acting via endothelial cell-specific receptor tyrosine kinases: VEGFs, angiopoietins, and ephrins in vascular development. *Genes Dev.* 1999;13:1055-1066.
- [54] Neufeld G, Cohen T, Shraga N, Lange T, Kessler O, Herzog Y. The neuropilins: multifunctional semaphorin and VEGF receptors that modulate axon guidance and angiogenesis. *Trends Cardiovasc Med.* 2002;12:13-19.
- [55] Herzog Y, Kalcheim C, Kahane N, Reshef R, Neufeld G. Differential expression of neuropilin-1 and neuropilin-2 in arteries and veins. *Mech Dev.* 2001;109:115-119.
- [56] Thurston G, Suri C, Smith K, et al. Leakage-resistant blood vessels in mice transgenically overexpressing angiopoietin-1. *Science (New York, NY).* 1999;286:2511-2514.
- [57] Maisonpierre PC, Suri C, Jones PF, et al. Angiopoietin-2, a natural antagonist for Tie2 that disrupts in vivo angiogenesis. *Science (New York, NY).* 1997;277:55-60.
- [58] Wang HU, Chen ZF, Anderson DJ. Molecular distinction and angiogenic interaction between embryonic arteries and veins revealed by ephrin-B2 and its receptor Eph-B4. *Cell.* 1998;93:741-753.
- [59] Adams RH, Wilkinson GA, Weiss C, et al. Roles of ephrinB ligands and EphB receptors in cardiovascular development: demarcation of arterial/venous domains, vascular morphogenesis, and sprouting angiogenesis. *Genes Dev.* 1999;13:295-306.

- [60] Adams RH, Klein R. Eph receptors and ephrin ligands. essential mediators of vascular development. *Trends Cardiovasc Med.* 2000;10:183-188.
- [61] Brew K, Dinakarbandian D, Nagase H. Tissue inhibitors of metalloproteinases: evolution, structure and function. *Biochim Biophys Acta.* 2000;1477:267-283.
- [62] Newman PJ. The biology of PECAM-1. *J Clin Invest.* 1997;99:3-8.
- [63] Radice GL, Rayburn H, Matsunami H, Knudsen KA, Takeichi M, Hynes RO. Developmental defects in mouse embryos lacking N-cadherin. *Dev Biol.* 1997;181:64-78.
- [64] Dejana E, Bazzoni G, Lampugnani MG. Vascular endothelial (VE)-cadherin: only an intercellular glue? *Exp Cell Res.* 1999;252:13-19.
- [65] Gory-Faure S, Prandini MH, Pointu H, et al. Role of vascular endothelial-cadherin in vascular morphogenesis. *Development (Cambridge, England).* 1999;126:2093-2102.
- [66] Eliceiri BP, Cheresh DA. The role of alphav integrins during angiogenesis: insights into potential mechanisms of action and clinical development. *J Clin Invest.* 1999;103:1227-1230.
- [67] Hynes RO. A reevaluation of integrins as regulators of angiogenesis. *Nat Med.* 2002;8:918-921.
- [68] Brooks PC, Clark RA, Cheresh DA. Requirement of vascular integrin alpha v beta 3 for angiogenesis. *Science (New York, NY).* 1994;264:569-571.
- [69] Risau W, Lemmon V. Changes in the vascular extracellular matrix during embryonic vasculogenesis and angiogenesis. *Dev Biol.* 1988;125:441-450.
- [70] Drake CJ, Davis LA, Walters L, Little CD. Avian vasculogenesis and the distribution of collagens I, IV, laminin, and fibronectin in the heart primordia. *J Exp Zool.* 1990;255:309-322.
- [71] Iso T, Hamamori Y, Keddes L. Notch signaling in vascular development. *Arteriosclerosis, thrombosis, and vascular biology.* 2003;23:543-553.
- [72] Alva JA, Iruela-Arispe ML. Notch signaling in vascular morphogenesis. *Curr Opin Hematol.* 2004;11:278-283.
- [73] Shawber CJ, Kitajewski J. Notch function in the vasculature: insights from zebrafish, mouse and man. *Bioessays.* 2004;26:225-234.
- [74] Hellstrom M, Kalen M, Lindahl P, Abramsson A, Betsholtz C. Role of PDGF-B and PDGFR-beta in recruitment of vascular smooth muscle cells and pericytes during embryonic blood vessel formation in the mouse. *Development (Cambridge, England).* 1999;126:3047-3055.

- [75] Lindahl P, Johansson BR, Leveen P, Betsholtz C. Pericyte loss and microaneurysm formation in PDGF-B-deficient mice. *Science (New York, NY)*. 1997;277:242-245.
- [76] Goumans MJ, Valdimarsdottir G, Itoh S, Rosendahl A, Sideras P, ten Dijke P. Balancing the activation state of the endothelium via two distinct TGF-beta type I receptors. *Embo J*. 2002;21:1743-1753.
- [77] Yamaguchi J, Kusano KF, Masuo O, et al. Stromal cell-derived factor-1 effects on ex vivo expanded endothelial progenitor cell recruitment for ischemic neovascularization. *Circulation*. 2003;107:1322-1328.
- [78] Askari AT, Unzek S, Popovic ZB, et al. Effect of stromal-cell-derived factor 1 on stem-cell homing and tissue regeneration in ischaemic cardiomyopathy. *Lancet*. 2003;362:697-703.
- [79] Aiuti A, Webb IJ, Bleul C, Springer T, Gutierrez-Ramos JC. The chemokine SDF-1 is a chemoattractant for human CD34+ hematopoietic progenitor cells and provides a new mechanism to explain the mobilization of CD34+ progenitors to peripheral blood. *J Exp Med*. 1997;185:111-120.
- [80] O'Reilly MS, Holmgren L, Shing Y, et al. Angiostatin: a novel angiogenesis inhibitor that mediates the suppression of metastases by a Lewis lung carcinoma. *Cell*. 1994;79:315-328.
- [81] O'Reilly MS, Boehm T, Shing Y, et al. Endostatin: an endogenous inhibitor of angiogenesis and tumor growth. *Cell*. 1997;88:277-285.
- [82] Unthank JL, Fath SW, Burkhart HM, Miller SC, Dalsing MC. Wall remodeling during luminal expansion of mesenteric arterial collaterals in the rat. *Circ Res*. 1996;79:1015-1023.
- [83] Djonov VG, Kurz H, Burri PH. Optimality in the developing vascular system: branching remodeling by means of intussusception as an efficient adaptation mechanism. *Dev Dyn*. 2002;224:391-402.
- [84] Oettgen P. Transcriptional regulation of vascular development. *Circ Res*. 2001;89:380-388.
- [85] Iljin K, Dube A, Kontusaari S, et al. Role of ets factors in the activity and endothelial cell specificity of the mouse Tie gene promoter. *Faseb J*. 1999;13:377-386.
- [86] Dube A, Akbarali Y, Sato TN, Libermann TA, Oettgen P. Role of the Ets transcription factors in the regulation of the vascular-specific Tie2 gene. *Circ Res*. 1999;84:1177-1185.
- [87] Kappel A, Schlaeger TM, Flamme I, Orkin SH, Risau W, Breier G. Role of SCL/Tal-1, GATA, and ets transcription factor binding sites for the regulation of flk-1 expression during murine vascular development. *Blood*. 2000;96:3078-3085.

- [88] Brown LA, Rodaway AR, Schilling TF, et al. Insights into early vasculogenesis revealed by expression of the ETS-domain transcription factor Fli-1 in wild-type and mutant zebrafish embryos. *Mech Dev.* 2000;90:237-252.
- [89] Hart A, Melet F, Grossfeld P, et al. Fli-1 is required for murine vascular and megakaryocytic development and is hemizygotously deleted in patients with thrombocytopenia. *Immunity.* 2000;13:167-177.
- [90] Gering M, Rodaway AR, Gottgens B, Patient RK, Green AR. The SCL gene specifies haemangioblast development from early mesoderm. *Embo J.* 1998;17:4029-4045.
- [91] Visvader JE, Fujiwara Y, Orkin SH. Unsuspected role for the T-cell leukemia protein SCL/tal-1 in vascular development. *Genes Dev.* 1998;12:473-479.
- [92] Cowan PJ, Tsang D, Pedic CM, et al. The human ICAM-2 promoter is endothelial cell-specific in vitro and in vivo and contains critical Sp1 and GATA binding sites. *The Journal of biological chemistry.* 1998;273:11737-11744.
- [93] German Z, Chambliss KL, Pace MC, Arnet UA, Lowenstein CJ, Shaul PW. Molecular basis of cell-specific endothelial nitric-oxide synthase expression in airway epithelium. *The Journal of biological chemistry.* 2000;275:8183-8189.
- [94] Gumina RJ, Kirschbaum NE, Piotrowski K, Newman PJ. Characterization of the human platelet/endothelial cell adhesion molecule-1 promoter: identification of a GATA-2 binding element required for optimal transcriptional activity. *Blood.* 1997;89:1260-1269.
- [95] Steingrimsson E, Tessarollo L, Reid SW, Jenkins NA, Copeland NG. The bHLH-Zip transcription factor Tfeb is essential for placental vascularization. *Development (Cambridge, England).* 1998;125:4607-4616.
- [96] Henderson AM, Wang SJ, Taylor AC, Aitkenhead M, Hughes CC. The basic helix-loop-helix transcription factor HESR1 regulates endothelial cell tube formation. *The Journal of biological chemistry.* 2001;276:6169-6176.
- [97] Myers C, Charboneau A, Boudreau N. Homeobox B3 promotes capillary morphogenesis and angiogenesis. *J Cell Biol.* 2000;148:343-351.
- [98] Belotti D, Clause N, Flagiello D, et al. Expression and modulation of homeobox genes from cluster B in endothelial cells. *Lab Invest.* 1998;78:1291-1299.
- [99] Boudreau N, Andrews C, Srebrow A, Ravanpay A, Cheresch DA. Induction of the angiogenic phenotype by Hox D3. *J Cell Biol.* 1997;139:257-264.
- [100] Liao W, Ho CY, Yan YL, Postlethwait J, Stainier DY. Hhex and scl function in parallel to regulate early endothelial and blood differentiation in zebrafish. *Development (Cambridge, England).* 2000;127:4303-4313.
- [101] Schreiber M, Wang ZQ, Jochum W, Fetka I, Elliott C, Wagner EF. Placental vascularisation requires the AP-1 component fra1. *Development (Cambridge, England).* 2000;127:4937-4948.

- [102] Xiong JW, Leahy A, Lee HH, Stuhlmann H. Vezf1: A Zn finger transcription factor restricted to endothelial cells and their precursors. *Dev Biol.* 1999;206:123-141.
- [103] Kuo CT, Veselits ML, Barton KP, Lu MM, Clendenin C, Leiden JM. The LKLF transcription factor is required for normal tunica media formation and blood vessel stabilization during murine embryogenesis. *Genes Dev.* 1997;11:2996-3006.
- [104] Wang GL, Jiang BH, Rue EA, Semenza GL. Hypoxia-inducible factor 1 is a basic-helix-loop-helix-PAS heterodimer regulated by cellular O<sub>2</sub> tension. *Proceedings of the National Academy of Sciences of the United States of America.* 1995;92:5510-5514.
- [105] Forsythe JA, Jiang BH, Iyer NV, et al. Activation of vascular endothelial growth factor gene transcription by hypoxia-inducible factor 1. *Molecular and cellular biology.* 1996;16:4604-4613.
- [106] Mazure NM, Chen EY, Laderoute KR, Giaccia AJ. Induction of vascular endothelial growth factor by hypoxia is modulated by a phosphatidylinositol 3-kinase/Akt signaling pathway in Ha-ras-transformed cells through a hypoxia inducible factor-1 transcriptional element. *Blood.* 1997;90:3322-3331.
- [107] Richard DE, Berra E, Gothie E, Roux D, Pouyssegur J. p42/p44 mitogen-activated protein kinases phosphorylate hypoxia-inducible factor 1alpha (HIF-1alpha) and enhance the transcriptional activity of HIF-1. *The Journal of biological chemistry.* 1999;274:32631-32637.
- [108] Hatzopoulos AK, Folkman J, Vasile E, Eiselen GK, Rosenberg RD. Isolation and characterization of endothelial progenitor cells from mouse embryos. *Development (Cambridge, England).* 1998;125:1457-1468.
- [109] Coffin JD, Harrison J, Schwartz S, Heimark R. Angioblast differentiation and morphogenesis of the vascular endothelium in the mouse embryo. *Dev Biol.* 1991;148:51-62.
- [110] Shi Q, Rafii S, Wu MH, et al. Evidence for circulating bone marrow-derived endothelial cells. *Blood.* 1998;92:362-367.
- [111] Yamaguchi TP, Dumont DJ, Conlon RA, Breitman ML, Rossant J. flk-1, an flt-related receptor tyrosine kinase is an early marker for endothelial cell precursors. *Development (Cambridge, England).* 1993;118:489-498.
- [112] Vajkoczy P, Blum S, Lamparter M, et al. Multistep nature of microvascular recruitment of ex vivo-expanded embryonic endothelial progenitor cells during tumor angiogenesis. *J Exp Med.* 2003;197:1755-1765.
- [113] Kupatt C, Hinkel R, Lamparter M, et al. Retroinfusion of embryonic endothelial progenitor cells attenuates ischemia-reperfusion injury in pigs: role of phosphatidylinositol 3-kinase/AKT kinase. *Circulation.* 2005;112:1117-122.
- [114] Kupatt C, Horstkotte J, Vlastos GA, et al. Embryonic endothelial progenitor cells expressing a broad range of proangiogenic and remodeling factors enhance

- vascularization and tissue recovery in acute and chronic ischemia. *Faseb J.* 2005;19:1576-1578.
- [115] Kaestner KH, Knochel W, Martinez DE. Unified nomenclature for the winged helix/forkhead transcription factors. *Genes Dev.* 2000;14:142-146.
- [116] Carlsson P, Mahlapuu M. Forkhead transcription factors: key players in development and metabolism. *Dev Biol.* 2002;250:1-23.
- [117] Weigel D, Jackle H. The fork head domain: a novel DNA binding motif of eukaryotic transcription factors? *Cell.* 1990;63:455-456.
- [118] Clark KL, Halay ED, Lai E, Burley SK. Co-crystal structure of the HNF-3/fork head DNA-recognition motif resembles histone H5. *Nature.* 1993;364:412-420.
- [119] Lehmann OJ, Sowden JC, Carlsson P, Jordan T, Bhattacharya SS. Fox's in development and disease. *Trends Genet.* 2003;19:339-344.
- [120] Weigel D, Jurgens G, Kuttner F, Seifert E, Jackle H. The homeotic gene fork head encodes a nuclear protein and is expressed in the terminal regions of the *Drosophila* embryo. *Cell.* 1989;57:645-658.
- [121] Lai E, Prezioso VR, Tao WF, Chen WS, Darnell JE, Jr. Hepatocyte nuclear factor 3 alpha belongs to a gene family in mammals that is homologous to the *Drosophila* homeotic gene fork head. *Genes Dev.* 1991;5:416-427.
- [122] Cirillo LA, Zaret KS. An early developmental transcription factor complex that is more stable on nucleosome core particles than on free DNA. *Mol Cell.* 1999;4:961-969.
- [123] Hellqvist M, Mahlapuu M, Blixt A, Enerback S, Carlsson P. The human forkhead protein FREAC-2 contains two functionally redundant activation domains and interacts with TBP and TFIIB. *The Journal of biological chemistry.* 1998;273:23335-23343.
- [124] Katoh M, Katoh M. Human FOX gene family (Review). *Int J Oncol.* 2004;25:1495-1500.
- [125] Sirotkin HI, Gates MA, Kelly PD, Schier AF, Talbot WS. Fast1 is required for the development of dorsal axial structures in zebrafish. *Curr Biol.* 2000;10:1051-1054.
- [126] Hoodless PA, Pye M, Chazaud C, et al. FoxH1 (Fast) functions to specify the anterior primitive streak in the mouse. *Genes Dev.* 2001;15:1257-1271.
- [127] Brody SL, Yan XH, Wuerffel MK, Song SK, Shapiro SD. Ciliogenesis and left-right axis defects in forkhead factor HFH-4-null mice. *Am J Respir Cell Mol Biol.* 2000;23:45-51.
- [128] Hong HK, Noveroske JK, Headon DJ, et al. The winged helix/forkhead transcription factor Foxq1 regulates differentiation of hair in satin mice. *Genesis.* 2001;29:163-171.

- [129] Brissette JL, Li J, Kamimura J, Lee D, Dotto GP. The product of the mouse nude locus, Whn, regulates the balance between epithelial cell growth and differentiation. *Genes Dev.* 1996;10:2212-2221.
- [130] Nehls M, Pfeifer D, Schorpp M, Hedrich H, Boehm T. New member of the winged-helix protein family disrupted in mouse and rat nude mutations. *Nature.* 1994;372:103-107.
- [131] Hulander M, Wurst W, Carlsson P, Enerback S. The winged helix transcription factor Fkh10 is required for normal development of the inner ear. *Nat Genet.* 1998;20:374-376.
- [132] Blixt A, Mahlapuu M, Aitola M, Pelto-Huikko M, Enerback S, Carlsson P. A forkhead gene, FoxE3, is essential for lens epithelial proliferation and closure of the lens vesicle. *Genes Dev.* 2000;14:245-254.
- [133] Weinstein DC, Ruiz i Altaba A, Chen WS, et al. The winged-helix transcription factor HNF-3 beta is required for notochord development in the mouse embryo. *Cell.* 1994;78:575-588.
- [134] Ang SL, Rossant J. HNF-3 beta is essential for node and notochord formation in mouse development. *Cell.* 1994;78:561-574.
- [135] Costa RH, Kalinichenko VV, Lim L. Transcription factors in mouse lung development and function. *Am J Physiol Lung Cell Mol Physiol.* 2001;280:L823-838.
- [136] Chen J, Knowles HJ, Hebert JL, Hackett BP. Mutation of the mouse hepatocyte nuclear factor/forkhead homologue 4 gene results in an absence of cilia and random left-right asymmetry. *J Clin Invest.* 1998;102:1077-1082.
- [137] Tichelaar JW, Lim L, Costa RH, Whitsett JA. HNF-3/forkhead homologue-4 influences lung morphogenesis and respiratory epithelial cell differentiation in vivo. *Dev Biol.* 1999;213:405-417.
- [138] Shu W, Yang H, Zhang L, Lu MM, Morrissey EE. Characterization of a new subfamily of winged-helix/forkhead (Fox) genes that are expressed in the lung and act as transcriptional repressors. *The Journal of biological chemistry.* 2001;276:27488-27497.
- [139] Peterson RS, Lim L, Ye H, Zhou H, Overdier DG, Costa RH. The winged helix transcriptional activator HFH-8 is expressed in the mesoderm of the primitive streak stage of mouse embryos and its cellular derivatives. *Mech Dev.* 1997;69:53-69.
- [140] Mahlapuu M, Ormestad M, Enerback S, Carlsson P. The forkhead transcription factor Foxf1 is required for differentiation of extra-embryonic and lateral plate mesoderm. *Development (Cambridge, England).* 2001;128:155-166.
- [141] Wehr R, Mansouri A, de Maeyer T, Gruss P. Fkh5-deficient mice show dysgenesis in the caudal midbrain and hypothalamic mammillary body. *Development (Cambridge, England).* 1997;124:4447-4456.

- [142] Xuan S, Baptista CA, Balas G, Tao W, Soares VC, Lai E. Winged helix transcription factor BF-1 is essential for the development of the cerebral hemispheres. *Neuron*. 1995;14:1141-1152.
- [143] Yuasa J, Hirano S, Yamagata M, Noda M. Visual projection map specified by topographic expression of transcription factors in the retina. *Nature*. 1996;382:632-635.
- [144] Montero-Balaguer M, Lang MR, Sachdev SW, et al. The mother superior mutation ablates foxd3 activity in neural crest progenitor cells and depletes neural crest derivatives in zebrafish. *Dev Dyn*. 2006;235:3199-3212.
- [145] Garry DJ, Meeson A, Elterman J, et al. Myogenic stem cell function is impaired in mice lacking the forkhead/winged helix protein MNF. *Proceedings of the National Academy of Sciences of the United States of America*. 2000;97:5416-5421.
- [146] Chen X, Rubock MJ, Whitman M. A transcriptional partner for MAD proteins in TGF-beta signalling. *Nature*. 1996;383:691-696.
- [147] Chen X, Weisberg E, Fridmacher V, Watanabe M, Naco G, Whitman M. Smad4 and FAST-1 in the assembly of activin-responsive factor. *Nature*. 1997;389:85-89.
- [148] Liu B, Dou CL, Prabhu L, Lai E. FAST-2 is a mammalian winged-helix protein which mediates transforming growth factor beta signals. *Molecular and cellular biology*. 1999;19:424-430.
- [149] Yeo CY, Chen X, Whitman M. The role of FAST-1 and Smads in transcriptional regulation by activin during early *Xenopus* embryogenesis. *The Journal of biological chemistry*. 1999;274:26584-26590.
- [150] Dou C, Lee J, Liu B, et al. BF-1 interferes with transforming growth factor beta signaling by associating with Smad partners. *Molecular and cellular biology*. 2000;20:6201-6211.
- [151] Rodriguez C, Huang LJ, Son JK, McKee A, Xiao Z, Lodish HF. Functional cloning of the proto-oncogene brain factor-1 (BF-1) as a Smad-binding antagonist of transforming growth factor-beta signaling. *The Journal of biological chemistry*. 2001;276:30224-30230.
- [152] Mahlapuu M, Enerback S, Carlsson P. Haploinsufficiency of the forkhead gene *Foxf1*, a target for sonic hedgehog signaling, causes lung and foregut malformations. *Development (Cambridge, England)*. 2001;128:2397-2406.
- [153] Perreault N, Katz JP, Sackett SD, Kaestner KH. *Foxl1* controls the Wnt/beta-catenin pathway by modulating the expression of proteoglycans in the gut. *The Journal of biological chemistry*. 2001;276:43328-43333.
- [154] Medema RH, Kops GJ, Bos JL, Burgering BM. AFX-like Forkhead transcription factors mediate cell-cycle regulation by Ras and PKB through p27kip1. *Nature*. 2000;404:782-787.



- [155] Kops GJ, Burgering BM. Forkhead transcription factors: new insights into protein kinase B (c-akt) signaling. *J Mol Med.* 1999;77:656-665.
- [156] Korver W, Roose J, Clevers H. The winged-helix transcription factor Trident is expressed in cycling cells. *Nucleic acids research.* 1997;25:1715-1719.
- [157] Nishimura DY, Swiderski RE, Alward WL, et al. The forkhead transcription factor gene FKHL7 is responsible for glaucoma phenotypes which map to 6p25. *Nat Genet.* 1998;19:140-147.
- [158] Mears AJ, Jordan T, Mirzayans F, et al. Mutations of the forkhead/winged-helix gene, FKHL7, in patients with Axenfeld-Rieger anomaly. *Am J Hum Genet.* 1998;63:1316-1328.
- [159] Mirzayans F, Gould DB, Heon E, et al. Axenfeld-Rieger syndrome resulting from mutation of the FKHL7 gene on chromosome 6p25. *Eur J Hum Genet.* 2000;8:71-74.
- [160] Semina EV, Brownell I, Mintz-Hittner HA, Murray JC, Jamrich M. Mutations in the human forkhead transcription factor FOXE3 associated with anterior segment ocular dysgenesis and cataracts. *Hum Mol Genet.* 2001;10:231-236.
- [161] Crisponi L, Deiana M, Loi A, et al. The putative forkhead transcription factor FOXL2 is mutated in blepharophimosis/ptosis/epicanthus inversus syndrome. *Nat Genet.* 2001;27:159-166.
- [162] Fang J, Dagenais SL, Erickson RP, et al. Mutations in FOXC2 (MFH-1), a forkhead family transcription factor, are responsible for the hereditary lymphedema-distichiasis syndrome. *Am J Hum Genet.* 2000;67:1382-1388.
- [163] Bell R, Brice G, Child AH, et al. Analysis of lymphoedema-distichiasis families for FOXC2 mutations reveals small insertions and deletions throughout the gene. *Hum Genet.* 2001;108:546-551.
- [164] Erickson RP, Dagenais SL, Caulder MS, et al. Clinical heterogeneity in lymphoedema-distichiasis with FOXC2 truncating mutations. *J Med Genet.* 2001;38:761-766.
- [165] Brice G, Mansour S, Bell R, et al. Analysis of the phenotypic abnormalities in lymphoedema-distichiasis syndrome in 74 patients with FOXC2 mutations or linkage to 16q24. *J Med Genet.* 2002;39:478-483.
- [166] Zhou Y, Kato H, Asanoma K, et al. Identification of FOXC1 as a TGF-beta1 responsive gene and its involvement in negative regulation of cell growth. *Genomics.* 2002;80:465-472.
- [167] Harris SE, Chand AL, Winship IM, Gersak K, Aittomaki K, Shelling AN. Identification of novel mutations in FOXL2 associated with premature ovarian failure. *Mol Hum Reprod.* 2002;8:729-733.
- [168] Frank J, Pignata C, Panteleyev AA, et al. Exposing the human nude phenotype. *Nature.* 1999;398:473-474.

- [169] Lai CS, Fisher SE, Hurst JA, Vargha-Khadem F, Monaco AP. A forkhead-domain gene is mutated in a severe speech and language disorder. *Nature*. 2001;413:519-523.
- [170] Lin L, Miller CT, Contreras JI, et al. The hepatocyte nuclear factor 3 alpha gene, HNF3alpha (FOXA1), on chromosome band 14q13 is amplified and overexpressed in esophageal and lung adenocarcinomas. *Cancer Res*. 2002;62:5273-5279.
- [171] Nakamura T, Furukawa Y, Nakagawa H, et al. Genome-wide cDNA microarray analysis of gene expression profiles in pancreatic cancers using populations of tumor cells and normal ductal epithelial cells selected for purity by laser microdissection. *Oncogene*. 2004;23:2385-2400.
- [172] Teh MT, Wong ST, Neill GW, Ghali LR, Philpott MP, Quinn AG. FOXM1 is a downstream target of Gli1 in basal cell carcinomas. *Cancer Res*. 2002;62:4773-4780.
- [173] Parry P, Wei Y, Evans G. Cloning and characterization of the t(X;11) breakpoint from a leukemic cell line identify a new member of the forkhead gene family. *Genes Chromosomes Cancer*. 1994;11:79-84.
- [174] Borkhardt A, Repp R, Haas OA, et al. Cloning and characterization of AFX, the gene that fuses to MLL in acute leukemias with a t(X;11)(q13;q23). *Oncogene*. 1997;14:195-202.
- [175] Hillion J, Le Coniat M, Jonveaux P, Berger R, Bernard OA. AF6q21, a novel partner of the MLL gene in t(6;11)(q21;q23), defines a forkhead transcriptional factor subfamily. *Blood*. 1997;90:3714-3719.
- [176] Cederberg A, Gronning LM, Ahren B, Tasken K, Carlsson P, Enerback S. FOXC2 is a winged helix gene that counteracts obesity, hypertriglyceridemia, and diet-induced insulin resistance. *Cell*. 2001;106:563-573.
- [177] Brunet A, Datta SR, Greenberg ME. Transcription-dependent and -independent control of neuronal survival by the PI3K-Akt signaling pathway. *Curr Opin Neurobiol*. 2001;11:297-305.
- [178] Iida K, Koseki H, Kakinuma H, et al. Essential roles of the winged helix transcription factor MFH-1 in aortic arch patterning and skeletogenesis. *Development (Cambridge, England)*. 1997;124:4627-4638.
- [179] Winnier GE, Kume T, Deng K, et al. Roles for the winged helix transcription factors MF1 and MFH1 in cardiovascular development revealed by nonallelic noncomplementation of null alleles. *Dev Biol*. 1999;213:418-431.
- [180] Kume T, Jiang H, Topczewska JM, Hogan BL. The murine winged helix transcription factors, Foxc1 and Foxc2, are both required for cardiovascular development and somitogenesis. *Genes Dev*. 2001;15:2470-2482.
- [181] Seo S, Fujita H, Nakano A, Kang M, Duarte A, Kume T. The forkhead transcription factors, Foxc1 and Foxc2, are required for arterial specification and lymphatic sprouting during vascular development. *Dev Biol*. 2006;294:458-470.

- [182] Sasaki H, Hogan BL. Differential expression of multiple fork head related genes during gastrulation and axial pattern formation in the mouse embryo. *Development* (Cambridge, England). 1993;118:47-59.
- [183] Hiemisch H, Monaghan AP, Schutz G, Kaestner KH. Expression of the mouse Fkh1/Mf1 and Mfh1 genes in late gestation embryos is restricted to mesoderm derivatives. *Mech Dev*. 1998;73:129-132.
- [184] Swiderski RE, Reiter RS, Nishimura DY, et al. Expression of the Mf1 gene in developing mouse hearts: implication in the development of human congenital heart defects. *Dev Dyn*. 1999;216:16-27.
- [185] Winnier GE, Hargett L, Hogan BL. The winged helix transcription factor MFH1 is required for proliferation and patterning of paraxial mesoderm in the mouse embryo. *Genes Dev*. 1997;11:926-940.
- [186] Kume T, Deng K, Hogan BL. Murine forkhead/winged helix genes Foxc1 (Mf1) and Foxc2 (Mfh1) are required for the early organogenesis of the kidney and urinary tract. *Development* (Cambridge, England). 2000;127:1387-1395.
- [187] Kume T, Deng KY, Winfrey V, Gould DB, Walter MA, Hogan BL. The forkhead/winged helix gene Mf1 is disrupted in the pleiotropic mouse mutation congenital hydrocephalus. *Cell*. 1998;93:985-996.
- [188] Kidson SH, Kume T, Deng K, Winfrey V, Hogan BL. The forkhead/winged-helix gene, Mf1, is necessary for the normal development of the cornea and formation of the anterior chamber in the mouse eye. *Dev Biol*. 1999;211:306-322.
- [189] Smith RS, Zabaleta A, Kume T, et al. Haploinsufficiency of the transcription factors FOXC1 and FOXC2 results in aberrant ocular development. *Hum Mol Genet*. 2000;9:1021-1032.
- [190] Seo S, Kume T. Forkhead transcription factors, Foxc1 and Foxc2, are required for the morphogenesis of the cardiac outflow tract. *Dev Biol*. 2006;296:421-436.
- [191] Hong HK, Lass JH, Chakravarti A. Pleiotropic skeletal and ocular phenotypes of the mouse mutation congenital hydrocephalus (ch/Mf1) arise from a winged helix/forkhead transcription factor gene. *Hum Mol Genet*. 1999;8:625-637.
- [192] Wilm B, James RG, Schultheiss TM, Hogan BL. The forkhead genes, Foxc1 and Foxc2, regulate paraxial versus intermediate mesoderm cell fate. *Dev Biol*. 2004;271:176-189.
- [193] Rice R, Rice DP, Olsen BR, Thesleff I. Progression of calvarial bone development requires Foxc1 regulation of Msx2 and Alx4. *Dev Biol*. 2003;262:75-87.
- [194] Rice R, Rice DP, Thesleff I. Foxc1 integrates Fgf and Bmp signalling independently of twist or noggin during calvarial bone development. *Dev Dyn*. 2005;233:847-852.

- [195] Yamagishi H, Maeda J, Hu T, et al. Tbx1 is regulated by tissue-specific forkhead proteins through a common Sonic hedgehog-responsive enhancer. *Genes Dev.* 2003;17:269-281.
- [196] Garlanda C, Parravicini C, Sironi M, et al. Progressive growth in immunodeficient mice and host cell recruitment by mouse endothelial cells transformed by polyoma middle-sized T antigen: implications for the pathogenesis of opportunistic vascular tumors. *Proceedings of the National Academy of Sciences of the United States of America.* 1994;91:7291-7295.
- [197] Dalby B, Cates S, Harris A, et al. Advanced transfection with Lipofectamine 2000 reagent: primary neurons, siRNA, and high-throughput applications. *Methods (San Diego, Calif.)* 2004;33:95-103.
- [198] Roth MJ, Tanese N, Goff SP. Purification and characterization of murine retroviral reverse transcriptase expressed in *Escherichia coli*. *The Journal of biological chemistry.* 1985;260:9326-9335.
- [199] Saiki RK, Gelfand DH, Stoffel S, et al. Primer-directed enzymatic amplification of DNA with a thermostable DNA polymerase. *Science (New York, NY.)* 1988;239:487-491.
- [200] Sanger F, Nicklen S, Coulson AR. DNA sequencing with chain-terminating inhibitors. *Proceedings of the National Academy of Sciences of the United States of America.* 1977;74:5463-5467.
- [201] Birnboim HC, Doly J. A rapid alkaline extraction procedure for screening recombinant plasmid DNA. *Nucleic acids research.* 1979;7:1513-1523.
- [202] Dagert M, Ehrlich SD. Prolonged incubation in calcium chloride improves the competence of *Escherichia coli* cells. *Gene.* 1979;6:23-28.
- [203] Williams RJ. Restriction endonucleases: classification, properties, and applications. *Molecular biotechnology.* 2003;23:225-243.
- [204] Tomkinson AE, Vijayakumar S, Pascal JM, Ellenberger T. DNA ligases: structure, reaction mechanism, and function. *Chemical reviews.* 2006;106:687-699.
- [205] Smith M. In vitro mutagenesis. *Annual review of genetics.* 1985;19:423-462.
- [206] Nelson M, McClelland M. Use of DNA methyltransferase/endonuclease enzyme combinations for megabase mapping of chromosomes. *Methods in enzymology.* 1992;216:279-303.
- [207] McDonnell MW, Simon MN, Studier FW. Analysis of restriction fragments of T7 DNA and determination of molecular weights by electrophoresis in neutral and alkaline gels. *Journal of molecular biology.* 1977;110:119-146.
- [208] Nolan T, Hands RE, Bustin SA. Quantification of mRNA using real-time RT-PCR. *Nature protocols.* 2006;1:1559-1582.

- [209] Zipper H, Brunner H, Bernhagen J, Vitzthum F. Investigations on DNA intercalation and surface binding by SYBR Green I, its structure determination and methodological implications. *Nucleic acids research*. 2004;32:e103.
- [210] Livak KJ, Schmittgen TD. Analysis of relative gene expression data using real-time quantitative PCR and the 2(-Delta Delta C(T)) Method. *Methods (San Diego, Calif)*. 2001;25:402-408.
- [211] Loken MR, Parks DR, Herzenberg LA. Two-color immunofluorescence using a fluorescence-activated cell sorter. *J Histochem Cytochem*. 1977;25:899-907.
- [212] Wood KV, de Wet JR, Dewji N, DeLuca M. Synthesis of active firefly luciferase by in vitro translation of RNA obtained from adult lanterns. *Biochemical and biophysical research communications*. 1984;124:592-596.
- [213] Lorenz WW, McCann RO, Longiaru M, Cormier MJ. Isolation and expression of a cDNA encoding *Renilla reniformis* luciferase. *Proceedings of the National Academy of Sciences of the United States of America*. 1991;88:4438-4442.
- [214] Burnette WN. "Western blotting": electrophoretic transfer of proteins from sodium dodecyl sulfate--polyacrylamide gels to unmodified nitrocellulose and radiographic detection with antibody and radioiodinated protein A. *Analytical biochemistry*. 1981;112:195-203.
- [215] Smith PK, Krohn RI, Hermanson GT, et al. Measurement of protein using bicinchoninic acid. *Analytical biochemistry*. 1985;150:76-85.
- [216] Welinder KG. Plant peroxidases. Their primary, secondary and tertiary structures, and relation to cytochrome c peroxidase. *European journal of biochemistry / FEBS*. 1985;151:497-504.
- [217] Das PM, Ramachandran K, vanWert J, Singal R. Chromatin immunoprecipitation assay. *BioTechniques*. 2004;37:961-969.
- [218] Gerhardt J, Jafar S, Spindler MP, Ott E, Schepers A. Identification of new human origins of DNA replication by an origin-trapping assay. *Molecular and cellular biology*. 2006;26:7731-7746.
- [219] Cartharius K, Frech K, Grote K, et al. MatInspector and beyond: promoter analysis based on transcription factor binding sites. *Bioinformatics (Oxford, England)*. 2005;21:2933-2942.
- [220] Morgenstern B, Frech K, Dress A, Werner T. DIALIGN: finding local similarities by multiple sequence alignment. *Bioinformatics (Oxford, England)*. 1998;14:290-294.
- [221] van Buul JD, Hordijk PL. Signaling in leukocyte transendothelial migration. *Arteriosclerosis, thrombosis, and vascular biology*. 2004;24:824-833.
- [222] Redick SD, Bautch VL. Developmental platelet endothelial cell adhesion molecule expression suggests multiple roles for a vascular adhesion molecule. *Am J Pathol*. 1999;154:1137-1147.

- [223] Albelda SM, Muller WA, Buck CA, Newman PJ. Molecular and cellular properties of PECAM-1 (endoCAM/CD31): a novel vascular cell-cell adhesion molecule. *J Cell Biol.* 1991;114:1059-1068.
- [224] Samatar AA, Wang L, Mirza A, Koseoglu S, Liu S, Kumar CC. Transforming growth factor-beta 2 is a transcriptional target for Akt/protein kinase B via forkhead transcription factor. *The Journal of biological chemistry.* 2002;277:28118-28126.
- [225] Schlaeger TM, Bartunkova S, Lawitts JA, et al. Uniform vascular-endothelial-cell-specific gene expression in both embryonic and adult transgenic mice. *Proceedings of the National Academy of Sciences of the United States of America.* 1997;94:3058-3063.
- [226] Nobrega MA, Ovcharenko I, Afzal V, Rubin EM. Scanning human gene deserts for long-range enhancers. *Science (New York, NY.* 2003;302:413.
- [227] West AG, Fraser P. Remote control of gene transcription. *Hum Mol Genet.* 2005;14 Spec No 1:R101-111.
- [228] Su AI, Wiltshire T, Batalov S, et al. A gene atlas of the mouse and human protein-encoding transcriptomes. *Proceedings of the National Academy of Sciences of the United States of America.* 2004;101:6062-6067.
- [229] Smith AD, Sumazin P, Zhang MQ. Tissue-specific regulatory elements in mammalian promoters. *Molecular systems biology.* 2007;3:73.
- [230] Pasqualini R, Ruoslahti E. Organ targeting in vivo using phage display peptide libraries. *Nature.* 1996;380:364-366.
- [231] Rajotte D, Arap W, Hagedorn M, Koivunen E, Pasqualini R, Ruoslahti E. Molecular heterogeneity of the vascular endothelium revealed by in vivo phage display. *J Clin Invest.* 1998;102:430-437.
- [232] Botella LM, Puig-Kroger A, Almendro N, et al. Identification of a functional NF-kappa B site in the platelet endothelial cell adhesion molecule-1 promoter. *J Immunol.* 2000;164:1372-1378.
- [233] Aird WC, Jahroudi N, Weiler-Guettler H, Rayburn HB, Rosenberg RD. Human von Willebrand factor gene sequences target expression to a subpopulation of endothelial cells in transgenic mice. *Proceedings of the National Academy of Sciences of the United States of America.* 1995;92:4567-4571.
- [234] Schlaeger TM, Qin Y, Fujiwara Y, Magram J, Sato TN. Vascular endothelial cell lineage-specific promoter in transgenic mice. *Development (Cambridge, England).* 1995;121:1089-1098.
- [235] Aird WC, Edelberg JM, Weiler-Guettler H, Simmons WW, Smith TW, Rosenberg RD. Vascular bed-specific expression of an endothelial cell gene is programmed by the tissue microenvironment. *J Cell Biol.* 1997;138:1117-1124.

- [236] Cabanas C, Sanchez-Madrid F, Bellon T, et al. Characterization of a novel myeloid antigen regulated during differentiation of monocytic cells. *Eur J Immunol.* 1989;19:1373-1378.
- [237] Goldberger A, Middleton KA, Newman PJ. Changes in expression of the cell adhesion molecule PECAM-1 (CD31) during differentiation of human leukemic cell lines. *Tissue Antigens.* 1994;44:285-293.
- [238] Almendro N, Bellon T, Rius C, et al. Cloning of the human platelet endothelial cell adhesion molecule-1 promoter and its tissue-specific expression. Structural and functional characterization. *J Immunol.* 1996;157:5411-5421.
- [239] Okouchi M, Okayama N, Imai S, et al. High insulin enhances neutrophil transendothelial migration through increasing surface expression of platelet endothelial cell adhesion molecule-1 via activation of mitogen activated protein kinase. *Diabetologia.* 2002;45:1449-1456.
- [240] Fujita H, Kang M, Eren M, Gleaves LA, Vaughan DE, Kume T. Foxc2 is a common mediator of insulin and transforming growth factor beta signaling to regulate plasminogen activator inhibitor type I gene expression. *Circ Res.* 2006;98:626-634.
- [241] Ma GT, Roth ME, Groskopf JC, et al. GATA-2 and GATA-3 regulate trophoblast-specific gene expression in vivo. *Development (Cambridge, England).* 1997;124:907-914.
- [242] Li Q, Estepa G, Memet S, Israel A, Verma IM. Complete lack of NF-kappaB activity in IKK1 and IKK2 double-deficient mice: additional defect in neurulation. *Genes Dev.* 2000;14:1729-1733.
- [243] Minami T, Kuivenhoven JA, Evans V, Kodama T, Rosenberg RD, Aird WC. Ets motifs are necessary for endothelial cell-specific expression of a 723-bp Tie-2 promoter/enhancer in Hprt targeted transgenic mice. *Arteriosclerosis, thrombosis, and vascular biology.* 2003;23:2041-2047.
- [244] Arany Z, Huang LE, Eckner R, et al. An essential role for p300/CBP in the cellular response to hypoxia. *Proceedings of the National Academy of Sciences of the United States of America.* 1996;93:12969-12973.
- [245] van der Heide LP, Smidt MP. Regulation of FoxO activity by CBP/p300-mediated acetylation. *Trends Biochem Sci.* 2005;30:81-86.
- [246] Vogt P. Potential genetic functions of tandem repeated DNA sequence blocks in the human genome are based on a highly conserved "chromatin folding code". *Hum Genet.* 1990;84:301-336.
- [247] Stallings RL. Distribution of trinucleotide microsatellites in different categories of mammalian genomic sequence: implications for human genetic diseases. *Genomics.* 1994;21:116-121.
- [248] Weber JL, Wong C. Mutation of human short tandem repeats. *Hum Mol Genet.* 1993;2:1123-1128.

- [249] Djian P. Evolution of simple repeats in DNA and their relation to human disease. *Cell*. 1998;94:155-160.
- [250] Tautz D. Hypervariability of simple sequences as a general source for polymorphic DNA markers. *Nucleic acids research*. 1989;17:6463-6471.
- [251] Iglesias AR, Kindlund E, Tammi M, Wadelius C. Some microsatellites may act as novel polymorphic cis-regulatory elements through transcription factor binding. *Gene*. 2004;341:149-165.
- [252] Johnson AC, Jinno Y, Merlino GT. Modulation of epidermal growth factor receptor proto-oncogene transcription by a promoter site sensitive to S1 nuclease. *Molecular and cellular biology*. 1988;8:4174-4184.
- [253] Hoffman EK, Trusko SP, Murphy M, George DL. An S1 nuclease-sensitive homopurine/homopyrimidine domain in the c-Ki-ras promoter interacts with a nuclear factor. *Proceedings of the National Academy of Sciences of the United States of America*. 1990;87:2705-2709.
- [254] Contente A, Dittmer A, Koch MC, Roth J, Dobbstein M. A polymorphic microsatellite that mediates induction of PIG3 by p53. *Nat Genet*. 2002;30:315-320.
- [255] Syagailo YV, Okladnova O, Reimer E, et al. Structural and functional characterization of the human PAX7 5'-flanking regulatory region. *Gene*. 2002;294:259-268.
- [256] Kashi Y, King D, Soller M. Simple sequence repeats as a source of quantitative genetic variation. *Trends Genet*. 1997;13:74-78.
- [257] Roth J, Koch P, Contente A, Dobbstein M. Tumor-derived mutations within the DNA-binding domain of p53 that phenotypically resemble the deletion of the proline-rich domain. *Oncogene*. 2000;19:1834-1842.
- [258] Gaudet J, Mango SE. Regulation of organogenesis by the *Caenorhabditis elegans* FoxA protein PHA-4. *Science (New York, NY)*. 2002;295:821-825.
- [259] Rubinsztein DC, Leggo J, Amos W. Microsatellites evolve more rapidly in humans than in chimpanzees. *Genomics*. 1995;30:610-612.
- [260] Odom DT, Dowell RD, Jacobsen ES, et al. Tissue-specific transcriptional regulation has diverged significantly between human and mouse. *Nat Genet*. 2007;39:730-732.
- [261] Zaret KS. Regulatory phases of early liver development: paradigms of organogenesis. *Nat Rev Genet*. 2002;3:499-512.
- [262] Baeuerle PA, Henkel T. Function and activation of NF-kappa B in the immune system. *Annu Rev Immunol*. 1994;12:141-179.
- [263] Collins T, Read MA, Neish AS, Whitley MZ, Thanos D, Maniatis T. Transcriptional regulation of endothelial cell adhesion molecules: NF-kappa B and cytokine-inducible enhancers. *Faseb J*. 1995;9:899-909.



**SUPPLEMENTAL TABLE**

Gene Symbol	Gene Name
<b>Category - Transcription Factors</b>	
<i>Ascl2</i>	Achaete-scute complex homolog-like 2
<i>Cited4</i>	Cbp/p300-interacting transactivator, with Glu/Asp-rich carboxy-terminal domain, 4
<i>c-myc</i>	Myelocytomatosis oncogene
<i>Egr1</i>	Early growth response 1
<i>Foxa2</i>	Forkhead box A2
<i>Foxc1</i>	Forkhead box C1
<i>Foxc2</i>	Forkhead box C2
<i>Gata4</i>	GATA binding protein 4
<i>Gata5</i>	GATA binding protein 5
<i>Gata6</i>	GATA binding protein 6
<i>Hes5</i>	Hairy and enhancer of split 5 (Drosophila)
<i>Id1</i>	Inhibitor of DNA binding 1
<i>Id3</i>	Inhibitor of DNA binding 3
<i>Klf2</i>	Kruppel like Factor 2
<i>Klf4</i>	Kruppel like Factor 4
<i>Sox7</i>	SRY-box containing gene 7
<i>Sox17</i>	SRY-box containing gene 17
<i>Sox18</i>	SRY-box containing gene 18
<b>Category - Ligands</b>	
<i>Ang2</i>	Angiopoietin-2
<i>Bmp2</i>	Bone morphogenetic protein 2
<i>Bmp4</i>	Bone morphogenetic protein 4
<i>Dkk1</i>	Dickkopf homolog 1
<i>Dkk2</i>	Dickkopf homolog 2
<i>Dkk3</i>	Dickkopf homolog 3
<i>Dll1</i>	Delta-like 1 (Drosophila)
<i>Dll4</i>	Delta-like 4 (Drosophila)
<i>ESL</i>	E-selectin Ligand
<i>Fgf2</i>	Fibroblast growth factor 2 (basic)
<i>PDGFB</i>	Platelet-derived growth factor beta polypeptide
<i>PSGL-1</i>	Selectin P ligand
<i>TGFβ1</i>	Transforming growth factor, beta 1
<i>VEGFA</i>	Vascular endothelial growth factor A

**Supplemental Table.** Gain of function analysis in eEPCs after transient transfection with CMV-Foxc1 and/or CMV-Foxc2. Table lists genes whose expression was analyzed by RT-PCR (continues next page).

Gene Symbol	Gene Name
<b>Category - Receptors/Adhesion Molecules</b>	
<i>c-Kit</i>	Proto-oncogene tyrosine-protein kinase Kit
<i>Cxcr4</i>	Chemokine (C-X-C motif) receptor 4
<i>Eng</i>	Endoglin
<i>EphA1</i>	EPH receptor A1
<i>EphB4</i>	EPH receptor B4
<i>Efnb2</i>	Ephrin B2
<i>E-selectin</i>	Selectin E
<i>Flk-1</i>	VEGF Receptor-2
<i>Flt-1</i>	VEGF Receptor-1
<i>Icam-1</i>	Intercellular adhesion molecule 1
<i>Integrin<sub>av</sub></i>	Integrin, alpha V
<i>Integrin<sub>b5</sub></i>	Integrin, beta 5
<i>Notch1</i>	Notch homolog 1 (Drosophila)
<i>Notch2</i>	Notch homolog 2 (Drosophila)
<i>Notch3</i>	Notch homolog 3 (Drosophila)
<i>PDGFR<math>\alpha</math></i>	Platelet-derived growth factor receptor alpha
<i>Pecam-1</i>	Platelet/endothelial cell adhesion molecule
<i>P-selectin</i>	Selectin P
<i>TGF<math>\beta</math>RII</i>	Transforming growth factor, beta receptor II
<i>Vcam-1</i>	Vascular Cell Adhesion Molecule-1
<i>VE-Cadherin</i>	Cadherin 5, type 2, (vascular epithelium)
<b>Category - Extracellular Matrix</b>	
<i>laminin<math>\alpha</math></i>	Laminin, alpha 2
<i>laminin<math>\beta</math></i>	Laminin, beta 1
<i>MMP2</i>	Matrix metalloproteinase 2
<i>MMP9</i>	Matrix metalloproteinase 9
<i>MMP13</i>	Matrix metalloproteinase 13
<i>TIMP-2</i>	Tissue inhibitor of metalloproteinase 2
<b>Category - Miscellaneous</b>	
<i>eNos</i>	Endothelial Nitric Oxide Synthase
<i>Tsp-2</i>	Thrombospondin 2
<i>tPA</i>	Plasminogen activator, tissue
<i>uPA</i>	Plasminogen activator, urokinase
<i>Dvl1</i>	Dishevelled, dsh homolog 1 (Drosophila)
<i>Dvl2</i>	Dishevelled, dsh homolog 2 (Drosophila)
<i>Dvl3</i>	Dishevelled, dsh homolog 3 (Drosophila)

Supplemental Table (continued).

**ABBREVIATIONS**

3T3	mouse fibroblast cell line
BAECs	Bovine Aortic Endothelial Cells
C57/BL6	mouse strain
cAMP	cyclic Adenosine-Monophosphate
CD	Cluster of Differentiation (leukocyte surface antigens)
CGR8	mouse embryonic stem cell line
ChIP	Chromatin Immunoprecipitation
Cos7	green monkey kidney cell line
Cy3	red fluorescence dye, conjugated to secondary antibodies
DNase	Deoxyribonuclease
dNTP	Deoxyribonucleosidtriphosphate/Deoxyribonucleotide
ECs	Endothelial Cells
EDTA	Ethylenediaminetetraacetate
eEPCs	Embryonic Endothelial Progenitor Cells
EGFP	Enhanced Green Fluorescence Protein
EMSA	Electrophoretic Mobility Shift Assay
EPCs	Endothelial Progenitor Cells
ES	Embryonic Stem cells
FACS	Fluorescence Activated Cell Sorting
FITC	Fluorescein-isothiocyanate (green dye conjugated to secondary antibodies)
fmol	femtomole ( $10^{-15}$ mole)
g	constant of gravity ( $9,81 \text{ m/s}^2$ ) or gram
H5V-ECs	mouse cardiac endothelial cell line
HSCs	Hematopoetic Stem Cells
HEPES	N-(2-Hydroxyethyl)piperazin-N`-2-ethansulfonic acid
IgG	Immunoglobuline
l	liter
M	molar (mol/l)
min	minutes
ml	milliliter ( $10^{-3}$ liter)

---

mM	millimolar ( $10^{-3}$ molar)
mol	mole ( $6.022 \times 10^{23}$ atoms or molecules)
mmol	millimole ( $10^{-3}$ mole)
$\mu$ l	microliter ( $10^{-6}$ liter)
$\mu$ M	micromolar ( $10^{-6}$ molar)
$\mu$ mol	micromole ( $10^{-6}$ mole)
MS1-EC	mouse pancreatic endothelial cell line
nmol	nanomole ( $10^{-9}$ mole)
ng	nanogram ( $10^{-9}$ gram)
o/n	overnight
PBS	Phosphate buffered saline
PCR	Polymerase Chain Reaction
PE	Phycoerythrin (red fluorescence dye conjugated to secondary antibodies)
pmol	picomole ( $10^{-12}$ mole)
qPCR	quantitative real-time PCR
RNase	Ribonuclease
RT-PCR	Reverse Transcriptase Polymerase Chain Reaction
sec	seconds
SMCs	Smooth Muscle Cells
FT4b	mouse eEPC line
T17b	mouse eEPC line
T19b	mouse eEPC line
TBE	Tris-borate EDTA
TIS	Transcription Initiation Site
Tris	Tris(hydroxymethyl)-aminomethane

**ACKNOWLEDGMENTS*****I want to thank***

- Dr. Antonis Hatzopoulos, leader of the Vascular Genetics group at the Hämatologikum GSF, and Associate Professor at the Cardiovascular Medicine Division at Vanderbilt University Medical Center, for the great opportunity to develop a Ph.D. thesis under his supervision and to work on this interesting project, as well as for his permanent support and help during the entire Ph.D. project.
- Prof. Dr. Dirk Eick, Hämatologikum GSF, and Department of Genetics at the Ludwig-Maximilians-University of Munich, for his willingness to supervise this Ph.D. thesis as doctoral thesis supervisor (Doktorvater) and for his continuous support during the entire Ph.D. project.
- Dr. Heike Beck, Hämatologikum GSF, for her help with tissue sectioning, histology and immunofluorescence.
- Dr. Jürgen Schoch, Hämatologikum GSF, for his help with primer design.
- Dr. Georgios Vlastos, Hämatologikum GSF, for his help with FACS Analysis.
- Dr. Reinhardt Mailhammer, Hämatologikum GSF, for his help with the LightCycler System.
- Albert Geishauser, Hämatologikum GSF, for his help with tissue sectioning and microscopy.
- Dr. Scott Baldwin, Vanderbilt University Medical Center, for providing the *Pecam-1* promoter plasmids and sharing ideas about the project.
- Drew Misfeld, Vanderbilt University Medical Center, for his great help with mouse embryo isolation and LacZ-staining.

- Dr. Jeannine Gerhardt, Vanderbilt University Medical Center, for her great help with and sharing ideas about ChIP analysis, and her help with the LightCycler System.
- Dr. Meena Rai, Vanderbilt University Medical Center, for her help with Western Blot analysis.
- Dr. Jingbo Yan, Vanderbilt University Medical Center, for his help with mouse embryo isolation and bioinformatics software.
- Dr. Tom Kume, Vanderbilt University Medical Center, for providing the Fox-expression plasmids.
- All lab members at Vanderbilt University for the great atmosphere and team work during my stay at Vanderbilt University.
- All lab members from the Vascular Genetics group for the great atmosphere and team work at the Hämatologikum, GSF.

---

**LIST OF PUBLICATIONS**

- **Lamparter M**, Misfeldt D, Gerhardt J, Baldwin HS, Hatzopoulos AK. Foxc1 regulates *Pecam-1* expression in embryonic endothelial progenitor cells. (In Preparation).
- **Lamparter M**, Hatzopoulos AK. In *Angiogenesis: Basic Science and Clinical Applications*. (Maragoudakis ME, Papadimitriou E, Eds). Transworld Research Network, Kerala, India. (2007).
- **Lamparter M**, Hatzopoulos AK. In *Therapeutic Neovascularization: Quo vadis?* (Deindl E, Kupatt C, Eds). Springer, Dordrecht, The Netherlands, pp. 197-214, 2007
- Ryzhov S, Solenkova NV, Goldstein AE, **Lamparter M**, Fleenor T, Young PP, Greelish JP, Byrne JG, Vaughan DE, Biaggioni I, Hatzopoulos AK, Feoktistov I. Adenosine Receptor Mediated Adhesion of Endothelial Progenitors to Cardiac Microvascular Endothelial Cells. *Circ Res*. 2007 Nov 21 [Epub ahead of print].
- Kupatt C, Hinkel R, **Lamparter M**, von Brühl ML, Pohl T, Horstkotte J, Beck H, Müller S, Delker S, Gildehaus FJ, Büning H, Hatzopoulos AK, Boekstegers P. Retroinfusion of embryonic endothelial progenitor cells attenuates ischemia-reperfusion injury in pigs: role of phosphatidylinositol 3-kinase/AKT kinase. *Circulation* 112:1117-122, 2005.
- Kupatt C, Horstkotte J, Vlastos GA, Pfosser A, Lebherz C, Semisch M, Thalgott M, Büttner K, Browarzyk C, Mages J, Hoffmann R, Deten A, **Lamparter M**, Müller F, Beck H, Büning H, Boekstegers P, Hatzopoulos AK. Embryonic endothelial progenitor cells expressing a broad range of proangiogenic and remodeling factors enhance vascularization and tissue recovery in acute and chronic ischemia. *FASEB J*. 19:1576-1578, 2005.

- Wei J, Blum S, Unger M, Jarmy G, **Lamparter M**, Geishauser A, Vlastos GA, Chan G, Fischer KD, Rattat D, Debatin KM, Hatzopoulos AK, Beltinger C. Embryonic endothelial progenitor cells armed with a suicide gene target hypoxic lung metastases after intravenous delivery. *Cancer Cell* 5:477-488, 2004.
- Vajkoczy P, Blum S, **Lamparter M**, Mailhammer R, Erber R, Engelhardt B, Vestweber D, Hatzopoulos AK. Multistep nature of microvascular recruitment of ex vivo-expanded embryonic endothelial progenitor cells during tumor angiogenesis. *J Exp Med* 197:1755-1765, 2003.



# Lebenslauf

## Persönliche Daten

---

Familienname	Lamparter
Vorname	Mathias
Geburtsdatum	03.12.1976
Geburtsort	München
Staatsangehörigkeit	deutsch

## Hochschulausbildung

---

10/2002-01/2008      **Promotion**  
Promotionsstudent an der Fakultät für Biologie der Ludwig-Maximilians Universität München;  
Ausführung der Promotion am Institut für Klinische Molekularbiologie und Tumorgenetik, Helmholtz Zentrum München (ehemals GSF Forschungszentrum für Umwelt und Gesundheit), Arbeitsgruppe Vaskuläre Genetik, **Dr. Antonis Hatzopoulos** (10/2002-01/2005);  
Fortsetzung der Promotion am Vanderbilt University Medical Center, Nashville, Tennessee, USA - Institute for Cardiovascular Medicine, **Prof. Dr. Antonis Hatzopoulos** (02/2005-11/2007);  
Doktorvater: **Prof. Dr. Dirk Eick**, Institut für Klinische Molekularbiologie und Tumorgenetik, Helmholtz Zentrum München (eick@helmholtz-muenchen.de)

11/1997-06/2002      **Biologiestudium** an der Technischen Universität München zur Erlangung des Grades Diplom-Biologe - Gesamtnote 1,1 (mit Auszeichnung bestanden)  
Hauptstudium - Schwerpunktfach: Technische Biologie  
Hauptstudium - Nebenfächer: Genetik, Virologie, Biochemie

11/2001-06/2002      **Diplomarbeit** am Institut für Klinische Molekularbiologie und Tumorgenetik, Helmholtz Zentrum München, Arbeitsgruppe Vaskuläre Genetik, **Dr. Antonis Hatzopoulos** Titel: "*Investigation of homing and activation of embryonic endothelial progenitor cells in tumor angiogenesis*" - (Note 1,0)

## Schulische Ausbildung

---

1996      **Abitur** am Heinrich-Heine-Gymnasium, München (Note: 2,8)